THE INVESTIGATION OF SEAWATER INTRUSION OF COASTAL AQUIFER IN KARAREIS (KARABURUN PENINSULA)

A Thesis Submitted to
the Graduate School of Engineering and Sciences of
İzmir Institute of Technology
in Partial Fulfillment of the Requirements for the Degree of

MASTER OF SCIENCE

in Environmental Engineering

by
Ahmed Y. S. MANSOUR

November 2016
IZMIR

We approve the thesis of **Ahmed Y. S. MANSOUR**

Examining Committee Members:

_____

Prof. Dr. Alper BABA
Department of Civil Engineering, Izmir Institute of Technology

_____

Assoc. Prof. Dr. Orhan GÜNDÜZ
Department of Environmental Engineering, Dokuz Eylül University

_____

Prof. Dr. Gökmen TAYFUR
Department of Civil Engineering, Izmir Institute of Technology

_____

Prof. Dr. Celalletin ŞİMŞEK
Department of Drilling Technology, Dokuz Eylül University

_____

Prof. Dr. Sait C. SOFUOĞLU
Department of Chemical Engineering, Izmir Institute of Technology

15 November 2016

_____

Prof. Dr. Alper BABA
Supervisor, Department of Civil Engineering
Izmir Institute of Technology

_____

Assoc. Prof. Dr. Orhan GÜNDÜZ
Co-Supervisor, Department of Environmental Engineering
Dokuz Eylül University

_____

Prof. Dr. Sait C. SOFUOĞLU
Head of the Department of Environmental Engineering

_____

Prof. Dr. Bilge KARAÇALI
Dean of the Graduate School of Engineering and Sciences

ACKNOWLEDGMENTS

I wish to express my sincere gratitude and appreciation to my advisor Prof. Dr. Alper BABA for his invaluable supervision, helpful suggestions, and encouragement during the period of my study.

I would like to express my especial gratitude to my co-supervisor Assoc. Prof. Dr. Orhan GÜNDÜZ for his great support, academic guidance, helpful advice and feedbacks. I want to thank Prof. Dr. Sait C. SOFUOĞLU for his helpful guidance and feedbacks. Furthermore, I really want to thank all the academic and administrative staff of the Environmental and Civil Engineering Department for their contributions during my study. I would also like to extend my thankfulness to Mehmet Sinan YILDIRIM for his encouragement and support during data the collection. Also, I would like to thank Presidency for Turks Abroad and Related Communities (YTB) for their priceless support during the period of my study in Turkey. Besides that, I do not want to forget to thank Scientific and Technological Research Council of Turkey (TÜBİTAK) for their support during this study.

Additionally, I would like to especially thank and appreciate to Turkish people for their honesty, hospitality, friendly environment and support in all aspects of my life. I would also like to express my deepest gratitude to the people of Palestine for their holistic supports.

Lastly, I would like to thank my father and mother for their supports, encouragement, and loves throughout my life. Also, I want to gratitude and thank my brothers and friends for their support, and acceptance of difficulties in very tough times of my life. Thanks a lot, and I am sorry that I could not individually name them, but I know without their supports and inspiration, I would not be able to accomplish MS program.

ABSTRACT

THE INVESTIGATION OF SEAWATER INTRUSION OF COASTAL AQUIFER IN KARAREIS (KARABURUN PENINSULA)

Seawater intrusion is a major problem to freshwater resources especially in coastal areas where fresh groundwater is surrounded and could easily be influenced by seawater. This study presents the development of conceptual and numerical model for the coastal aquifer of Karareis region in the western part of Turkey. The study also presents the interpretation and the analysis of the groundwater levels recorded by groundwater data loggers. Groundwater pumping from Karareis aquifer has increased significantly during the summer period to meet the agriculture and domestic water demands. Levels of groundwater were measured at nine locations in Karareis region; also water samples were collected and analyzed for some parameters. For this study SEAWAT code is used to solve the numerical model for the coupled density dependent flow system. The model was calibrated using the average of one-year dataset of collected groundwater levels. Model validation was handled using the average of groundwater levels measured over more one year. Five scenarios were tested to understand the effects of pumping and climate change on groundwater levels and seawater intrusion in the next ten years.

The result of analysis demonstrated a high concentration of electrical conductivity and chloride along the coastal part of the study area. As a result of the numerical model, seawater intrusion will extent about 420 m towards the land in the next ten years of increased pumping scenario, while a little change in water level and TDS concentration was recognized in climate change scenario. Results also showed that reducing the pumping from Karareis wells will be necessary to protect the freshwater from contamination by seawater.

Keywords Seawater Intrusion, Electrical Conductivity, Chloride, Density Dependent Flow, SEAWAT, TDS, Karareis, Karaburun

ÖZET

KARAREİS (KARABURUN YARIMADASI) KIYI AKİFERİNE DENİZ SUYU GİRİŞİMİNİN ARAŞTIRILMASI

Deniz suyu girişimi, özellikle deniz tarafından çevrelenen kıyı akiferlerde, tatlı su kaynaklarını tehdit eden en önemli problemlerden biridir. Bu çalışma kapsamında, Türkiye'nin batısında bulunan Karareis bölgesindeki kıyı akiferi için kavramsal ve numerik modelleme çalışmaları yapılmış olup ayrıca spesifik olarak deniz suyu girişimini dikkate alan değişken yoğunluklu yeraltı suyu akım modelleme çalışması sunulmuştur. Bununla beraber akiferdeki yeraltı suyu seviyelerinin ölçümü ve tahminine yönelik çalışmalar da bu tez kapsamında değerlendirilmiştir. Yapılan çalışmada, Karareis kıyı akiferinde yazın tarım ve günlük kullanıma bağlı olarak yeraltı suyu çekimi belirgin olarak artmakta olduğu saptanmıştır. Bölgenin hidrolojik ve hidrojeolojik parametrelerinin tayini için bölgede dokuz farklı lokasyonda yer alan sondaj kuyularında yeraltı suyu seviyesi ölçülmüştür. Kıyı akiferlerindeki deniz suyu girişimi etkisi altındaki yeraltı suyu akımları SEAWAT isimli matematiksel model sürümü ile belirlenmiştir. Model kalibrasyonu ve test için iki yıl boyunca kuyulardan düzenli ölçülen yeraltı suyu seviye verilerinden yararlanılmıştır. Gelecek on yıl için pompaj kuyularından su çekiminin, iklim değişiminin ve deniz suyu girişiminin yeraltı suyu seviyesine etkisini anlamak için beş senaryo test edilmiştir.

Yapılan incelemelerde, çalışma alanının özellikle kıyı kesimlerinde, yüksek klorür konsantrasyonu ve elektriksel iletkenlik değerlerinin gözlendiği, deniz suyu girişiminin gelecek on yıllık artan su çekimi senaryosu kapsamında değerlendirilip modellenmesi sonucunda, bölgenin iç kesimlerine doğru 420 metreye kadar tuzlu su girişiminin ilerleyebileceği görülmüştür. Senaryo kapsamında yeraltı suyu seviyesinin veya TDS miktarının minimal düzeyde değişeceği ayrıca ortaya konulmuştur. Son olarak, Karareis bölgesi akiferinde yeraltı suyu çekiminin planlanması ile deniz suyu girişiminin tatlı suyu kaynaklarına etkisi azaltılmış olacak, bölgenin yeraltı suyu kaynaklarının niteliği ve niceliği korunmuş olacaktır.

Anahtar kelimeler Deniz suyu Girişimi, Elektriksel İletkenlik, klorür, Yoğunluk Bağlı Akım, SEAWAT, TDS, Karaburun, Karareis

TABLE OF CONTENTS

LIST OF FIGURES

LIST OF TABLES

LIST OF ABBREVIATIONS

Agr.Well	Agricultural Well
DC	Direct Current
EC	Electrical Conductivity
ESRI	Environmental Systems Research Institute
FDEM	Frequency Domain Electromagnetic Methods
FDM	Finite Difference Method
FEM	Finite Element Method
G.S	Ground Surface
G.W	Groundwater
MODFLOW	Modular Finite-Difference Ground-Water Flow Model
MSL	Mean Sea Level
MT3D	Modular Three-dimensional Transport Model
MT3DMS	Three-Dimensional Multispecies Transport Model
OBS. Well	Observation Well
PCG	Preconditioned Conjugate Gradient
PDE	Partial Differential Equation
PEST	Non Linear Parameter Estimator
RMSE	Root Mean Square Error
SEAWAT	Three-Dimensional Variable-Density Groundwater Flow Model
SIP	Strongly Implicit Procedure
SOR	Successive Over Relaxation
SRTM	Shuttle Radar Topography Mission
St.	Station
TDEM	Time Domain Electromagnetic Methods
TDS	Total Dissolved Solids
Temp	Temperature
UAE	United Arab Emirates
USA	United State of America
USACE	United States Army Corps of Engineers
USEPA	United States Environmental Protection Agency
USGS	United States Geological Survey

LIST OF SYMBOLS

Cl^-	Chloride
Na^+	Sodium
Ca^{2+}	Calcium
K^+	Potassium
Mg^{+2}	Magnesium
HCO_3^-	Bicarbonate
SO_4^{2-}	Sulfate
Br	Bromine
K_{xx}, K_{yy}, K_{zz}	Hydraulic conductivities along x, y, and z coordinate axes (LT^{-1})
h	Potentiometric head (L)
W	Local source or sink of water per unit volume (T^{-1})
S_s	Specific storage of the porous material (L^{-1})
t	Time (T)
δ^{18} O	Oxygen isotope
δ^2 H	Hydrogen isotope
C	Concentration of contaminates dissolved in groundwater (ML^{-3})
D_{lJ}	Hydrodynamic dispersion coefficient along I and J direction (L^2T^{-1})
v_i	Seepage velocity (LT^{-1})
q_s	Volumetric flux of water per unit volume of aquifer (T^{-1})
C_s	Concentration of sources or sinks (ML^{-3})
θ, α	Porosity (-)
R_k	Chemical reaction term ($ML^{-3}T^{-1}$)
ρ_s	Density of the saline water (ML^{-3})
ρ_f	Density of fresh water (ML^{-3})
g	Acceleration of gravity (LT^{-2})
h_f	Elevation of the water table above sea level (L)
x_w	Distance of well from shoreline (L)
B	Depth to bedrock below mean sea level (L)
$Q'_\circ$	Freshwater flow per unit length of shoreline (L3/T/L)
Q_w	Constant pumping rate (L^3/T)

Q_c	Critical pumping rate (L^3/T)
T	Transmissivity (L^2/T)
mg/L	Milligrams Per Liter
ppb	Parts Per Billion

CHAPTER 1

INTRODUCTION

1.1. Background

Water is very essential for life on the Earth, and within the fact that 99.4% of all the water on the Earth is surface water and groundwater occurs only as 0.6% of the total. However, most of the surface water is in the form of saltwater in oceans and seas (97%). Fresh surface water accounts for only 2% of the total volume of water. The proportion between surface water and subsurface water without taking into account the saltwater will be 78% and 22%, respectively. A further breakdown of fresh water shows that almost 77% of the total volume of fresh water is in the form of ice locked in ice-caps and glaciers in Polar Regions. The fresh water resources that are accessible for human consumption are in lakes and streams with 0.3% and 0.003%, respectively (Bear et al., 1999).

The central focus of hydrology is the hydrologic cycle consisting of the continuous processes; water evaporates from the oceans and the land surfaces to become water vapor which is carried over the earth by atmospheric circulation. The water vapor condenses and precipitates on the land and oceans. The precipitated water discharges as surface runoff or infiltrate into the ground, flows through the soil as subsurface flow. Infiltrated water may recharge groundwater and later become spring flow or become stream flow. Evapotranspiration is process consists of two parts, first evaporation directly from the land surface and second transpiration through the plant leaves. Groundwater is a component of the hydrologic cycle and it is the water which occupies the voids in saturated zone of earth's crust. Water formations of the earth's crust act as conduits for transmission and as reservoir for storage of water. Water enters the system from the ground surface or from bodies of surface water, and then travels slowly for varying distance until it returns to surface by plants or humans or by actions of natural flow. Naturally, discharge of groundwater occurs as a flow into surface water bodies, such as streams, springs and oceans. Groundwater near the surface may return to atmosphere by either evaporation or transpiration. Pumping from the groundwater

system is considered to be the major artificial discharge of groundwater (Todd & Mays, 1980).

Seawater intrusion is the most common problem in fresh groundwater. Seawater intrusion occurs where saline water displaces or mixes with fresh water in an aquifer. If the extraction of fresh water from a coastal aquifer exceeds the natural recharge of freshwater from rainfall or river leakage into aquifer then brackish water can be drawn to the aquifer. In hydrogeological systems, hydraulic gradient and the distribution of hydraulic conductivity can determine the rate and the pathway of transport (Bear et al., 1999). Seawater intrusion generally results inadvertently from human activities. This problem starts to spread out in many European and Mediterranean coastal aquifers such as Greece (Kallioras et al., 2006), Turkey (Cobaner et al., 2012), and (Kaya et al., 2015), Palestine (Qahman & Larabi, 2006), Tunisia (Paniconi et al., 2001) and (Gaaloul et al., 2012) and Syria (Allow, 2011). Seawater intrusion takes place either at typical coastal aquifers due to over-pumping of fresh water quantities such as the study aquifer in Gaza Strip in Palestine (Qahman & Larabi, 2006) and (Sarsak & Almasri, 2013) and coastal aquifer of Wadi Ham in United Arab Emirates (UAE) (Sherif et al., 2012).

Turkey is located in the Mediterranean part of Alpine belt and has a coastalline of 8,000 km. The population is increasing, especially along the coastal areas, and parallel to population increase and economic growth, the demand of water has increased significantly. This has led to excessive consumption of the aquifer by local people, without expert control, which caused serious problems such as seawater intrusion. In Turkey there are two common types of aquifers along the coast, namely alluvial aquifers (with primary permeability) and karstic and fractured (with primary and secondary permeability). Alluvial aquifers are widespread in almost all regions, while karstic aquifers are the major aquifers in southern Anatolia and fractured aquifers are the main aquifers in northwestern and northern Anatolia (Land et al., 1997).

Aquifer which is contaminated by saline water, remediation and reinstatement of its freshwater can be a difficult task. The major problem for all aquifers, however, is mismanagement of ground water resources; excessive pumping gives rise to saltwater intrusion. Therefore, effective techniques are generated to investigate the complex geohydrologic structures and their behavior, and the hydrologic systems as a whole are studied, not only aquifers.

1.2. Problem Identification

The Overexploitation of groundwater from shallow alluvial aquifer of Karareis region, has induced a rise in the saline-fresh interface (seawater intrusion) and thus, a degradation of the quality of the groundwater.

Karareis alluvial aquifer has been chosen to carry out this study because of many reasons; the boundary conditions in that region were defined by many boreholes which were dug in that region, and this makes the aquifer simple to be simulated numerically. Also, it will consider to be a representative example for alluvial coastal aquifers which have the same geological characteristic in Turkey. Additionally, the results will contribute to understand the groundwater system in Karareis and other similar aquifers located in arid region. Finally the alluvial aquifer of Karareis region is considered to be sensitive aquifer in view of its hydrogeological characteristics, therefore sustainable management techniques should be carried out to control intrusion from various sources, and to protect the aquifer from collapse.

1.3. Aim and Objectives

The aim of this study is to investigate the potential effect of seawater intrusion to the unconfined aquifer in the coastal area of Karareis, and to investigate the effects of the fluctuations of pumping quantity on seawater intrusion by applying the SEAWAT code which is based on density-dependent groundwater flow model. While, the objectives of the current study, are:

- To install investigation wells into study area at approximately depth of 50 m
- To characterize the hydrogeology and obtain the hydrogeological modeling parameters for the coastal aquifer
- To sample groundwater in the coastal area for general chemical constituents and environmental isotopes
- To develop conceptual model for the process of groundwater flow and seawater intrusion in the coastal aquifer
- To create groundwater flow numerical model using Visual MODFLOW, and calibrate the flow model to observed data

- To examine model results using Visual MODFLOW Explorer and assess the threat of seawater intrusion into the unconfined aquifer

1.4. Thesis Structure

This thesis contains five chapters. The chapters are briefly explained in the following:

CHAPTER 1. INTRODUCTION. This chapter briefly gives general information about the water cycle and occurrence of groundwater; then starts to give an idea about groundwater pollution due to seawater intrusion. Also, this chapter clarifies the aim and the objectives of this study, and finally structure the overall of the thesis (Figure 1.1).

CHAPTER 2. LITERATURE REVIEW. This chapter reviews the methodologies for geophysical, geochemical and numerical investigation that are used to detect the presence of saltwater in coastal aquifer. Also, a number of case studies on seawater intrusion in coastal aquifers using different simulation codes have been conducted and reported in this chapter.

CHAPTER 3. METHODOLOGY. This chapter describes the study area with respect to geology, hydrogeology, and climate. Also, it summarizes the methods that are used to obtain the information about the concerned aquifer (location, thickness and permeability) and about the groundwater (flow direction, movement, and quality). Finally it presents the groundwater modeling code which was used in the seawater intrusion simulation.

CHAPTER 4. RESULTS AND DISCUSSION. This chapter presents the steps used to construct the conceptual and numerical model. Also, it presents the calibration and validation of the numerical model; showing the results of SEAWAT model regarding the significance of TDS contamination in Karareis groundwater. Also, it covers some of the suggested management scenarios in order to understand the effect of pumpage on the extent of seawater intrusion. Finally it demonstrates some of methods that are used to control seawater intrusion in the aquifer.

CHAPTER 5. SUMMARY, CONCLUSIONS AND RECOMMENDATIONS. This chapter concludes the overall subjects of the thesis and the author’s comments/ suggestions based on the study results.

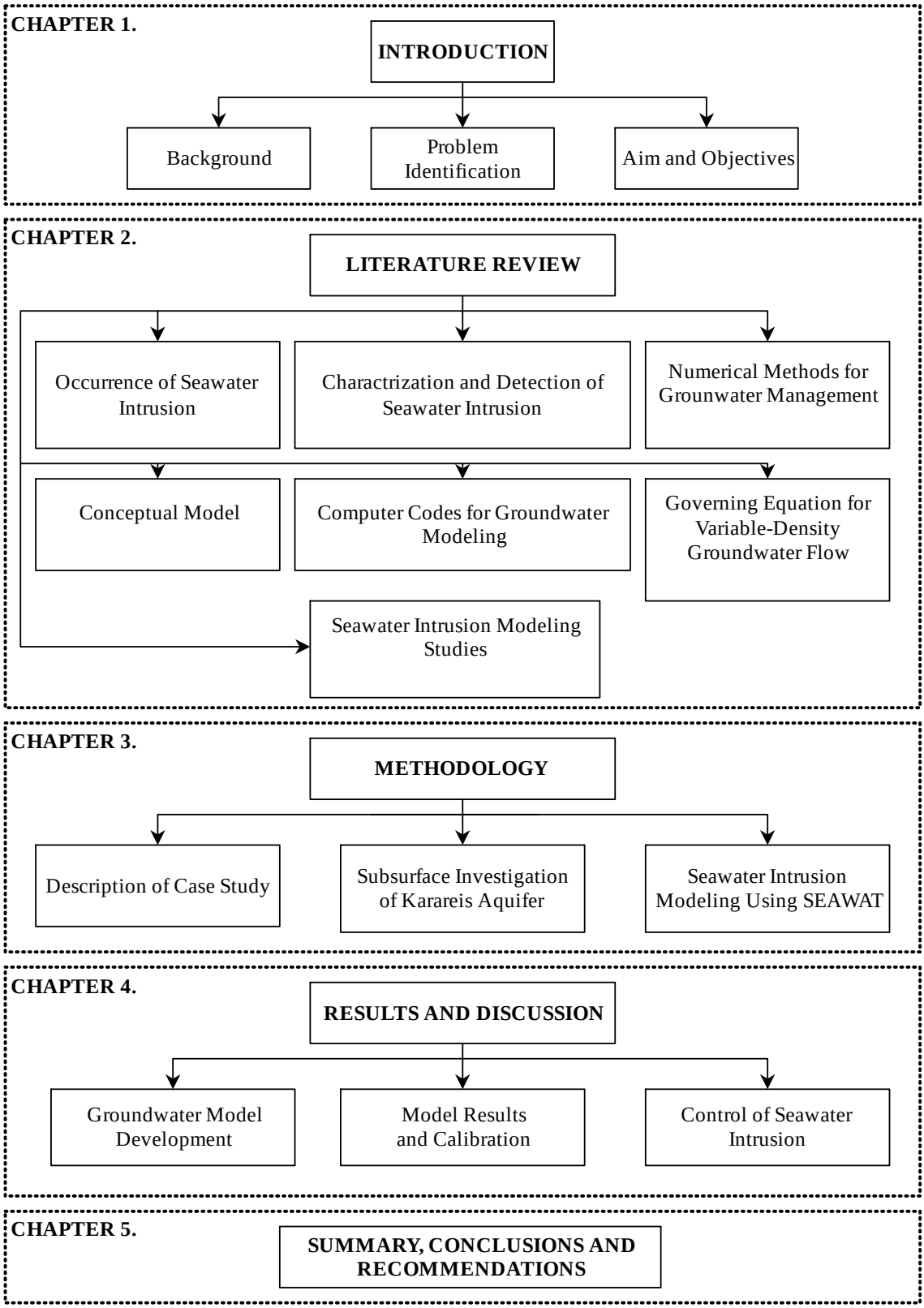

Figure 1.1. Thesis structure

CHAPTER 2

LITERATURE REVIEW

2.1. Occurrence of Seawater Intrusion

Seawater intrusion is the mass transport of saline water into zones of freshwater. Mass transport rates and directions are determined by hydraulic gradient and distribution of hydraulic conductivity (Bear et al., 1999). Seawater intrusion into freshwater generally results inadvertently from human activities. Saline water may be derived from any several sources (Todd & Mays, 1980):

1. Overtaking of seawater in coastal areas
2. Salt in salt domes, thin beds, or disseminated in geologic formations
3. Seawater that entered aquifers during past geologic time
4. Return flows from irrigated lands
5. Human saline wastes

Naturally, freshwater flows to the oceans and mixes with saltwater by the processes of dispersion and molecular diffusion. The freshwater and saltwater zones within coastal aquifer are separated by a transition zone (zone of dispersion) which there is mixing between fresh water and saltwater. The transition zone is characterized by measurements of the chloride concentration or the TDS of sampled groundwater at observation wells. There are no standard method for defining the transition zone, concentration of TDS ranging from 1000 to 35000 mg/L and of chloride ranging from 250 to 19000 mg/L are common indicators of the zone (Barlow, 2003). Generally, seawater intrusion in coastal aquifers is caused by two mechanisms:

- Lateral encroachment from oceans due to excessive discharge from coastal aquifer, or
- Upward movement (upconing) from deeper saline water near pumping wells

Seawater intrusion into freshwater is also influenced by factors such as tidal fluctuations, long-term climate change and sea level changes, fractures in coastal rock formations and seasonal changes in evaporation and recharge rates. Recharging can also be lowered in areas with increased urbanization and thus impervious surfaces. Construction of drainage canals can also cause intrusion according to the decrease in

water levels (Barlow, 2003). Reduction or reversal of groundwater gradient, which permits denser saline water to displace fresh water, occurs in coastal aquifers when pumping of wells disturbs the natural hydrodynamic balance (Todd & Mays, 1980). The occurrence of seawater intrusion is extensive and represents a special category of pollution. A List of examples of intrusion has been presented in this chapter, to reveals that the problem exists in localities of most parts of the populated coastal aquifer in the world.

2.2. Characterization and Detection of Seawater Intrusion

Since the early 1900s, field studies have been documented the locations and the movements of saline water in coastal aquifers. These studies are the basis for understanding the mechanisms that cause seawater intrusion in different hydro-geologic settings. Several geophysical and geochemical techniques are used to detect the presence of seawater intrusion in coastal aquifers.

2.2.1. Water Sampling

Water sampling or boreholes fluid are used to obtain the position of fresh-salt water interface. However, several important considerations should be taken into account, such as boreholes locations and borehole's screen length and distribution (Bear & Cheng, 2010; Land et al., 1997). This method consists of drilling boreholes (observation wells) at locations of studied area. When the screen of the well is short, wrong results may be obtained, and it cannot be known at which depth this water is present in the formation. However, when the well consists of multiple short screens the water starts to enter the well from various depths and then mixed in the well. Therefore, before taking water sample from well, water should be recycled a few times to be sure that the taken sample represents the water in the aquifer. Currently, to get unmixed representative water sample at different depths, various tools have been used, such as packers which can take water samples from different depths without mixing. The data obtained by this method is considered to be the most direct and, may be the most accurate, and sometimes is be used to calibrate data obtained by other methods, such as geophysical methods (Bear & Cheng, 2010). However, one of the main disadvantages

of this method is that, the associated costs are sometimes high, particularly when the studied area is large.

2.2.2. Geophysical Characterization Methodologies

Various techniques have been used to identify the morphology of underground saline water bodies. Geophysical techniques make use of physical properties, such as the electrical conductivity, electromagnetic permeability, thermal conductivity, etc., of the geomaterials, such as the soil, and the water occupying the void space, with the latter varying with the concentration of dissolved matter (Bear & Cheng, 2010).

2.2.2.1. Direct Current (DC) Resistivity

This method is one of the earliest geophysical methods that used to detect saltwater underground in coastal aquifers by mapping of fresh/salt-water interfaces. The method is based on the increase in electrical conductivity with increasing water salinity (Bear & Cheng, 2010). In DC method, the resistivity of subsurface materials is measured by introducing an electrical current into the ground by a pair of surface electrodes (current electrodes) and measuring the resulting potential field (voltage) between a pair of a second electrodes (potential electrodes) (Boulding, 1996). The measured resistance represents the integrated resistivity over the electrically heterogeneous soil. The effectiveness of this technique is limited and, may not be strong enough to accurately determine a continuously varying salt concentration in a transition zone (Bear & Cheng, 2010).

2.2.2.2. Electromagnetic Methods

Electromagnetic methods are useful to study fresh-salt water relationships. The saltwater body acts as an underground conductor. This method is based on the electromagnetic response of the earth to electrical currents that are induced to flow in the ground (Barlow, 2003). In this method, two wire coils are used, one to generate an alternative magnetic field, and the other to detect the resultant magnetic field generated in the sub-surface. The method is less applicable for greater depths and, may be used to

obtain general information at shallow depths over large areas (frequency domain electromagnetic profiling FDEM), or to collect more detailed quantitative data about the electrical profile of the subsurface (time domain electromagnetic sounding TDEM).

One of the main disadvantages of geoelectrical methods is their difficultly to detect thin clay layers, and to distinguish clay that contain fresh or brackish water from sand saturated with saline water (Land et al., 1997).

2.2.3. Geochemical Characterization Methodologies

In many coastal aquifers around the world, the geochemical techniques are used to characterize the occurrence of seawater intrusion and to identify the origin of salinity. The two most common approaches to determine the presence of saline water are measurement of electrical conductivity (EC) and chloride concentration (Cl^-). Also, geochemical isotopes are important tools can be used to describe the mixing process between saline water and fresh water (Bear & Cheng, 2010). In generally, seawater can be characterized by the predominance of $Cl^-$and Na^+, with a molar ratio of 0.86, and excess of Cl^-over alkali ions (Na and K), and Mg^{+2} greater than Ca^{2+} (Mg/Ca = 4.5-5.2). On the other hand, fresh groundwater's predominant anions are HCO_3^-, SO_4^{2-} and Cl^-. The fundamental cations are Ca^{2+} and Mg^{2+} which Ca^{2+} is greater than Mg^{2+} and, to lesser extent, the alkali ions Na^+ and K^+ (Bear & Cheng, 2010). To interpret the salinization process geological and hydrochmeical criteria have to be studied. Several geochemical criteria are used to define the origin and to distinguish the sources of salinization.

2.2.3.1. Salinity

Chloride is usually found at a low concentration in groundwater (excepting deep groundwater), but it is the dominate anion in the seawater. Therefore, chloride is a good indicator to show the possibility of seawater intrusion in coastal aquifers. Thus, time-serious chloride concentrations can record the early development of salinization processes.

2.2.3.2. Major Ion Ratios

Major ion ratios are often used to interpret the processes of salinization within the mixing zone. The ionic chemical distribution of the groundwater samples such as Na/Cl, Mg/Cl, Ca/Mg, SO4/Cl, and Ca/Cl are used to group the water samples in to main categories according to their chemical composition and their ions dominations (Lollar, 2005). Na/Cl ratio is the most frequently used geochemical parameter in order to study the mechanism of seawater intrusion. Low Na/Cl, combined with other geochemical constituents indicate seawater intrusion. Na/Cl can also be used to separate between seawater intrusion and other sources of saltwater. In coastal aquifers, when seawater intrudes in coastal fresh water, cations starts to exchange between saline and fresh water, and the analysis of this exchange has been used to identify the process of salinization (Appelo & Postma, 2005). Sometimes, Cl versus tracer elements such as Cl/Br ratios can be used to understand the processes of intrusion within the mixing zone (Bear & Cheng, 2010). Presence of high amount of Cl an Br in groundwater is an indicator of the influence of seawater (Nair et al., 2015).

2.2.3.3. Ca/Mg, Ca/ (HCO_3+SO_4)

One of the most prominent features of seawater intrusion is commonly the enrichment of Ca over its concentration in seawater. High Ca/Mg and Ca/ (HCO_3+SO_4) ratios (>1) are indicators of the arrival of seawater intrusion (Bear et al., 1999).

2.2.3.4. Oxygen and Hydrogen Isotopes

Environmental isotope values can be used to describe the mixing process between saline water and freshwater in a similar way as the ion composition. In order to study the origin and dynamics of groundwater, the analysis of variations in the stable isotopes of Oxygen (δ^{18} O) and Hydrogen (δ^{2} H) has to be carried out. The distribution of these isotopes is used to investigate the source of various water and interconnection between them. The isotopic signatures of each water body differ from place to place and a high contrast between groundwater and seawater has been used to describe the seawater intrusion mechanism (Nair et al., 2015).

2.3. Numerical Methods for Groundwater Management

Groundwater modeling has become a very important process in managing groundwater resources. Over the past forty years, it was considered to be one of the primary tools, which was used to understand groundwater flow and seawater movement in coastal aquifer. Numerical models are based on mathematical models which derived from Darcy's law and the law of conservation of mass. The accuracy of model predictions is dependent on the reliability of the estimated model parameters and the accuracy of the boundary conditions (Todd & Mays, 1980).

Numerical models have been developed to solve the groundwater flow equations or groundwater flow in combination with solute transport by using Finite Difference Method (FDM) or Finite Element Method (FEM) or combination of these. However, it will be difficult to develop and solve groundwater flow and solute transport more than groundwater flow alone. In coastal aquifers, density of water and concentration of chemical can vary throughout the modeled area; this makes aquifer difficult to be simulated numerically. To simplify this problem two approaches have been used, the first is to assume that freshwater and saline water zones are immiscible and separated by sharp interface, while the second is to consider that freshwater and salt water are single fluid and have a spatially variable salt concentration that influences the fluid's density; this approach is the principle of density-dependent groundwater flow and solute-transport modeling. Several computer codes that have been developed by individual researchers are used for solving groundwater flow transport problems (Bear & Cheng, 2010).

2.3.1. Three-Dimensional Groundwater Model

Groundwater flow in three dimensions in a porous media of constant density for heterogeneous and anisotropic medium which is derived by combining a water balance equation with Darcy's law can be expressed by the following partial differential equation (PDE):

$$\frac{\partial}{\partial x}\left(K_{xx}\frac{\partial h}{\partial x}\right)+\frac{\partial}{\partial y}\left(K_{yy}\frac{\partial h}{\partial y}\right)+\frac{\partial}{\partial z}\left(K_{zz}\frac{\partial h}{\partial z}\right)+W=S_s\frac{\partial h}{\partial t} \qquad (2.1)$$

where K_{xx}, K_{yy}, and K_{zz} are the hydraulic conductivities along x, y, and z coordinate axes parallel to the major axes of hydraulic conductivity; h is the potentiometric head; W is local source or sink of water per unit volume; S_s is specific storage of the porous material; and t is the time. Under steady condition, Eq. (2.1) is equal to zero as continuity requires that the amount of water flowing in to a representative elemental volume is equal to the amount flowing out, this leads to Eq. (2.2)

$$\frac{\partial}{\partial x}\left(K_{xx}\frac{\partial h}{\partial x}\right)+\frac{\partial}{\partial y}\left(K_{yy}\frac{\partial h}{\partial y}\right)+\frac{\partial}{\partial z}\left(K_{zz}\frac{\partial h}{\partial z}\right)+W=0 \qquad (2.2)$$

Transient conditions are formulated by applying the law of conservation of mass over an elemental volume in the flow field in function of time. The solution of Eq. (2.1) requires deterministic models which can be further classified as analytical or numerical. Numerical models can be further classified as FDM and FEM. Generally, numerical modeling employs approximation methods to solve partial differential equation which describes the flow in porous medium. FDM is much easier in programing and application than FEM (Director, 2007; Todd & Mays, 1980).

2.3.2. Finite Difference Method (FDM)

One of the established solution techniques available for solving the governing equations of the model is FDM. It's an old method made more useful with the advent of high speed for digital computers (Magnus U, 2011). The FDM works by replacing the region over which the independent variables in the PDE are defined by a finite grid of points at which the dependent variable is approximated. The partial derivatives in the PDE at each grid point are approximately estimated from neighboring values (Causon & Mingham, 2010).

The application of FDM replaces the continuous system described by PDE with a finite set of discrete points in space and time. The continuous medium in FDM is replaced by a discrete set of points called nodes which are points within cells (grid) where the head is calculated and various hydrogeological parameters are assigned. According to that, a set of finite difference equations, one for each node is, thus, obtained. In order to solve a finite difference equation, one has to start with the initial

distribution of heads and compute heads at later time instants. This iterative process has been developed to solve the set of algebraic equations obtained through discretization of Eq. (2.1). To solve Eq. (2.1) the head '*h*' is a function of both space and time, which are discretized during discretization process. Time is discretized into stress period and time steps (Director, 2007).

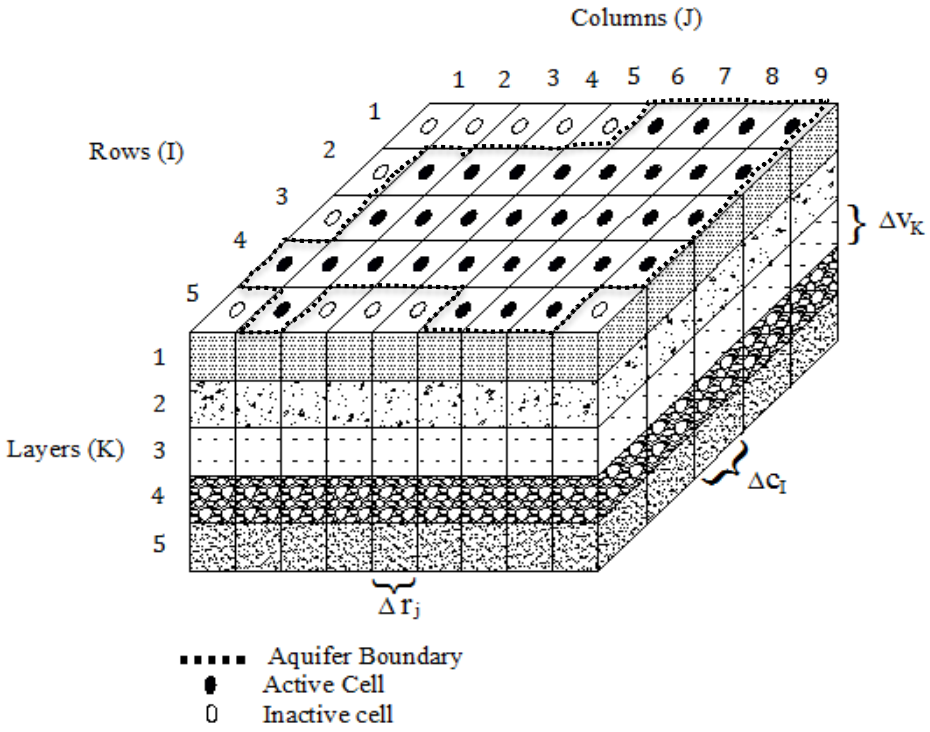

Figure 2.1. A discretized hypothetical aquifer system
(Source: McDonald & Harbaugh, 1988)

Figure 2.1 shows an aquifer system has been discretized into a mesh of blocks called cells, described by rows, columns, and layers. I, J, and K represent rows, columns, and layers respectively. The symbols Δr_j, ΔC_I, and ΔV_K represent dimensions of cells along the row, column, and vertical direction, respectively. Layers generally refer to horizontal geohydrologic units, so K denotes changes from along z-direction. Rows are considered parallel to the x axis and columns, are parallel to y axis. FDM is also used to solve the hydrodynamic dispersion part of the mass transport equation Eq. (2.3) as given below.

One of the main disadvantages of FDM is that it cannot represent the exact irregular boundary of the continuous medium.

2.3.3. Governing Equation for Solute Transport

Solute transport calculations have two component, molecular diffusion and advection. Surely, in real systems the situation is more complicated, particularly dispersion in porous media. One of the main reasons that makes transport in porous media difficult to model is that model must include at least two phases (solid and water or solid and air) (Logan, 2012). Advection and dispersion are the two processes that control flux into and out of elemental volume of porous media. Advection is the primary transport mechanism by which pollutant can be transported by the flowing groundwater (bulk groundwater flow), expressed by Darcy's law, while dispersion occurs when contaminated groundwater mixes with non-contaminated groundwater, resulting in a dilution of contaminate. The conservation of mass for solutes in porous media is considered to be the first step for derivation of solute (reactive or conservative) transport equations (Todd & Mays, 1980).

The transport of solute mass in groundwater can be described by the following partial differential equation (Zheng & Bennett, 2002):

$$\frac{\partial C}{\partial t} = \frac{\partial}{\partial x_i}\left(D_{IJ}\frac{\partial C}{\partial x_j}\right) - \frac{\partial}{\partial x_i}(v_i C) + \frac{q_s}{\theta}C_s + \sum_{k=1}^{N} R_k \qquad (2.3)$$

where C is the concentration of contaminates dissolved in groundwater, t is the time, x_i is the distances along the respective cartesian coordinate axis, D_{IJ} is the hydrodynamic dispersion coefficient along I and J direction, v_i is the seepage velocity, q_s is the volumetric flux of water per unit volume of aquifer, C_s is the concentration of sources or sinks, θ is the porosity, and R_k is the chemical reaction.

Form the right side of Eq. (2.3), the first term represents the change in concentration due to hydrodynamic dispersion, while the second term represents the effect of advection. The third and the last term represent source-sink and the chemical reaction, respectively. The advection phenomenon is due to groundwater flow velocity, which can be obtained from the solution of flow equation Eq. (2.1), so it is desirable to solve the flow balance before contaminant transport modeling begins.

2.3.4. Sharp Interface Model

More than 100 years ago, the relationship between groundwater levels and the depth of the saline water wedge was developed by two groups of researchers, working independently along the European coast (Badon Ghyben, 1889; Herzberg, 1901)[1]. This relationship is due to static conditions between two fluids with different densities. However, groundwater is not static and this relationship doesn't occur under field conditions. The relationship between fresh and saline water as shown in Figure 2.2 can be illustrated as following (Geta, 2003; Todd & Mays, 1980):

$$\rho_s g z = \rho_f g (z + h_f) \tag{2.4}$$

where ρ_s is the density of the saline water, ρ_f is the density of fresh water, g is the acceleration of gravity, and z is the depth of the fresh-saline interface below sea level and h_f is the elevation of the water table above sea level. Solving for z yield:

$$z = \frac{\rho_f}{\rho_s - \rho_f} h_f \tag{2.5}$$

For typical seawater conditions, the corresponding densities for the fresh water and salt water are $\rho_f = 1.000$ g/cm^3 and $\rho_s = 1.025$ g/cm^3 respectively, so that

$$z = 40\ h_f \tag{2.6}$$

When seawater is in a dynamic equilibrium or not, subsequent investigations have shown that Eq. (2.6) is a good first approximation to the extent of salt water wedge for nearly horizontal conditions (Director, 2007). However, the above equations have limitations. Ghyben-Herzberg relationship assumes hydrostatic conditions, and only applies when there is no vertical gradient in groundwater levels within the aquifer. It

[1] In 1889, the Dutchman Badon Ghyben, who did research for the public water supply in a dune area for the city of Amsterdam and in 1901, independently the German Herzberg developed the equilibrium equation for this phenomenon in groundwater (Geta, 2003).

has been recognized that the thickness of freshwater zone to be represented as a zero where the elevation of water table is zero. Actually, freshwater zone must have some thickness for freshwater to discharge to the sea (Barlow, 2003).

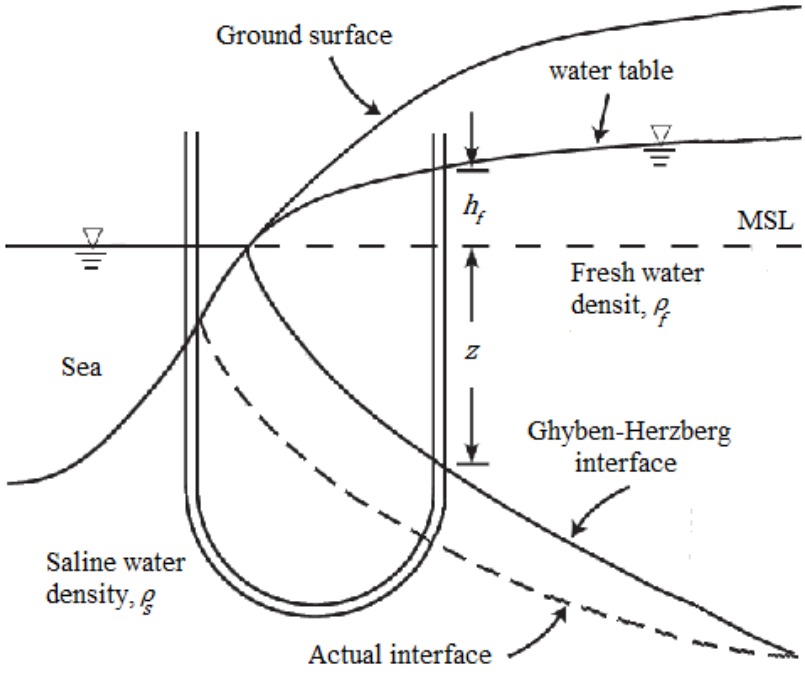

Figure 2.2. Location of the Ghyben-Herzberg and actual salt-fresh water interface (Source: Bear & Cheng, 2010)

The boundary between fresh and saline water as described above doesn't occur under field conditions. Actually, the two fluids are miscible and are separated by a zone with finite thickness, which is called transition zone (sometimes referred to as the zone of dispersion). The thickness of this zone depends upon the structure of the aquifer and some external influences which effects on the displacement of the interface such as, tidal, recharge and pumping of wells (Todd & Mays, 1980). The transition zone becomes wider and more diffused as the interface moves in response to the external influences mentioned before. The transition zone can be determined by measurement of chloride concentration of the water samples extracted from different depths at observation well. Figure 2.3 shows a transition zone in Biscayne aquifer near Miami, Florida, in which the numbered lines represent the concentration of chloride in mg/L, and the points represent the places from which water samples were taken (Barlow, 2003; Todd & Mays, 1980). In generally, the vertical thickness of the zone of transition

is much smaller than the horizontal (or lateral) thickness and is limited by the thickness of the aquifer.

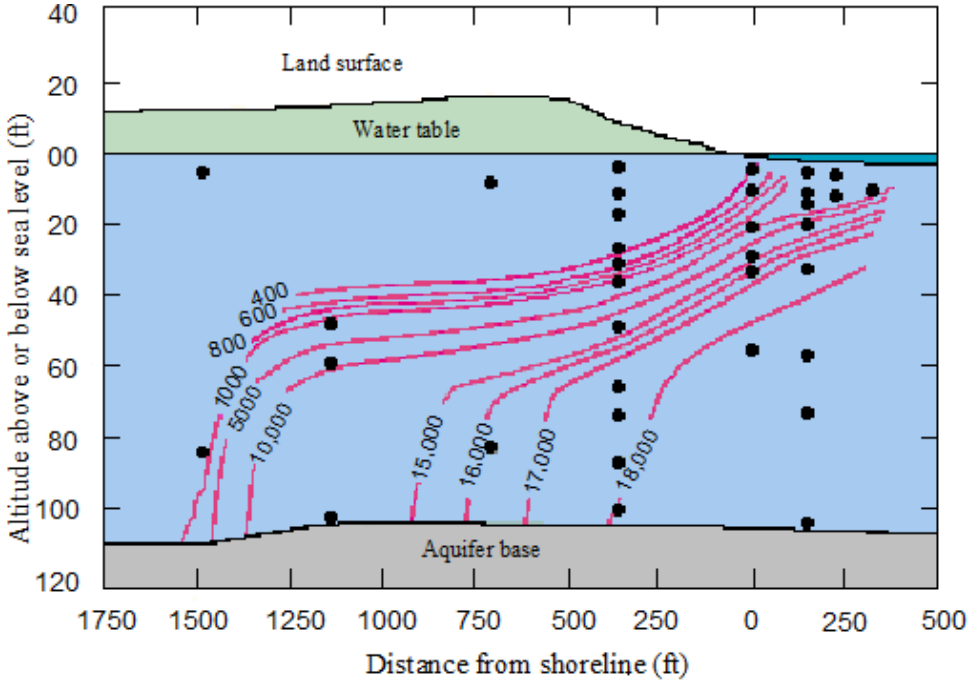

Figure 2.3. Cross section through the transition zone of the Biscayne aquifer (Source: Barlow, 2003)

2.3.5. Effect of Pumping on Seawater Intrusion

The water stored in the ground can be compared to money kept in a bank account. If the average amount of money withdrawn from the account was larger than the amount deposited then over the long term account-supply problems will appear. Similarly, pumping groundwater at a faster rate than it can be recharged can cause several problems over the long term such as depletion which is defined as long term water level declines. Drying up of wells, reduction of water streams and lakes, and salinization of water are considered to be some of the negative effects of groundwater depletion. Naturally, the boundary between salt-fresh water tends to be relative stable, but pumping can disturb this natural hydrodynamic balance, resulting saltwater occupation inland and upward. Strack (1976) developed a technique to evaluate the effect of wells on saline-fresh water interface. The equation using to determine the position of the toe of an interface under steady state conditions, can be illustrated as following:

$$\frac{(1+\delta)B^2}{2\delta} = \frac{Q'_\circ}{K}x + \frac{Q_w}{4\pi K}\ln\left[\frac{(x-x_w)^2+y^2}{(x+x_w)^2+y^2}\right] \tag{2.7}$$

$$\delta = \frac{\rho_f}{\rho_s - \rho_f} \tag{2.8}$$

where x_w is the distance of well from shoreline, B is the depth to bedrock below mean sea level, $Q'_\circ$ is the freshwater flow per unit length of shoreline, Q_w is the constant pumping rate, K is the hydraulic conductivity, and (x ,y) is the coordinates of the toe of the interface.

When Q_w increases, the toe of the interface starts to advance inland toward pumping well. As pumping rate continues to increase, the toe location forms a wedge and touches the low potential zone surrounding the well which is called the critical situation. In this situation, the calculated pumping rate is called critical pumping rate and it is denoted by Q_C. Figure 2.4 shows comparison between the locations of the toe of the seawater wedge corresponding to different pumping rates (Bear & Cheng, 2010).

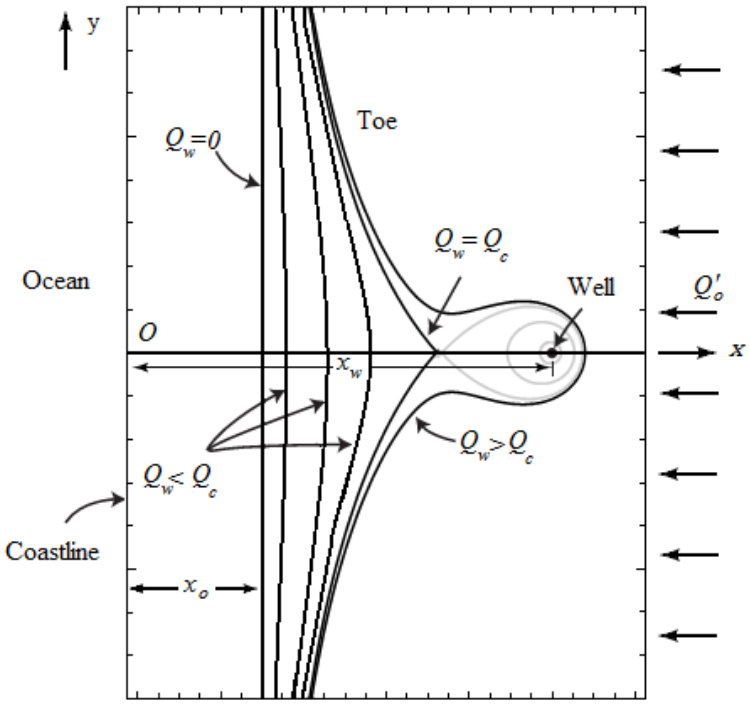

Figure 2.4. Locations of the toe corresponding to different pumping rate (Source: Bear & Cheng, 2010)

2.3.6. Upconing of Saline Water

Saltwater upconing is described as the local rise of salt-fresh water interface below the pumping well when it's operated. Pumping freshwater by a well located above the transition zone will produce upconing over the long term, resulting salinization of the pumped water. However, when pumping is stopped, the saline water tends to settle downward and return to its position due to the different in densities. Upconing is not a simple phenomenon, however in recent years, research studies have been done to formulate the design and the operation of wells for skimming fresh water from above saline water (Todd & Mays, 1980). The two mainly approaches used for modeling saltwater upconing are sharp interface and miscible displacement (variable density flow and transport). Several studies have been presented the analysis of saltwater upconing and decay beneath a pumping well, such as Reilly and Goodman (1987), and Zhou et al. (2005). From these studies it's important to determine the optimum location, depth, pumping rate and pumping sequence which provides the largest amount of freshwater with high quality in concentration (minimize mixing of fresh-saline water underground).

2.4. Conceptual Model

Developing a conceptual model is considered to be the first step in the modeling process. Furthermore, it is the most important step in groundwater model process. Conceptual model is a hydrogeologist's mental representation of the groundwater system. It should be presented based on geologic setting, hydrogeological parameters, and the three dimensional flow systems. Therefore, investigations are often undertaken, including field and laboratory work and analysis of available data. Conceptual model provides better understanding of the physical setting related to groundwater flow. Conceptual model usually includes items such as (Bear & Cheng, 2010):

- Geometry of boundary and the initial condition within the domain
- Dimensionality of the model (1, 2, or 3D)
- The behavior of the system: steady state or transient
- Types of the soil, distribution of the hydrogeologic layers, domain's stratigraphy, etc.

The conceptual model must be as much as representative of the real (natural) system as possible, because it will be the basis for developing the numerical model. An increased level of the effort in creating the conceptual model leads to better prediction and reduces the time for calibrating the numerical model.

2.5. Computer Codes for Groundwater Modeling

Once a numerical has been constructed, computer codes have been used to solve, or to find (approximate) solution of the PDEs of the groundwater flow and mass transport by using FDM or FEM. Computer codes have been developed by individual researchers, commercial entities, or by governmental agencies. United States Geological Survey (USGS) and U.S Environmental Protection Agency (USEPA) have the most codes that are accessible to the public for free. The following codes are the most used codes in groundwater modeling.

2.5.1. MODFLOW

Modular Finite-Difference Ground-Water Flow Model (MODFLOW) is a computer program can simulate one, two or three-dimensional groundwater flow using finite difference solution of the model. MODFLOW which is developed by McDonald and Harbaugh (1988) went through several revisions until it reached to the current version MODFLOW-2005 (Harbaugh, 2005). MODFLOW is considered to be the most used computer code because it's a public domain, open source code. It's used to simulate steady and nonsteady flow in an aquifer which its layer can be confined, unconfined, or a combination of them. MODFLOW is designed to simulate groundwater systems where saturated-flow conditions exist, Darcy's Law is applied, and the density of groundwater is constant. MODFLOW-2000 and any other version that came after it are divided into a serious of independent subroutines called modules. The modules are grouped into packages that deal with a single aspect of simulation. Depending on the problem individual packages may or may not be required, such as Well Package (WEL), Recharge Package (RCH), and General Head Package (GHB). Also MODFLOW includes solver packages used to solve groundwater flow equations,

such as Strongly Implicit Procedure (SIP), Successive Over Relaxation (SOR), and Preconditioned Conjugate Gradient (PCG).

Visual MODFLOW is the most common computer software used by hydrologists and researcher to simulate groundwater flow modeling. It supports MODFLOW, MT3D, MODPATH and SEAWAT codes.

2.5.2. MT3DMS

MT3DMS is three-dimensional groundwater contaminant and solute model used to simulate advection, dispersion, and chemical reaction of dissolved constituents in groundwater. The code was first released as Modular Three-dimensional Transport Model (MT3D) by the USEPA (Zheng, 1990) which is used to simulate changes in concentration of a single species miscible contaminants in groundwater. Later MT3D was extended and released by U.S Army Corps of Engineers (USACE), Engineering and Research Development Center (Zheng & Wang, 1999), as MT3DMS, in which 'MS' stands for multispecies transport. Its most current resale is version 5 (Zheng, 2006).

2.5.3. SEAWAT

SEAWAT is a computer code was developed to simulate three-dimensional variable-density groundwater flow. The original code was released by W Guo and Bennett (1998). SEAWAT combines MODFLOW and MT3DMS in to a single computer code for the purpose of simulating saltwater intrusion. For conventional MODFLOW-MT3DMS applications, total simulation time is divided into stress period. First, a complete solution is developed for heads in each stress period. Latter, MT3DMS divides stress period into transport steps, then calculates the concentration at each step. However, in SEAWAT stress period are divided into time steps, then both flow and transport equations are solved during a time steps. This means that MT3DMS runs for a time step, and then MODFLOW runs for the same time step using the last concentration from MT3DMS to calculate the density term in the flow equation.

SEAWAT includes both explicit and implicit methods for coupling the flow and solute transport equations. With explicit method, the fluid densities are calculated with

solute concentrations from the previous time step. With implicit methods, solutions to the flow and transport equations are repeated, and concentrations and densities are updated with each time step until the maximum difference in fluid density at a single cell for consecutive iterations is less than a user-specified value (Guo & Langevin, 2002). The SEAWAT has been tested with many applications (Bakker, 2003), (Bakker et al., 2004), (Langevin, 2003), (Dausman & Langevin, 2005), (Schneider & Kruse, 2006) and (Zimmermann et al., 2006).

2.6. Governing Equation for Variable-Density Groundwater Flow

The governing equation for variable-density groundwater flow in terms of freshwater head, which is solved by MODFLOW routines in SEAWAT code, is derived by Weixing Guo and Langevin (2002) as follows:

$$\begin{aligned}\frac{\partial}{\partial\alpha}\left\{\rho K_{f\alpha}\left[\frac{\partial h_f}{\partial\alpha}+\frac{\rho-\rho_f}{\rho_f}\frac{\partial Z}{\partial\alpha}\right]\right\}+\frac{\partial}{\partial\beta}\left\{\rho K_{f\beta}\left[\frac{\partial h_f}{\partial\beta}+\frac{\rho-\rho_f}{\rho_f}\frac{\partial Z}{\partial\beta}\right]\right\}\\ +\frac{\partial}{\partial\gamma}\left\{\rho K_{f\gamma}\left[\frac{\partial h_f}{\partial\gamma}+\frac{\rho-\rho_f}{\rho_f}\frac{\partial Z}{\partial\gamma}\right]\right\}\\ =\rho S_f\frac{\partial h_f}{\partial t}+\theta\frac{\partial\rho}{\partial C}\frac{\partial C}{\partial t}-\bar{\rho}q_s\end{aligned} \tag{2.9}$$

where α, β, γ are orthogonal coordinate axes, aligned with the principal directions of permeability; $K_{f\alpha}$, $K_{f\beta}$, $K_{f\gamma}$ are the hydraulic conductivities in three dimensional; h_f is the equivalent freshwater head; ρ_f is the density of freshwater; Z is the elevation above the datum of the center of a model cell; S_f is the equivalent freshwater specific storage; $\bar{\rho}$ is density of water entering from a source or leaving through sink; q_s is the volumetric flow rate of sources or sinks per unit volume of aquifer; C is the concentration of contaminates dissolved in groundwater; t is the time.

SEAWAT code utilizes MT3DMS routines to solve solute transport governing equation Eq. (2.3), which was mentioned before in Section 2.3.3. For a coupled variable density flow and solute-transport simulation, fluid density is assumed to be a function only of solute concentration (Langevin et al., 2003). A linear equation was used in this code, to convert solute concentration to fluid density.

$$\rho = \rho_f + \frac{\partial \rho}{\partial C} C \tag{2.10}$$

where $\frac{\partial \rho}{\partial C}$ is the slope of the equation which depends on the units used for the simulation; For example, if meters and kilograms are used for simulation, $\frac{\partial \rho}{\partial C}$ is a set of value of 0.7143, which approximately equals the change in fluid density divided by the change in solute concentration for freshwater and seawater.

2.7. Seawater Intrusion Modeling Studies

Qahman and Larabi (2006) developed a numerical assessment of seawater intrusion in Gaza, Palestine, by applying 3-D variable density groundwater flow model. The excessive pumping of groundwater from the water supply wells near to the coast is considered the main cause of seawater intrusion into the aquifer, to prevent the aquifer from the future intrusion a future decrease in groundwater withdraw is very important consideration. To simulate variable density effects on groundwater flow, the coupled flow and transport code SEAWAT was used. The model domain and finite deference grid used to simulate ground water flow within the Gaza coastal aquifer are consist of 115 row, and 35 columns with 4025 regular cells. The model covers an area of 365 km^2, and discretized vertically into 12 layers. The numerical model was calibrated and tested against both steady state and transient data. During calibration, observed and calculated heads (water levels) were compared. SEAWAT was applied to examine how far inland the seawater transition zone has moved since intrusion began. Simulation results indicate that the proposed schemes successfully simulate the intrusion mechanism. Two pumping schemes were designed by using calibrated model for calculation the future changes in the water level and quality of water in a period of another 17 years, to evaluate the impact on the aquifer for two future scenarios of pumping. The results show that seawater intrusion will exacerbate in the aquifer if the rate of pumping continue at the same rate. Alternative solutions were proposed to prevent the deterioration of the aquifer include, elimination of ground water pumping and encouraging the artificial recharger on the aquifer.

Sherif et al. (2012) presented the simulation of seawater intrusion in the coastal aquifer of Wadi Ham, United Arab Emirates, and the assessment of the effects of different scenarios of groundwater pumping. Pumping from Kalba and Fujairah coastal aquifer of UAE has increased during the last two decades to meet the agricultural and domestic demands. Due to lack of natural recharge from rainfall, groundwater levels have started to decline causing an intrusion of coastal aquifer of Wadi Ham. A number of field visits have been conducted in order to determine the locations of pumping and observation wells. A number of farms have been visited to evaluate the groundwater salinity on the soil and crop productivity. The hydrological and geological data have been collected from previous studies. The topography of the study was determined using the digital elevation model of SRTM. Groundwater is used to irrigate the cultivated areas along the Wadi and for domestic uses. In this study, seawater intrusion simulation is conducted in two-dimensional horizontal or vertical views. Initial head values were obtained through steady state simulation using available data of groundwater levels when the aquifer under the steady state condition. The developed model was calibrated against 5 years dataset, and verified against another 11years dataset. To simulate the salt concentration, after the model calibrated, MT3D was employed. Results showed that the salinity of water under the current pumping rate expected to exceed 10,000 mg/L, and showed that reducing of pumping from Kalba wells will help to reduce the seawater intrusion into the aquifer.

Gopinath et al. (2016) developed a numerical model to investigate the seawater intrusion in Nagapattinam coast aquifer of Tamilnadu, India. The significant economic development of the study area is agricultural and some industries like soap manufacturing and coir. Large amount of groundwater has been withdrawn in order to satisfy the water needs for the study area. A finite difference mesh has been used to discretize the study area, by dividing into 40 rows and 40 columns for a total of 7 layers. The aquifer thickness was determined using the log data for 32 locations. Model calibration has been attempted by considering two key parameters (recharge rates and hydraulic conductivity). The model has been calibrated for hydraulic head to 61 observation wells, and then the calculated model was simulated for 50 years using the same hydrological parameters to assess the extent of seawater intrusion due to the pumping in the study area. The simulations indicate that upconing phenomena founded

to be active along the coastal line of study area. Therefore, there was significant impact of groundwater on the aquifer around the pumping wells.

Lin et al., (2009) developed a numerical model of variable-density groundwater flow and miscible salt transport to investigate the extent of seawater intrusion in the Gulf coast aquifer Alabama, USA. The groundwater is the only source of freshwater for industrial, municipal and private uses. The input parameters to the model were determined from analysis of well logs, and pumping tests. In this area, excessive pumping of groundwater from the aquifer is considered as the most important factor to cause seawater intrusion, particularly in deep aquifer. However, coastal flooding of lowland areas as a result of tropical storms and hurricanes may increase the salinity of water in shallow aquifer. The model has been discretized to 61 columns and 51 rows with uniform grid spacing of 402.3 m in both directions. In the vertical direction, the model consists of 7 layers representing the hydrostratigraphy of the aquifer. The hydraulic conductivity maps were created using the hydraulic conductivity values determined by pumping tests. In this study SEAWAT code was used to simulate the seawater intrusion into coastal aquifer. Due to the scarcity of the observed chloride concentrations and continuously head data, the model was only calibrated against the observed heads at the end of simulation. The calibration was achieved through a trial-and-error approach by adjusting the values of two key parameters (hydraulic conductivity and recharge rates), until the hydraulic head values match the observed values to acceptable degree. During calibration, a total of 35 observed hydraulic head values were used. Prediction of the extent of seawater intrusion in coastal aquifer was carried out by running the calibrated model 40 years forwards with the same conditions. As the population continues to grow and the demand of groundwater increase, it can be expected the actual extent of seawater intrusion in the future may be increased more than the model prediction.

Cobaner et al. (2012) developed a model to investigate the current condition of salinization by examining seawater intrusion in the Silifke-Goksu Deltaic plain, Turkey, and to investigate the effects of pumping quantity on seawater intrusion. SEAWAT code was used to model the seawater intrusion mechanism of the study area along the Mediterranean coast of Turkey. A finite-difference mesh in SEAWAT was used to discretize the aquifer system. The study area was discretized into 42 rows, 38 columns

and 20 layers while the aquifer thickness extends to 600 m below sea level. The groundwater recharge consists of precipitation, flow from areas, seepage from drains and rivers, was estimated with the help of groundwater level data of the aquifer system. The model was calibrated using field measured data including static groundwater head, electrical conductivity, and chloride concentration values collected from 23 observation wells. The model successfully simulated saltwater intrusion in the aquifer by locating the saltwater-freshwater interface and determining the spatial and temporal distribution of the TDS concentration in the aquifer. The result of this study indicate that the groundwater flow and TDS transport of the study area is very sensitive to increases in groundwater pumpage. This model can be used to establish some management policies in groundwater extraction.

Kallioras et al. (2006) developed a conceptual model for the management of a coastal aquifer in northern Greece. The analysis of the groundwater level recordings and piezometric maps of the study area were presented in this study. During this study, 612 groundwater wells have been recorded between June 2001 and October 2005, while the groundwater samples were taken during the period 2003 to 2005. The sampling methods included physiochemical parameters such as temperature, EC and pH, while the rest analysis included geochemical analysis such as major ions. Spatial distribution of the hydrochmeical types of the groundwater samples was presented throughout the area of investigation. Also, chloride concentration profile during irrigation period was drawn. Additionally, this study provided the preparation of the results of chemical analysis of groundwater samples of the study area. Finally, it assessed the lack of groundwater resources management of the area by the local water authorities.

CHAPTER 3

METHODOLOGY

3.1. Description of Case Study

3.1.1. Location of Case Study

Karareis is located in the extreme western end of Karaburun Peninsula which is located about 100 km to the west of city of Izmir. The study area covers approximately an area of 2.34 km^2 between 26°24′46″- 26°26′22″ longitudes and 38°28′32″- 38°29′56″ latitudes. The location of Karareis is shown in Figure 3.1. The surface of the study area is characterized by a plain with normal regression and there is a seasonal stream divides the area to unequal two parts. The study area is surrounded by mountains from three sides and the fourth side is occupied by the sea. The land cover of study area includes agricultural fields, grassland, and settlement areas (summerhouses) which have been increasing rapidly since 1980. Topographic conditions and trade routes forced the people to build their settlements on the coastal line. The number of summerhouses in that region is estimated to be around 750 houses. For these houses the only source of freshwater is through groundwater. Due to this fact there are six legal pumping wells that function in order to supply the water needs for the summerhouses.

3.1.2. Climate

The climate in Karareis is typical Mediterranean climate with hot/dry summers and mild/rainy winters. The mean annual temperature of the peninsula ranges from 15°C to 20°C. As shown in Figure 3.2, the average daily maximum temperature ranges from 32°C to 20°C and minimum temperatures from 20°C to 8°C in the summer and winter, respectively.

Rainfall data of Karareis have been collected by Karaburun 18032 station. Figure 3.3 shows the total daily precipitation (mm) during the period 2012 to 2015. The annual rainfall varied from 1200 mm/yr to 1900 mm/yr in 2012 and 2013, respectively

and 450 mm/yr to 1200 mm/year in 2014 and 2015, respectively. Most of rainfall occurs in the period from November to March, and the rest of the year is being completely to semi dry.

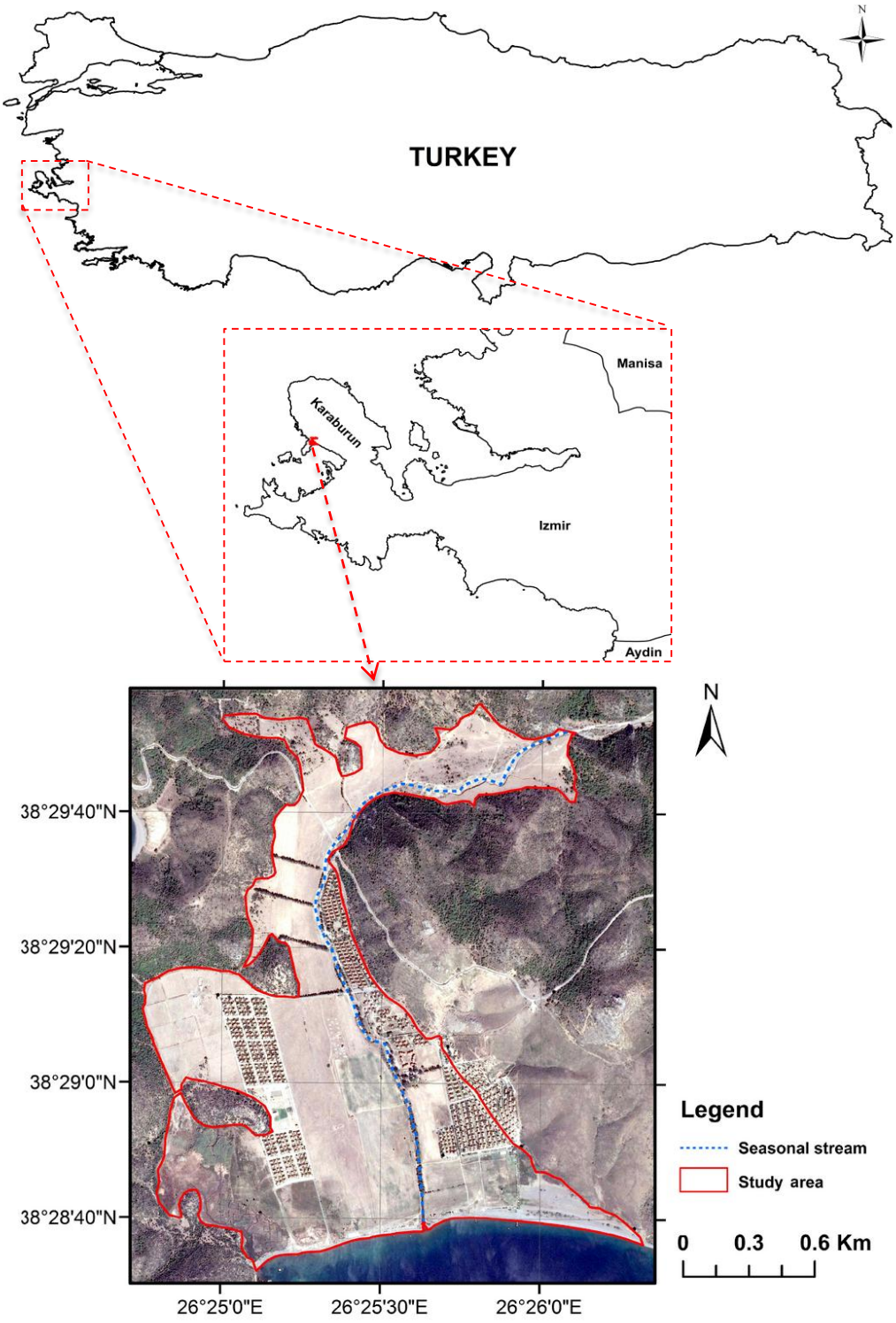

Figure 3.1. Location map of the study area (Karareis)

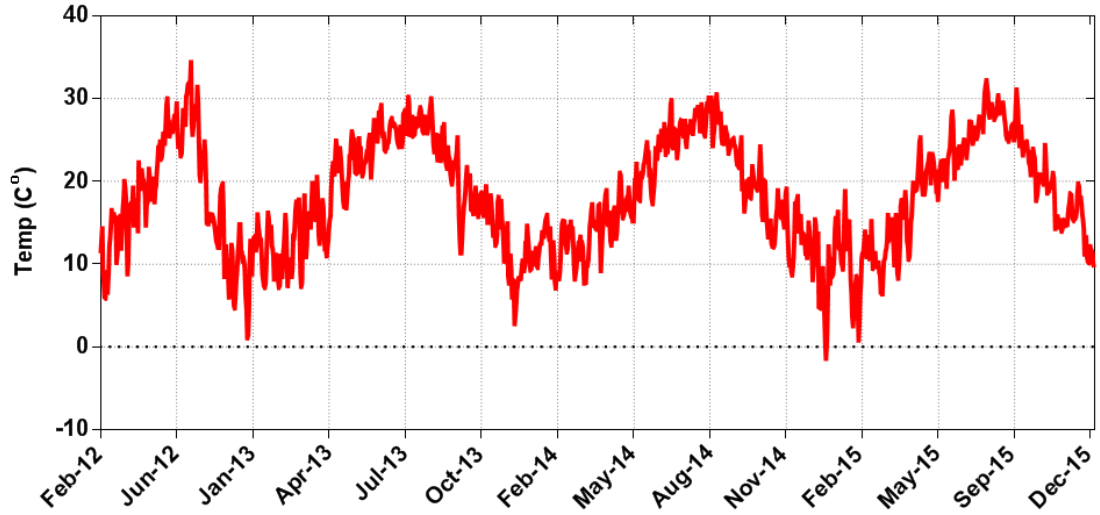

Figure 3.2. Typical daily temperature values for Karaburun Peninsula

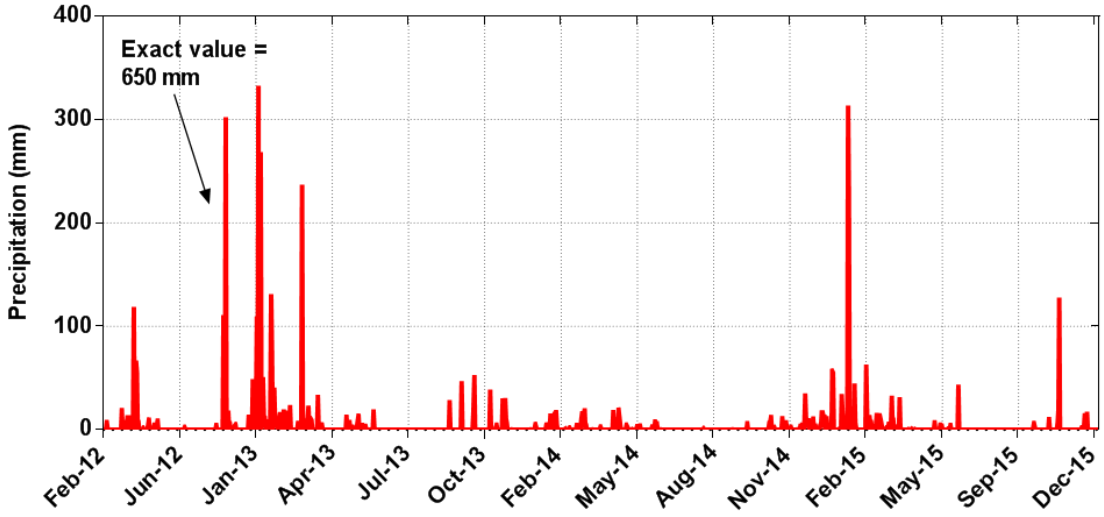

Figure 3.3. Daily precipitation values for Karaburun Peninsula

3.1.3. Topography

The topography of study area was determined using the digital elevation model of SRTM (Jarvis et al., 2008). The land surface elevation of the study area ranges from mean sea level (MSL) to about 40 m above mean sea level. Figure 3.4 shows the distribution of ground surface elevations of Karareis region, the three-dimensional view was drawn using Visual MODFLOW.

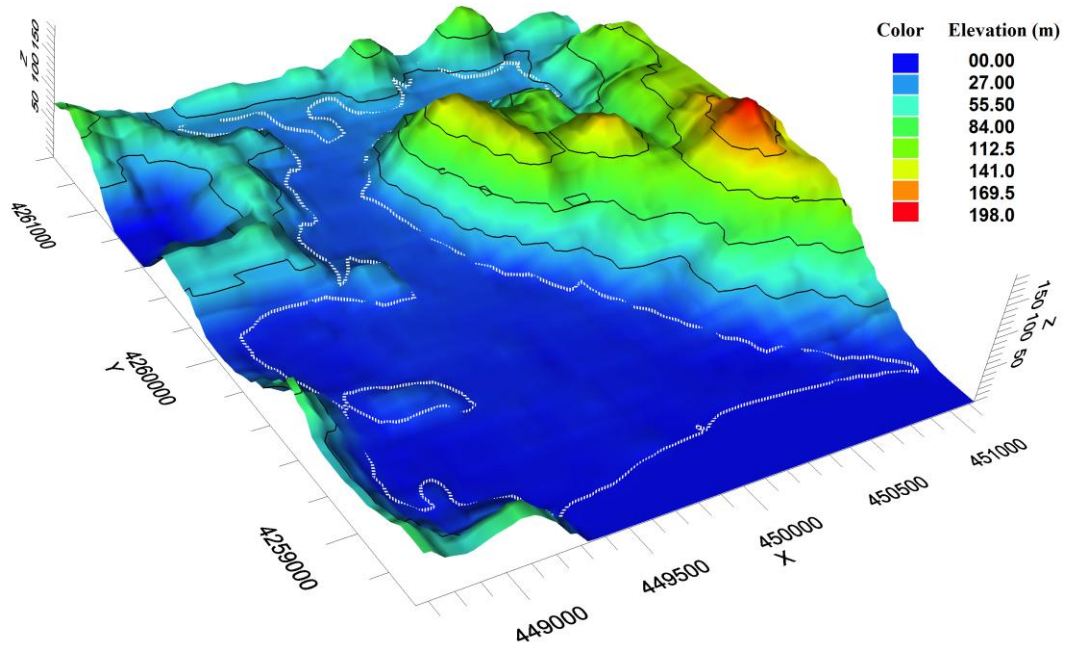

Figure 3.4. Three-Dimensional view of topographical map for Karareis region

3.2. Subsurface Investigation of Karareis Aquifer

Subsurface investigation can obtain many needed information about the aquifer of Karareis, such as location, thickness, permeability and yield. In addition, these investigations can obtain the groundwater characteristics such as flow direction, movement and quality. Subsurface investigation is considered to be the first step for detection of seawater intrusion in coastal aquifers. Also, it includes many applications, such as geologic log, water level measurement, and subsurface hydrogeological parameters.

3.2.1. Geology and Drilling

The basement rock of study are is the Early–Middle Carboniferous Alandere Formation, which consists of marine limestone (Erdogan, 1990). The unit is unconformably overlain by Triassic-Jurassic rocks of Karaburun Platform Carbonates and Upper Cretaceous to Paleocene rocks of Bornova Flysch Zone. The flysch-type metasediments crop out around the Karareis site. These metasediments are subdivided into a sequence of weakly deformed brown and grey phyllites, and a pack of highly

deformed dark sericitic meta-pelites. Generally, these units consist of mudstone, sandstone, pebble and limestone around Karareis region. These units are not permeable and have not any wells around Karareis. It is unconformably overlain by costal alluvium aquifer.

Nine locations (SK-1 to SK-9) were selected within the study area for the installation of new monitoring wells (Figure 3.5). Also, they were used to determine the main geological characteristics which compose the aquifer system. The depth of monitoring wells was approximately 50 m. The geological map of Karareis shows that there are geological fault pass near to SK-7 (Figure 3.5).

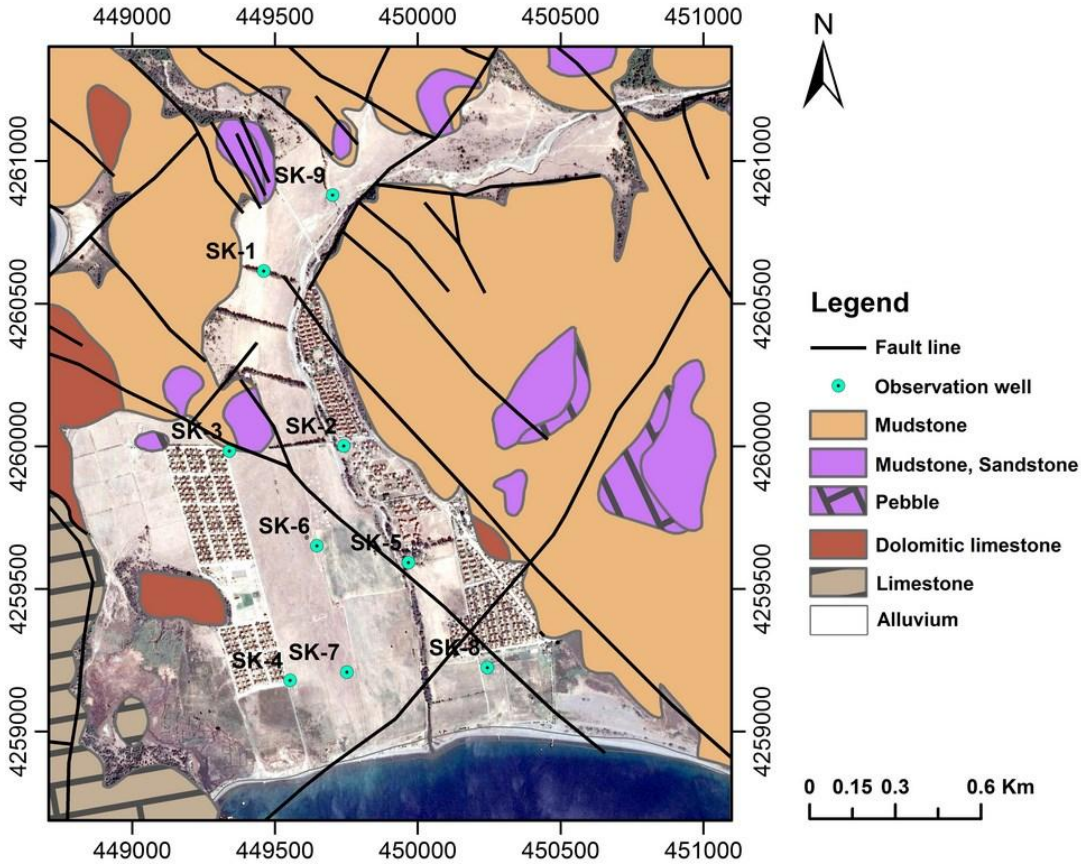

Figure 3.5. Geological map of Karareis region and locations of monitoring wells

3.2.2. Groundwater Level and Salinity Monitoring

Groundwater level (water table of an unconfined aquifer or the piezometric surface of a confined aquifer) is affected by several factors, such as recharge from

rainfall, or discharge by pumping wells. When recharge is less than the discharge, the water level will fall, and vice versa.

In the study area the groundwater level measurements were carried out using two methods. For SK-1, SK-2, SK-3, SK-4, SK-7 and SK-8 automatic groundwater data loggers have been used, and the remaining wells (SK-5, SK-6 and SK-9) manual groundwater level meter was used. The automatic data loggers take one record each hour for electrical conductivity, water level and temperature then store them in its memory. Later, the stored data can be downloaded from the loggers using computer software. In the study area, three types of data loggers were used in order to record the fluctuation of groundwater physical parameters for the period July 2014-July 2015. Baro-Diver which was used to compensate for variations in the atmospheric pressure was placed in SK-6. In SK-7 Corrosion Proof Multi-Parameter Groundwater Data logger (CTD-Diver) which measures the electrical conductivity, temperature, and water level was used, and in the remaining wells (SK-1, SK-2, SK-3, SK-4 and SK-8), Mini-Divers for measurement of temperature and water level were used. Beside that for communications with the divers, USB Reading Unit was used for reading or downloading the stored data (Figure 3.6).

Figure 3.6. Examples of groundwater level measurement instruments. (A) Manual meter. (B) USB Reading Unit. (C) Different types of data loggers. (D) Multi Parameter Meter

Under natural conditions, groundwater flow in the study area is towards the Aegean Sea, where it discharges to the sea. By establishing a number of observation wells spreading over the study area, the fluctuation in groundwater level and electrical conductivity were monitored every hour for two years.

For electrical conductivity measurements of this study, two different methods were conducted. As mentioned before, automatic CTD-diver was used in order to record the variations of electrical conductivity during the study period. For the remaining wells, the electrical conductivity was measured using manual meter (HQ40d Portable pH, Conductivity, Dissolved Oxygen, Multi-Parameter Meter) (Figure 3.6). Electrical conductivity can be considered as a crude indicator of water quality for many purposes, since it is related to the sum of all ionized solutes or TDS content. The relationship between conductivity and TDS is not directly linear; however as a rough approximation, the relationship between electrical conductivity and TDS commonly used is (Chang et al., 1983; Walton, 1989):

$$TDS\left(\frac{mg}{l}\right) = EC\left(\frac{\mu S}{cm}\right) \times 0.67 \qquad (3.\ 1)$$

During the field work, groundwater samples were collected from the observation wells within the study area in September 2014, April 2015 and September 2015. The samples were analyzed for chloride to establish an understanding of the intrusion in the aquifer.

3.2.3. Porosity and Specific Yield

The porosity and the specific yield of the unconsolidated geologic materials can be determined by the distribution of their sizes. In order to determine the materials size distribution, soil samples were collected at different depths from the geological logs located in the study area, then evaluated by using sieve analysis test which was conducted in geotechnical laboratory.

3.2.4. Determination of Hydraulic Conductivity

In the practical work, the hydraulic conductivity tests are employed. The hydraulic conductivity can be determined by a variety of methods, including tracer test, pumping test of wells, and laboratory methods.

3.2.4.1. Tracer Test

The hydraulic conductivity of the aquifer was determined by conducting tracer test. Sodium fluorescein was used as a tracer due to the ease of detection, for not being expensive, and for being safe to the environment. Figure 3.7 shows the cross section of a portion of an aquifer with groundwater flowing from SK-2 toward (OBS.Well).

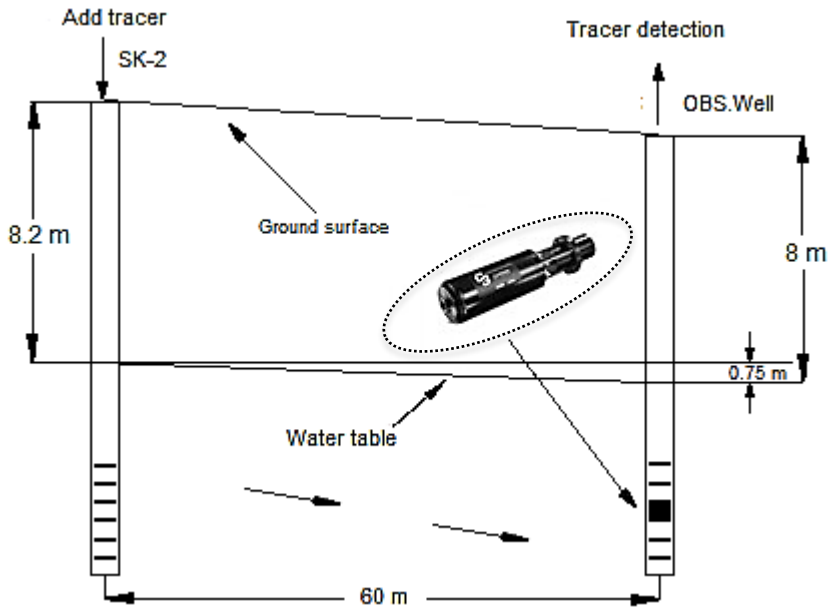

Figure 3.7. Cross section of the aquifer illustrating tracer test for determining hydraulic conductivity

To compute the hydraulic conductivity K of the aquifer, the average interstitial velocity v_a is giving by:

$$v_a = \frac{K}{\alpha}\frac{h}{L} \qquad (3.\ 2)$$

where h is the difference in water level; L is the distance between the two observation wells; α is the porosity. v_a is also determined by:

$$v_a = \frac{L}{t} \tag{3. 3}$$

where t is the travel time of the tracer between the two observation wells. Substitution of Eq. (3.2) into Eq. (3.3) gives

$$K = \frac{\alpha}{h}\frac{L^2}{t} \tag{3. 4}$$

3.2.4.2. Pumping Test

Pumping test of well is considered to be the most reliable method for determination the aquifer hydraulic conductivity. The test is conducted by pumping water from each well at a constant rate equal to 4 L/s, and then the drawdown was recorded in the well using groundwater data loggers. Cooper-Jacob method was used to calculated the hydraulic conductivity and the transmissivity (Cooper & Jacob, 1946).

3.2.4.3. Laboratory Tests

The hydraulic conductivity for the samples collected from the study area was determined by a constant head permeameter. Water enters the cylinder of the devise from the bottom and is collected as overflow after passing upward through the soil sample. From Darcy's law the hydraulic conductivity can be determined from (Todd & Mays, 1980):

$$K = \frac{VL}{Ath} \tag{3. 5}$$

where V is the flow volume in time t, and the other dimensions, A, L and h is the dimensions of the sample in the permeameter cylinder (Figure 3.8). The test was

conducted for soil samples taken from different depths, and then equivalent hydraulic conductivity was calculated.

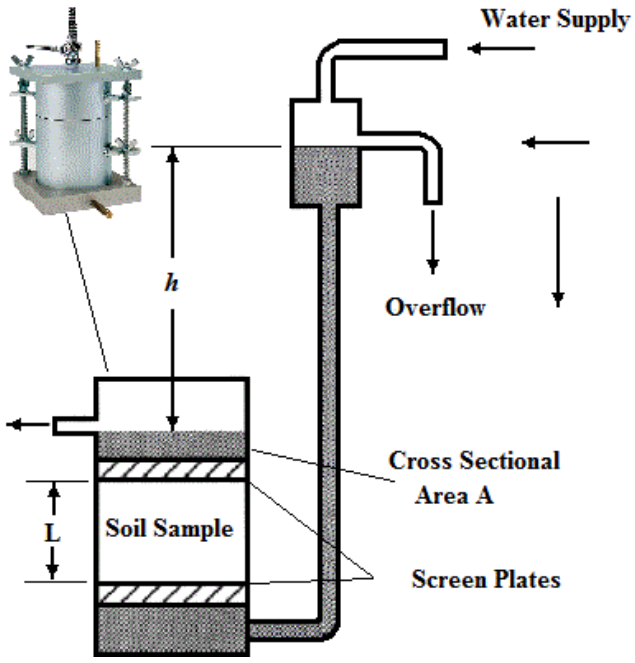

Figure 3.8. Constant head permeameter for measuring hydraulic conductivity

3.3. Seawater Intrusion Modeling Using SEAWAT

SEAWAT code was chosen for the simulation of the seawater intrusion in the coastal aquifer of Karareis for many reasons:

- SEAWAT is based on the approach of variable density groundwater flow. For Karareis aquifer the thickness of transition zone is not negligible.
- SEAWAT is compatible with MODFLOW and MT3DMS that are very famous and good tools for simulation the groundwater flow in combination with solute transport.
- SEAWAT code was tested by simulating five benchmark problems involving variable-density groundwater flow, including the Elder problem (Guo & Langevin, 2002)
- Users of MODFLOW and MT3DMS can easily apply SEAWAT to variable-density groundwater flow model

Using of computer model does not always minimize the need for sample data, boring, wells, etc. In fact more data may be required to adequately calibrate the model to fit existing site conditions. In this study groundwater flow and transport model will be developed in order to simulate seawater intrusion into fresh water aquifer.

3.3.1. Preparation of MODFLOW Input Packages for SEAWAT

The MODFLOW input packages for SEAWAT are:

- Basic (BAS) package which is used to specify the locations of active, inactive and specified head.
- Output Control (OC) option which is used to control the results that are saved from the flow portion of the variable-density simulation.
- Well (WEL) package which is used to simulate a specified flux to individual cells.
- Recharge (RCH) package which is used to simulate a specified flux distributed over the top of the model. It can be positive or negative. If a positive value is specified, it means the fluid is recharging to the model. If a negative value is specified, fluid is withdrawn from the model.
- Time varying constant head (CHD) package which is required to simulate specified head boundaries that can change with or between stress periods.
- Solver (SIP, SOR, and PCG) packages, one of the three solver packages can be implemented to solve the variable-density groundwater flow model equations.

CHAPTER 4

RESULTS AND DISCUSSION

4.1. Groundwater Model Development

A general flow chart of the modeling process of study area is given in the schematic block diagram (Figure 4.1). Visual MODFLOW software version 2011.1 Pro and Visual MODFLOW Flex version 2014.1 were used for modeling purpose.

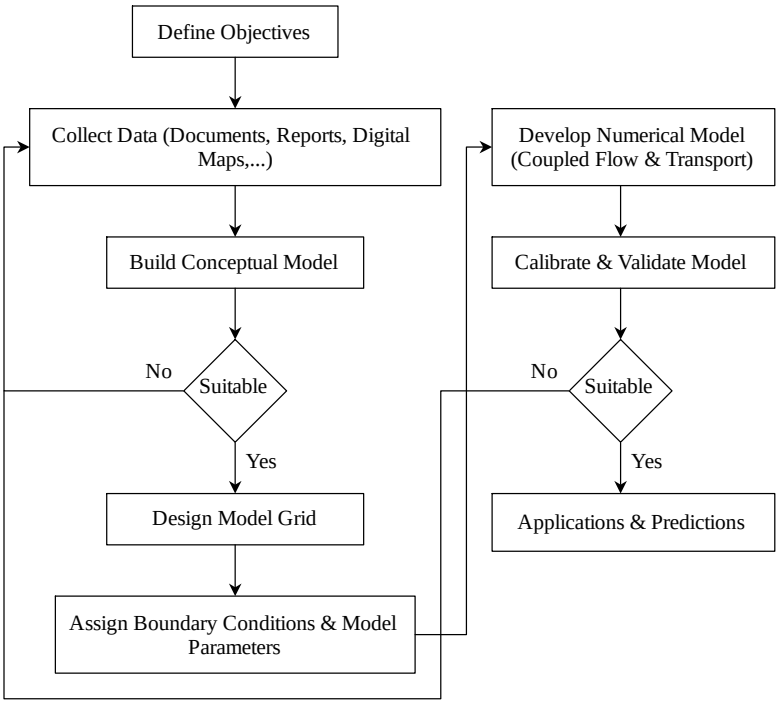

Figure 4.1. The modeling procedure of Karareis aquifer

4.1.1. Conceptual Model

4.1.1.1. Base Map

A georeferenced map was used to gain a perspective of the dimension of the model. Also, it used for locating the important characteristics of the model such as, boundary condition. The map was georeferenced before by using Arc Map version

10.2.2 with UTM Zone 35N (WGS84) coordinate system. In MODFLOW base map does not contain any specific data used in the numerical calculations, and does not have any effect to the results of simulation. Figure 4.2 shows GIS-based 3D base map for the study area.

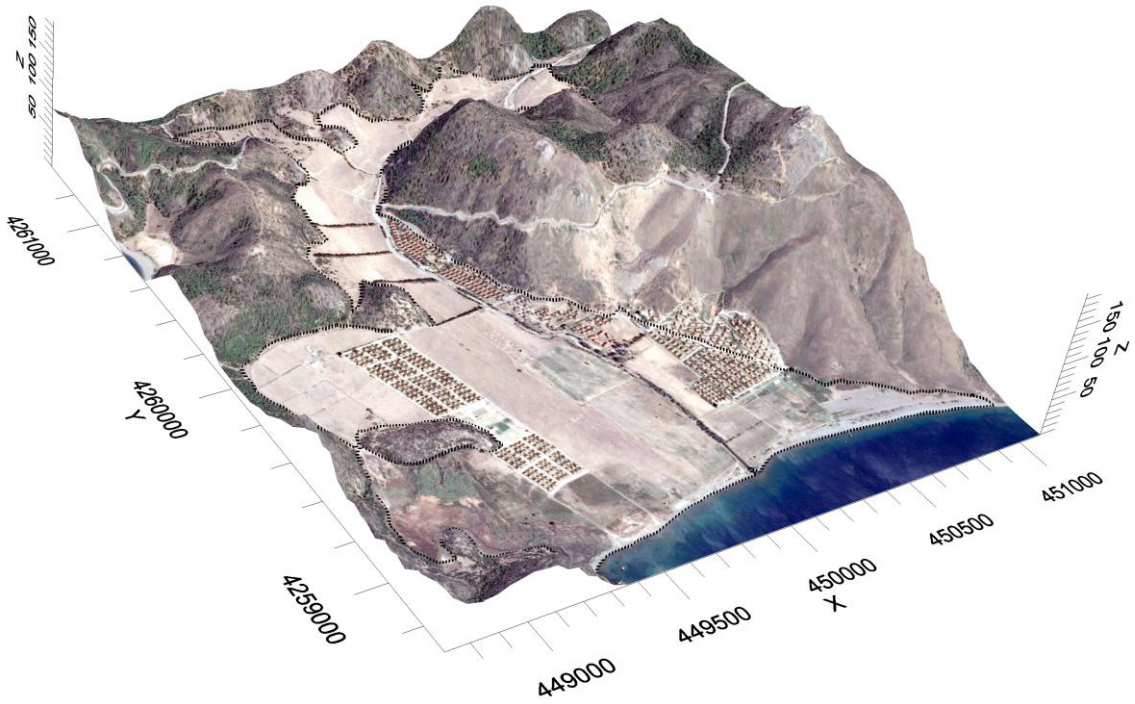

Figure 4.2. GIS-based 3D base map for Karareis region

4.1.1.2. Model Structure

The alluvial materials were found to be in the first forty meters. Alluvial deposits extend to maximum depth of 52 m below land surface. The thickness of the aquifer decreases with the increase of the distance from the shoreline. The alluvium mainly consists of mixture of gravel, sand and sandy gravel, while the aquifer base is composed of flysch which is a type of sedimentary rocks. The flysch has a small permeability value which considered to be around the average of 4.6×10^{-7} m/sec (Marinos et al., 2011) compared with the permeability in the first forty meters (Figure 4.3).

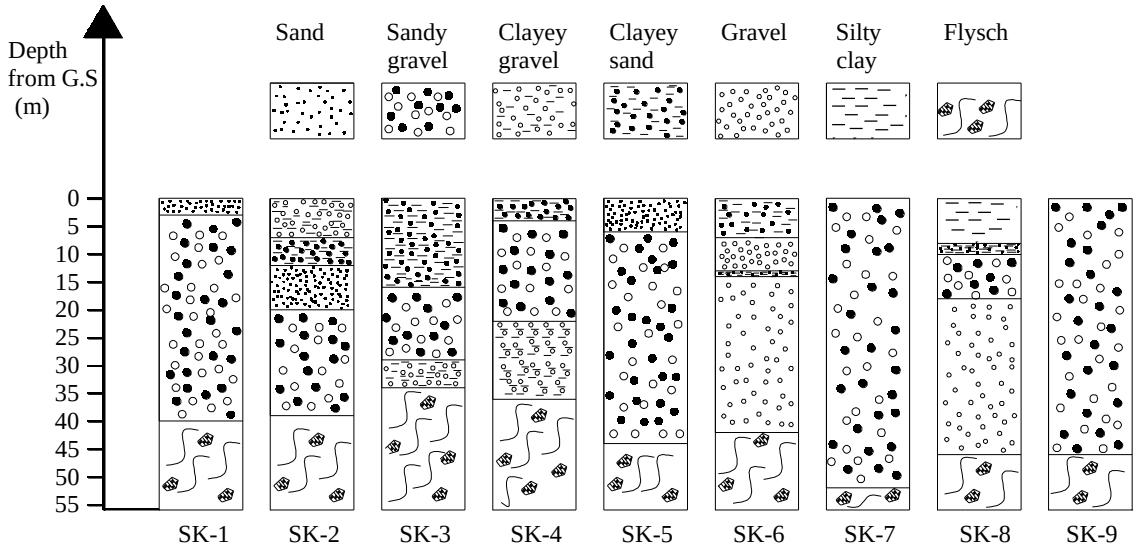

Figure 4.3. Geological log for the wells in unconsolidated alluvial aquifer

The model domain includes the alluvial region and comprises an area of 2.34 km^2. The information of existing boreholes were used to construct the conceptual model of that region. For model structure one layer is considered along the entire stretch of the study area. The aquifer thickness was determined by geophysical investigations of the log data for nine locations which is mentioned in Section 3.2.1. The actual elevations of the ground surface was provided by using the topographical map of the study area (Figure 3.4). This layer was underlined by the consolidated materials of flysch. Based on the available geological information, the base of the aquifer was built by an interpolation of the depths of the alluvium material. Figure 4.4 shows the surface of the aquifer base for Karareis region.

In MODFLOW Flex, horizons which are 2-dimentional surfaces with topography can be created by clipping or extending interpolated surface to the boundary of the conceptual model (Figure 4.5). When horizons are created, the geologic formation (Structural Zone) of the aquifer can be generated, which can be used later to define the hydrogeological parameters (Figure 4.6).

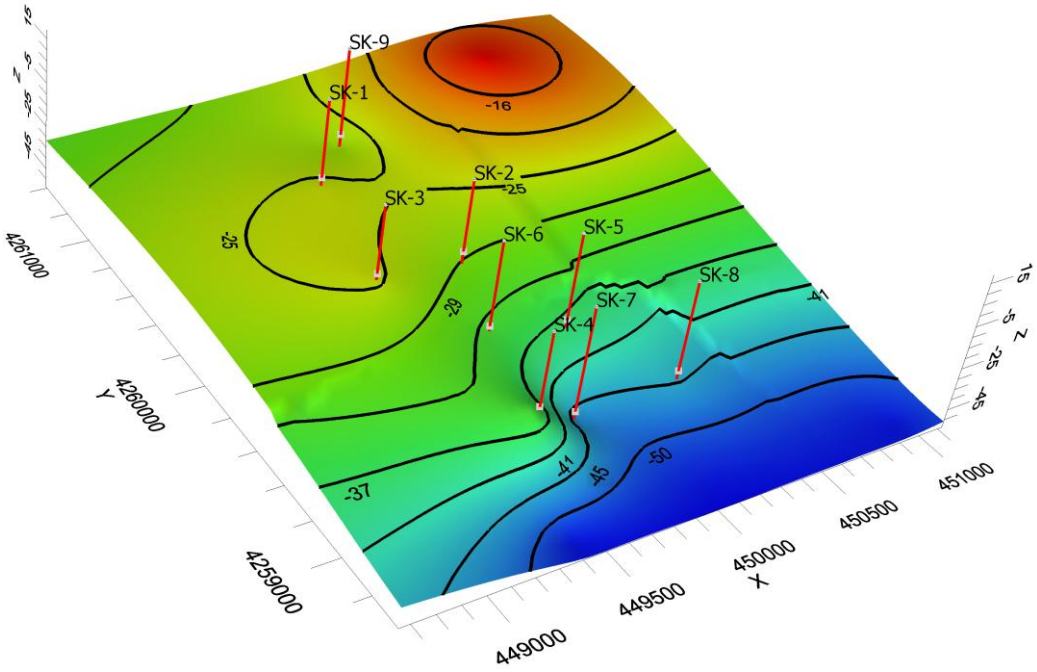

Figure 4.4. Surface of the aquifer base prepared by Kriging interpolation

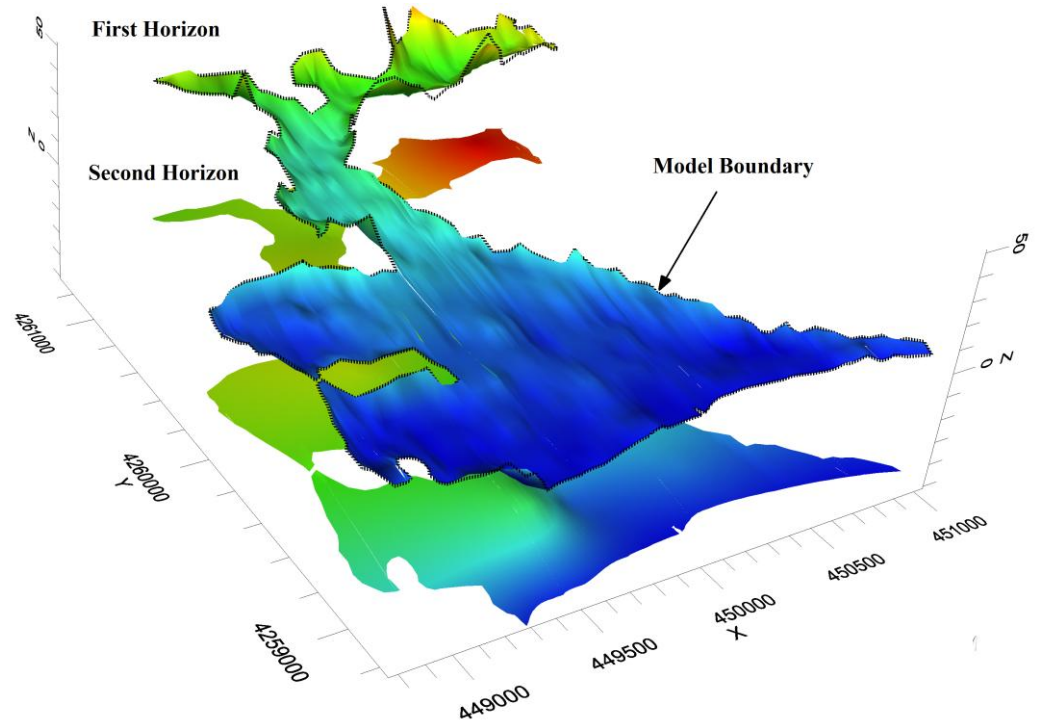

Figure 4.5. Aquifer surface and base horizons

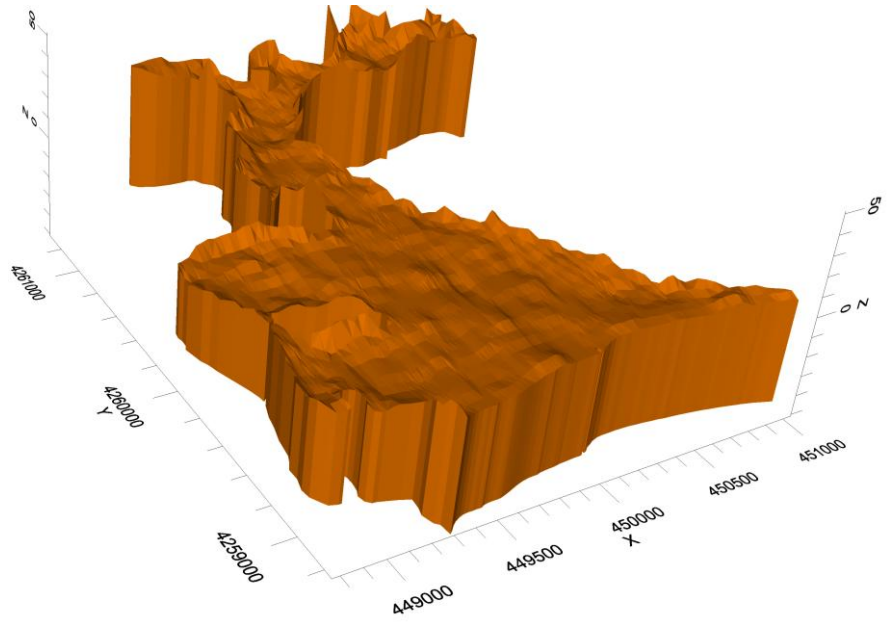

Figure 4.6. 3D view of the aquifer geologic structure as drawn by VMODFLOW

4.1.2. Groundwater level and Salinity

An overall view of the groundwater fluctuation shows that the groundwater level reached its lowest point in the end of July of 2014, and it was stable at that point until mid of December of 2014. After that, infiltration of rainfall caused a rise in groundwater level between December 2014 and April 2015. A peak in groundwater level was monitored in the mid of March 2015. Figure 4.7 to Figure 4.12 show the fluctuation of groundwater levels of the aquifer for the period from July-2014 to October 2015.

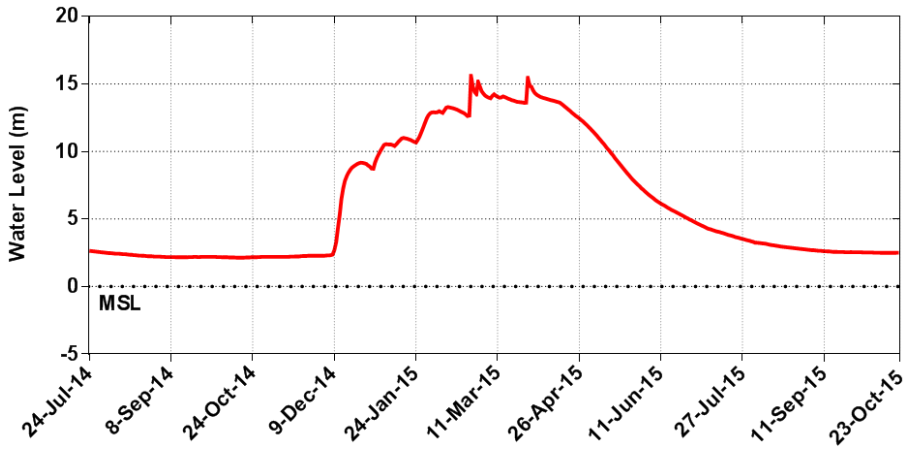

Figure 4.7. Fluctuation of groundwater level measured in SK-1

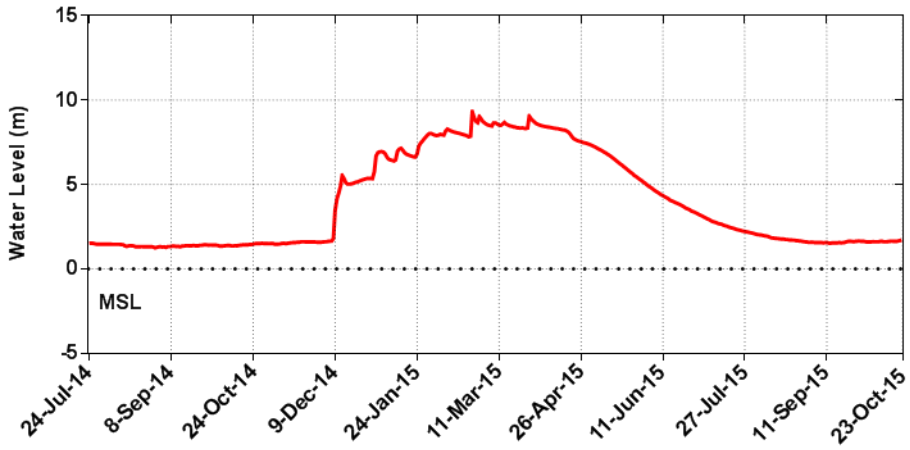

Figure 4.8. Fluctuation of groundwater level measured in SK-2

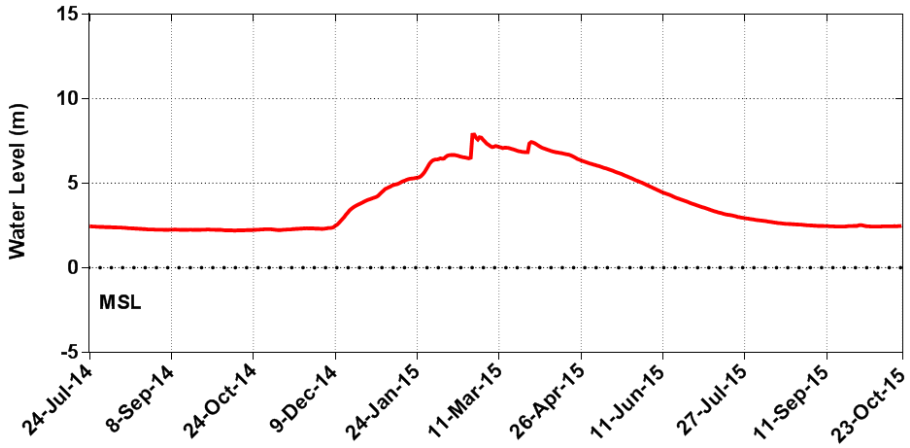

Figure 4.9. Fluctuation of groundwater level measured in SK-3

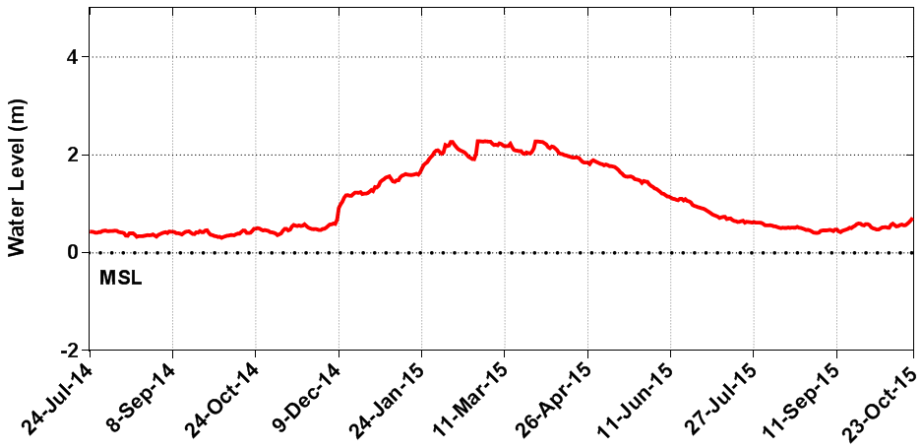

Figure 4.10. Fluctuation of groundwater level measured in SK-4

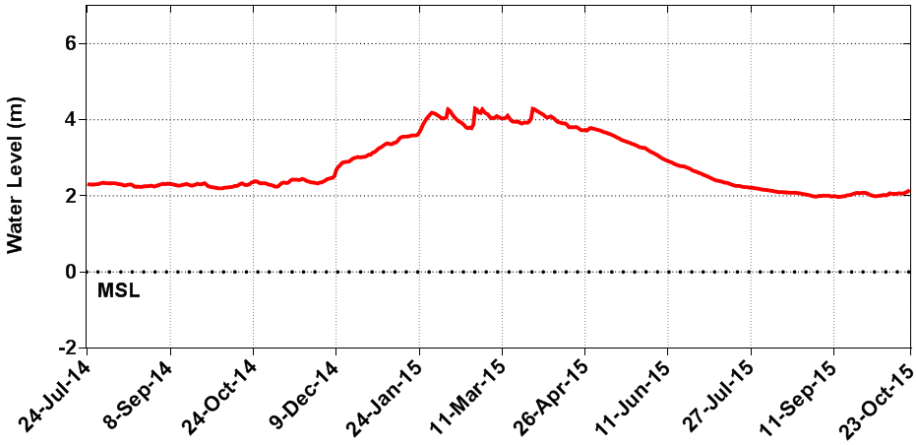

Figure 4.11. Fluctuation of groundwater level measured in SK-7

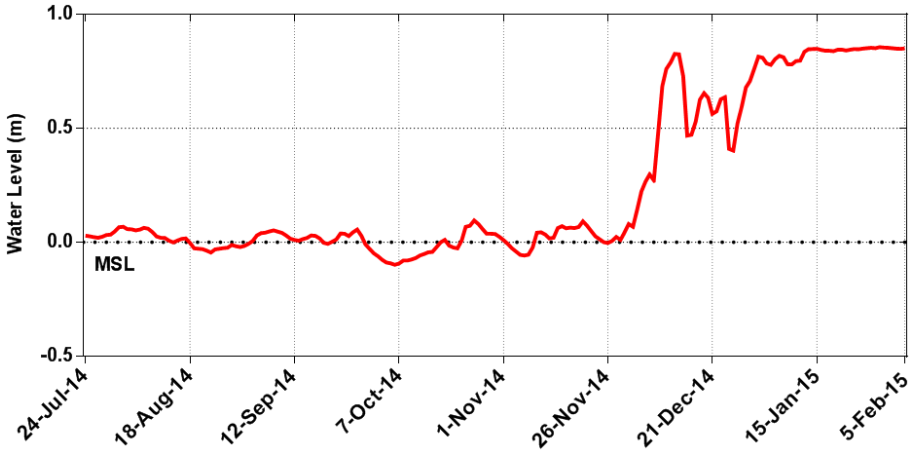

Figure 4.12. Fluctuation of groundwater level measured in SK-8

For the remaining wells (SK-5, SK-6 and SK-9) water level was measured using manual meter for six times at that period. The date and the water level values are listed in Table 4.1. While, Table 4.2 listed the average heads were calculated for the period (2014-2015) and (2015-2016) in order to use it for model calibration and validation. However, the average head of (SK-5, SK-6 and SK-9) was calculated by estimation using the values of the other observation wells.

Table 4.1. Groundwater levels (m) for the period July 2014-February 2015

	Observation well		
Date	SK-5	SK-6	SK-9
7/23/2014	1.52	1.67	6.15
8/22/2014	1.31	1.550	5.730
9/18/2014	1.26	1.650	5.640
6/12/2015	3.02	2.480	8.300
9/02/2015	1.18	1.070	5.740
2/11/2016	4.05	3.63	14.49

Table 4.2. Average groundwater levels (m) for the period (2014-2015) and (2015-2016)

Target well	Screen depth (m)	Average head (2014-2015)	Average head (2015-2016)
SK-1	40	7.15	7.79
SK-2	39	4.53	3.65
SK-3	34	4.22	3.69
SK-4	36	1.15	0.98
SK-5	44	2.62	2.73
SK-6	42	2.35	2.49
SK-7	52	2.25	2.52
SK-8	46	0.25	0.63
SK-9	46	8.23	10.19

As it is known that the electrical conductivity measurement provides a good indication for the salinity. Table 4.3 shows a typical electrical conductivity values obtained during the study period by using a portable meter. Figure 4.13 shows that there is an evident relationship between the electrical conductivity and the amount of precipitation. The change in the electrical conductivity of the water mainly depends on the amount of recharged water due to rainfall, which can be indicated by the change in water level. The electrical conductivity reached the highest level in the driest (summer) period after which it starts falling to reach the lowest peak during the storm period.

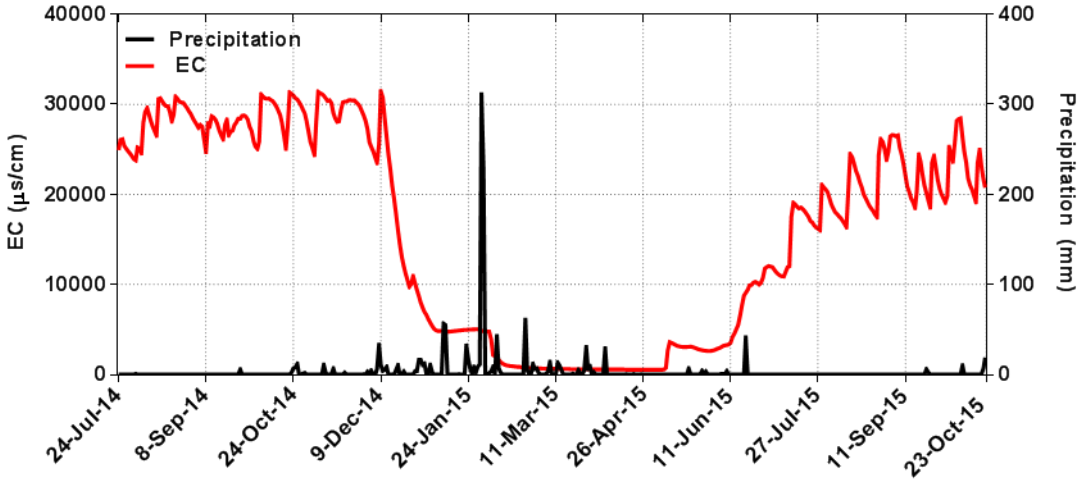

Figure 4.13. Variations in electrical conductivity of groundwater measured in SK-7 and daily precipitation recorded by Karaburun St.

Table 4.3. Typical EC values (µs/cm) obtained by using portable meter

	Observation well								
Date	SK-1	SK-2	SK-3	SK-4	SK-5	SK-6	SK-7	SK-8	SK-9
7/23/2014	704	485	1251	605	1549	750	7148	856	1513
8/22/2014	1757	1222	3122	1485	3797	1812	16060	2440	3690
9/18/2014	581	420	2268	608	1382	2645	1315	865	2408
4/16/2015	618	481	877	554	1730	579	626	932	453
6/12/2015	1752	750	974	612	1231	662	5711	1045	997
9/02/2015	1797	592	952	605	1009	610	20765	1201	932

Based on the observations between July-2014 and September-2015 except SK-7, the electrical conductivity varied from 420 to 3797 µs/cm (Figure 4.14, 4.15). The electrical conductivity reached the highest level in August 2014 then it started to fall progressively to reach the lowest level in April 2015.

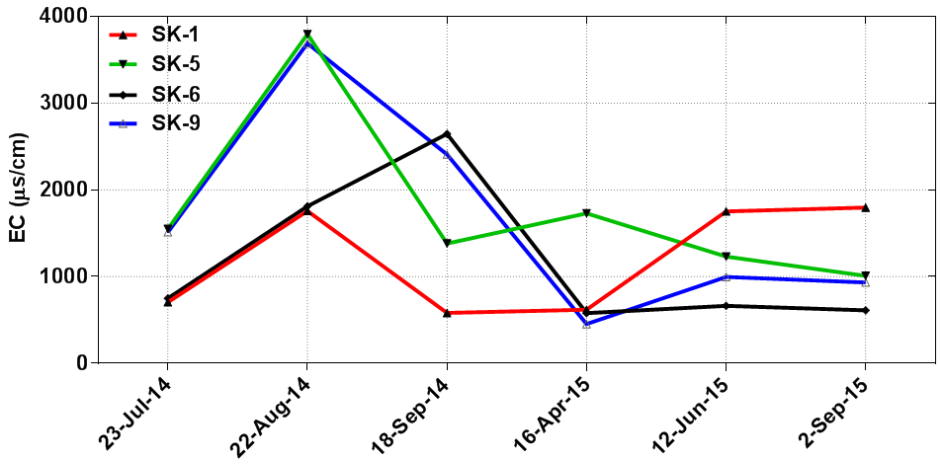

Figure 4.14. Variations in electrical conductivity of groundwater measured in SK-1, SK-5, SK-6 and SK-9

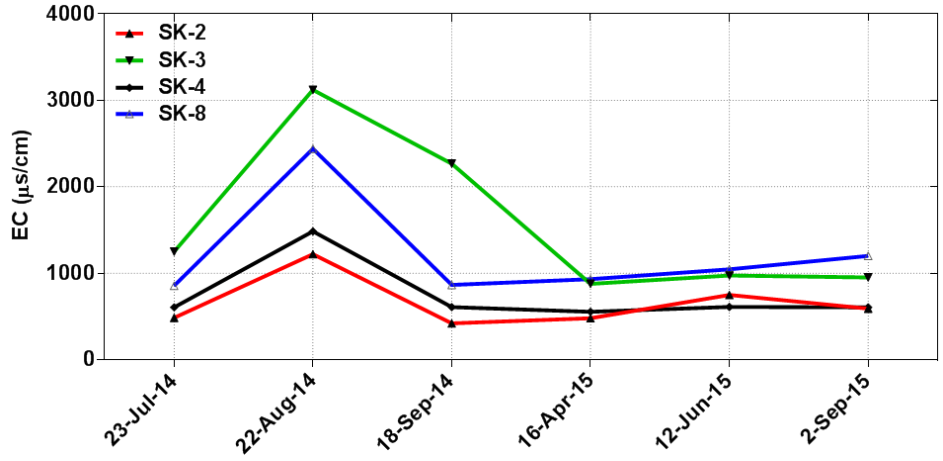

Figure 4.15. Variations in electrical conductivity of groundwater measured in SK-2, SK-3, SK-4 and SK-8

As shown in Table 4.4 the water samples from SK-1 to SK-9 except SK-7 are characterized with law concentration of chloride which ranged from 35 to 66 mg/L. However, in SK-7 samples the chloride concentration exceeded 6000 mg/L in September 2015.

In MODFLOW heads at the locations of specified observation wells for every time steps are calculated. This allows the user to compare the simulated (calculated) heads with observed heads, produce calibration statistics. Data of observation wells period (2014-2015) is used for the calibration of the model. The water level was monitored in nine wells; the location of these wells can be seen in Figure 3.5 or in 3D view in Figure 4.17.

Table 4.4. Concentration of chloride (mg/L) for the period (2014 – 2015)

Observation well	Sep (2014)	Apr (2015)	Sep (2015)
SK-1	-	44.17	234.47
SK-2	41.8	33	35.76
SK-3	-	62.14	66.17
SK-4	-	41.79	42.96
SK-5	-	49.03	46.39
SK-6	109	46.3	40.61
SK-7	2217	50.47	6709.56
SK-8	-	37.81	38.92
SK-9	63.7	36.28	37.97

- Chloride concentration was not measured

A general observation of water level data at monitoring wells, suggest that the water tends to rise during the December to April, and start declining from April to November. As mentioned before that the rise and the fall of water level depends upon the amount, duration and the intensity of the rain fall, specific yield and the slope of the aquifer toward the sea.

4.1.3. Estimation of Groundwater Extraction

The groundwater is considered the only source of freshwater used in Karareis region. In Karareis there are six legal pumping wells that work in order to satisfy the domestic needs, and one agricultural well is used for agricultural irrigation. Figure 4.16 shows the location of pumping wells within the study area. By carrying of field study the groundwater abstraction was roughly estimated for the domestic and the irrigation uses. The rates of pumping for the two periods (summer and winter) are listed in Table 4.5. The table also shows the numbers of summerhouses are being supplied by water due to the work of pumping wells. The amount of water used by summerhouse for domestic use averages 1.3 m^3/d; however, the actual water used in that location is

greater than the estimated, due to illegal pumping wells. Agriculture is the major water consumer, with typical water use to be on order of 120 m^3/d over the year.

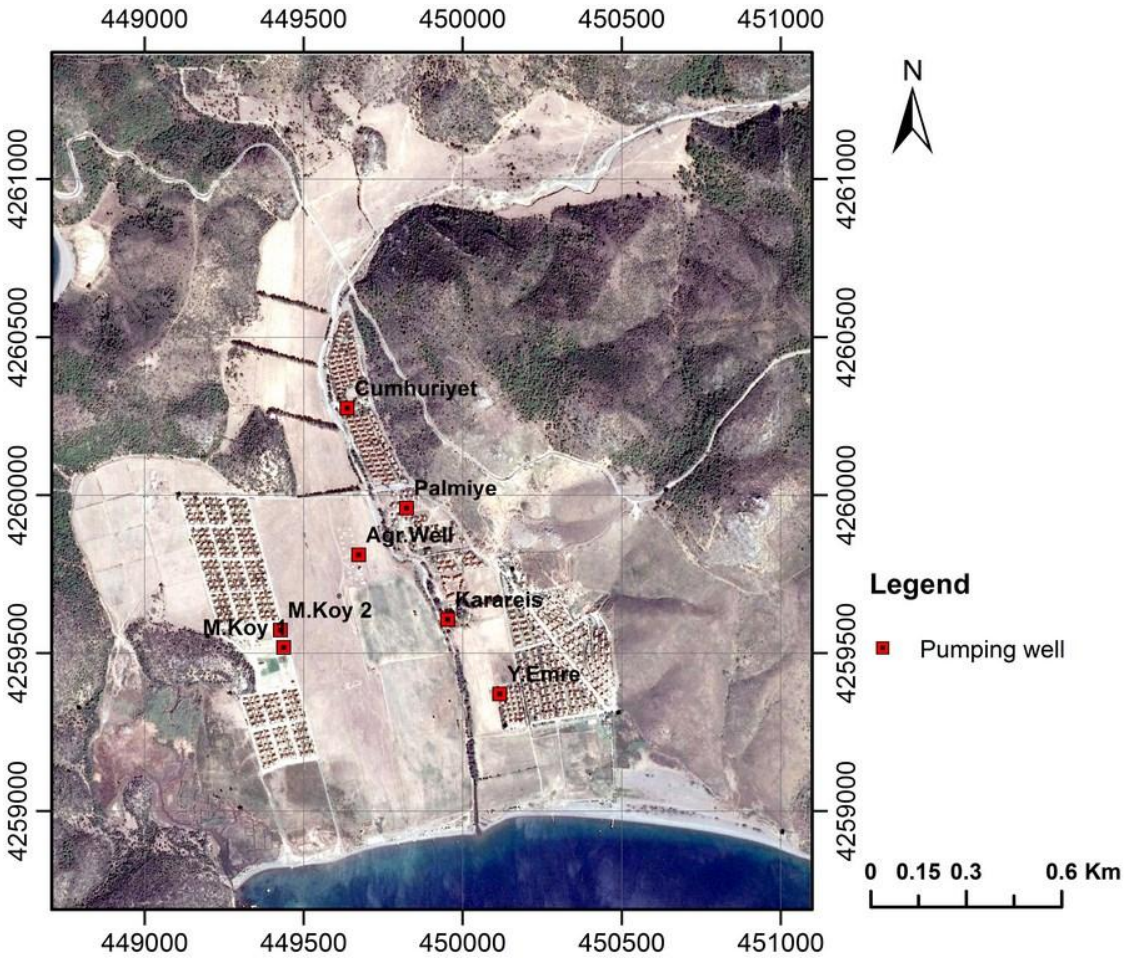

Figure 4.16. Location of pumping wells within the study area

The pumping wells are located in the model grid and the pumping rate was entered. In MODFLOW the well is considered to be located in the center of the cell and the pumping from the aquifer is considered to be in negative rates. The pumping rate was specified continuously for all the stress periods. Figure 4.17 shows 3D view for the locations of the pumping wells within the conceptual model of the study area.

Table 4.5. Rate of water pumping in winter and summer period

		Summer		Winter		Average
Well ID	No. SH[1]	No. SH	Q (m^3/d)	No. SH	Q (m^3/d)	Q (m^3/d)
Palmiye	30	30	40	9	3	12
Cumhuriyet	180	130	130	10	4	35
Karareis	305	270	270	30	10	74
M.Koy 1	100	100	100	10	4	27
M.Koy 2	100	100	100	10	4	27
Y.Emre	25	20	20	2	1	5
Agr.Well[2]	-	120		120		120

1 Summerhouse 2 Agricultural well

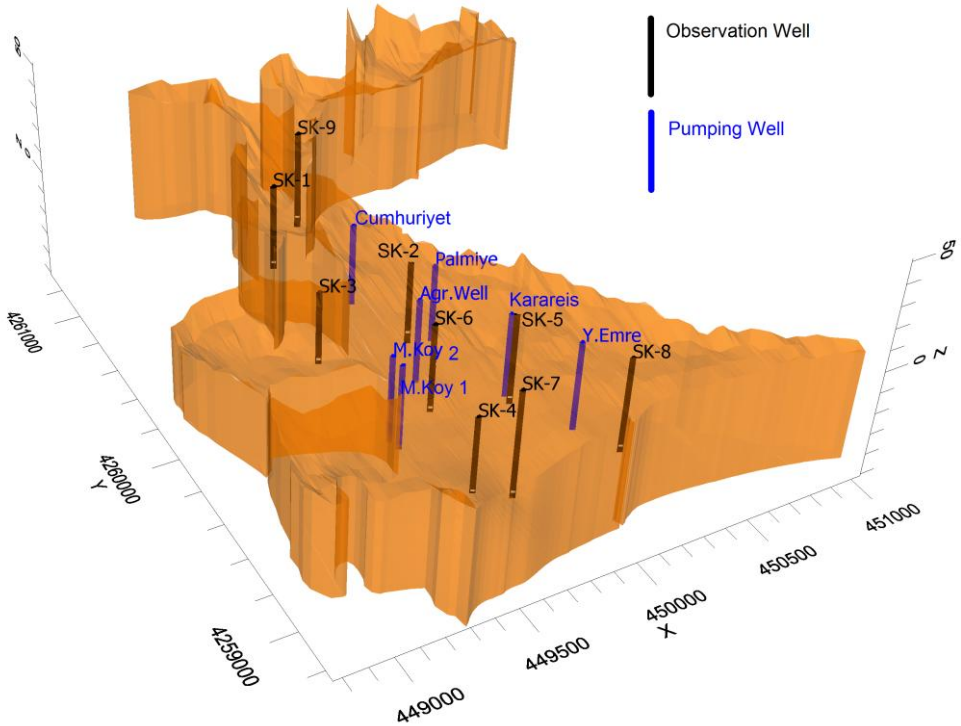

Figure 4.17. Distribution of pumping and observation wells throughout the model domain

4.1.4. Model Discretization and Boundary Conditions

A finite difference grid (Figure 4.18) has been used to discretize the study area, by dividing into 100 rows and 100 columns for one layer. A vertical cross section depicting the vertical discretization of the flow domain is shown in Figure 4.19.

Specification of appropriate boundary conditions is considered to be the most difficult task in constructing the model because it is one of the major contributors of the uncertainty in the model. Boundary conditions are mathematical statement specifying the heads or fluxes at the boundaries of the model. Boundary condition in Karareis aquifer consists of no-flow and constant head boundaries. The northern, eastern and western boundaries are assumed to be no-flow boundaries. Because basement of study area consists of mudstone and sandstone which has low permeability (Figure 3.5). Many wells were dug showed that groundwater does not occur in these units. The constant head and concentration was specified to the model cells along the coast. The constant sea water head and concentration of total dissolved solid assumed for the model were 0 m and 35000 mg/L, respectively. However, the exact position of this boundary is not known due to the scarcity and uncertainty of data (Figure 4.18).

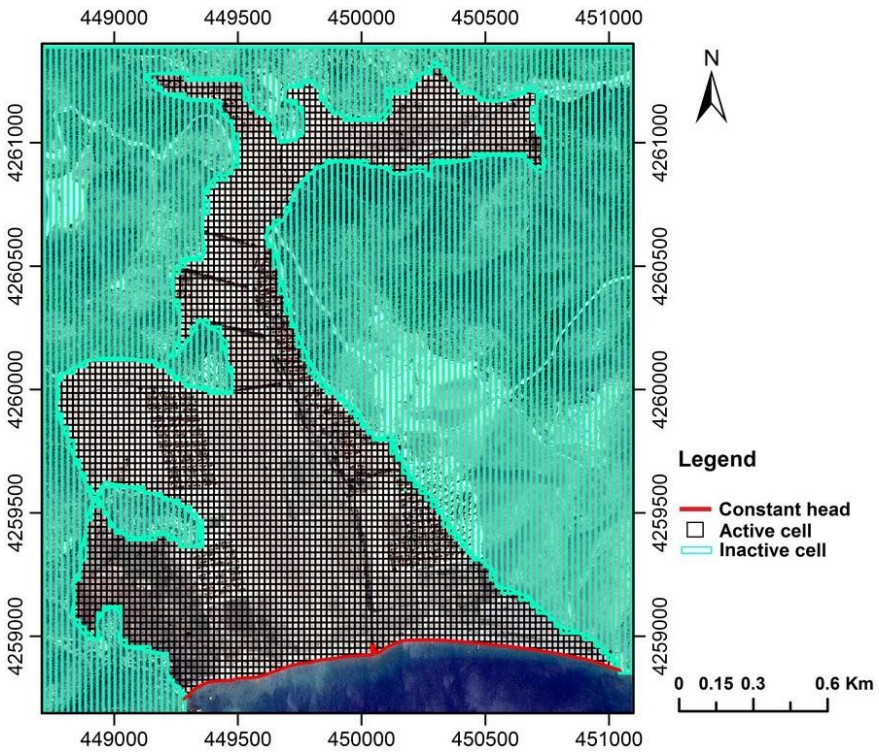

Figure 4.18. Finite different grid and boundary conditions for Karareis model

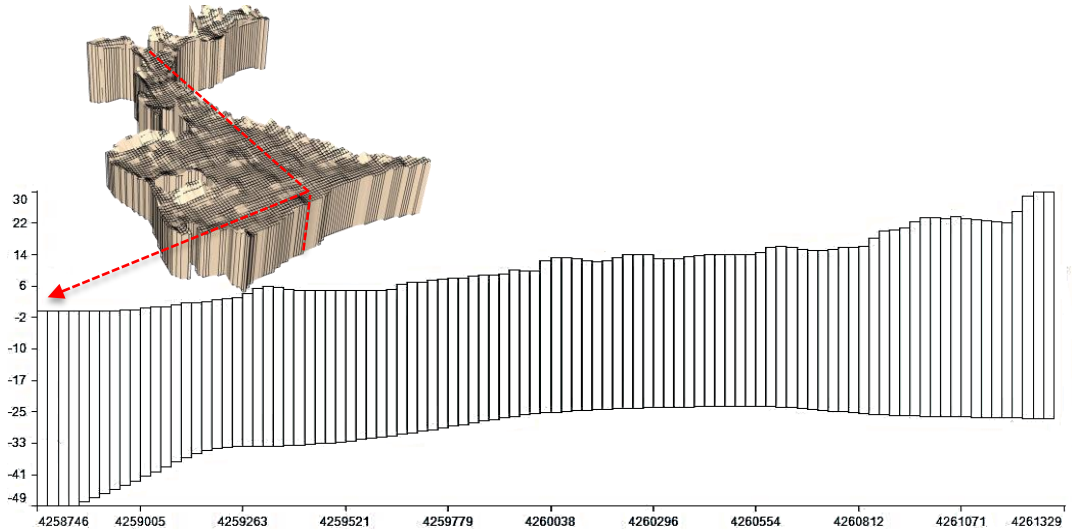

Figure 4.19. Vertical cross section through model, (column 32)

A reference density of 1025 kg/m^3 was used for seawater which will be used by SEAWAT to calculate the fluid densities relative to simulated concentrations of dissolved salts in the model.

4.1.5. Initial Conditions

The initial head and concentrations were set at the beginning time of the simulation in order to start solving the flow equations. MODFLOW needs an initial "guess" for the head values in the model. A good initial head guess for the simulation can reduce the required run time significantly in the transient sate. Within the model of Karareis, the initial water level of zero elevation from the mean sea level was set to the model.

The initial concentration assumed for the aquifer was evaluated by interpolating the concentration of total dissolved solid for various samples listed in Table 4.6 (Figure 4.20). The results of the steady state run will used as initial conditions for transient simulation of seawater intrusion.

Table 4.6. Typical TDS values (mg/L) obtained by using (TDS-EC) relationship[1]

Observation well	Average of EC (µs/cm)	Average of TDS (mg/L)
SK-1	1082.4	725
SK-2	672	450
SK-3	1698	1138
SK-4	773	518
SK-5	1938	1298
SK-6	1290	864
SK-7	6172	4135
SK-8	1228	823
SK-9	1812	1214

1 equation (3. 1) shows the relationship between TDS and EC

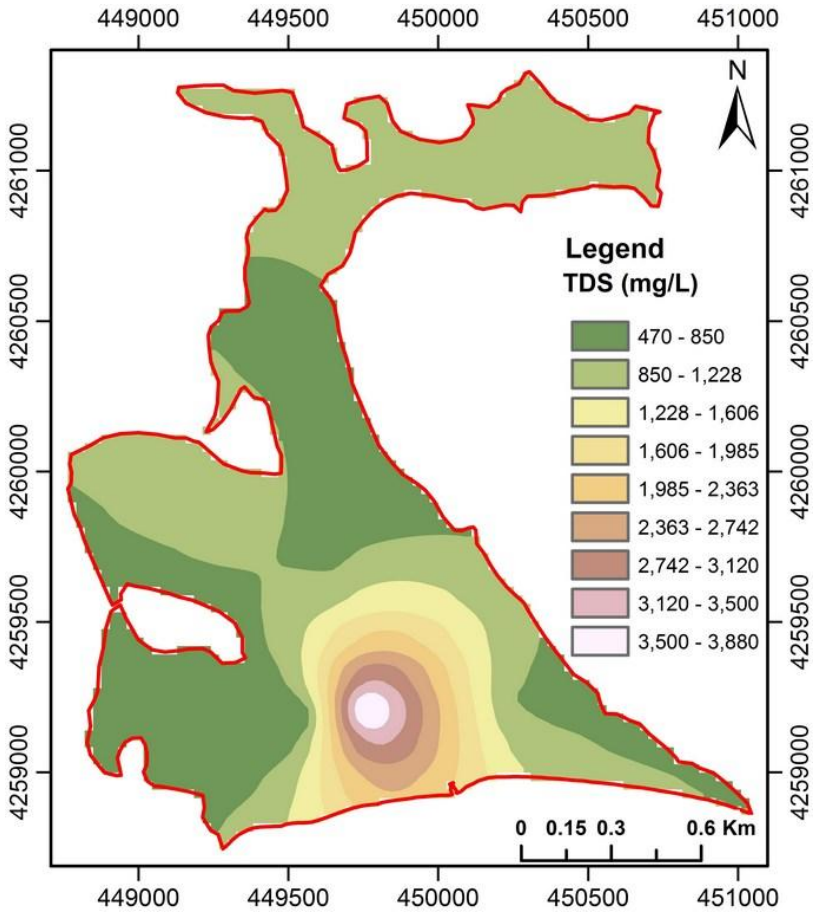

Figure 4.20. TDS map (mg/L) prepared by Kriging interpolation

4.1.6. Recharge

Groundwater recharge consists of precipitation, seepage flow from the seasonal stream and percolations from irrigated area. The major portion of the recharge to groundwater is from stream and precipitation; therefore, the groundwater level in the aquifer rises continuously during the rainy season of the year. During the dry season (no-recharge), the groundwater levels fall depending on discharge amount. Based on these facts, the amount of recharge due to precipitation, stream flow and due to other reasons can be determined with help of the groundwater level data of the aquifer system. The recharge is often used as a calibration parameter and is varied along with hydrogeologic material properties. The general procedure for estimating recharge amount was to multiply the annual rainfall quantity in each zone by infiltration coefficient of the soil. Due to lack of data, the recharge quantity was estimated to be 320 mm/year which is 24% of the annual rainfall for the period (2014-2015), and 130.8 mm/year for the next year.

4.1.7. Hydrogeological Parameters

4.1.7.1. Porosity and Specific Yield

From the grain size distribution it can be said that 70% of soil samples can be classified as well graded sand (SW) according to the uniformity coefficient which is greater than 6 and the rest can be classified as poorly graded sand (SP). The percentage of silt and clay in the samples was less than 5% except the soil samples which was taken from the first 5 meters.

Morris and Johnson (1967) developed a classification system used to divide the soil samples according to their particle size distribution (Table 4.7). According to Sieve analysis test, it was found that the majority of the samples collected from the study area are composed of coarse sand and fine gravel. The value of porosity for this type of samples ranges from 0.23 to 0.43 and the value of specific yield ranges from 0.13 to 0.40 (Das, 2013; Morris & Johnson, 1967).

Table 4.7. Soil classification based on particle size
(Source: Morris & Johnson, 1967)

Material	Particle size, mm
Clay	<0.004
Silt	0.004 – 0.062
Very fine sand	0.062 – 0.125
Fine sand	0.125 – 0.25
Medium sand	0.25 – 0.5
Coarse sand	0.5 – 1.0
Very coarse sand	1.0 – 2.0
Very fine gravel	2.0 – 4.0
Fine gravel	4.0 – 8.0
Medium gravel	8.0 – 16.0
Coarse gravel	16.0 – 32.0
Very coarse gravel	32.0 – 64.0

4.1.7.2. Hydraulic Conductivity

For the tracer method, the tracer that was injected in SK-2 arrived in 3 days to the second observation well. The dye (sodium fluorescein) was detected by Submersible Multi-Parameter Fluorometer which was placed in (OBS. Well). The water depth from the ground surface in the two observation wells 60 m apart were 8.2 m and 8 m. With taking in consideration that there is approximately one meter difference in the ground elevation between the two wells. Figure 4.21 shows the concentration of sodium fluorescein detected after 2 days of injection.

Given α = 0.25, L = 60 m, h = 0.75 m, and t = 3 days or 259.2×10^3 second, K equals:

$$K = \frac{(0.25)(60\ m)^2}{(0.75\ m)(259.2 \times 10^3\ s)} = 4.63 * 10^{-3}\ m/s$$

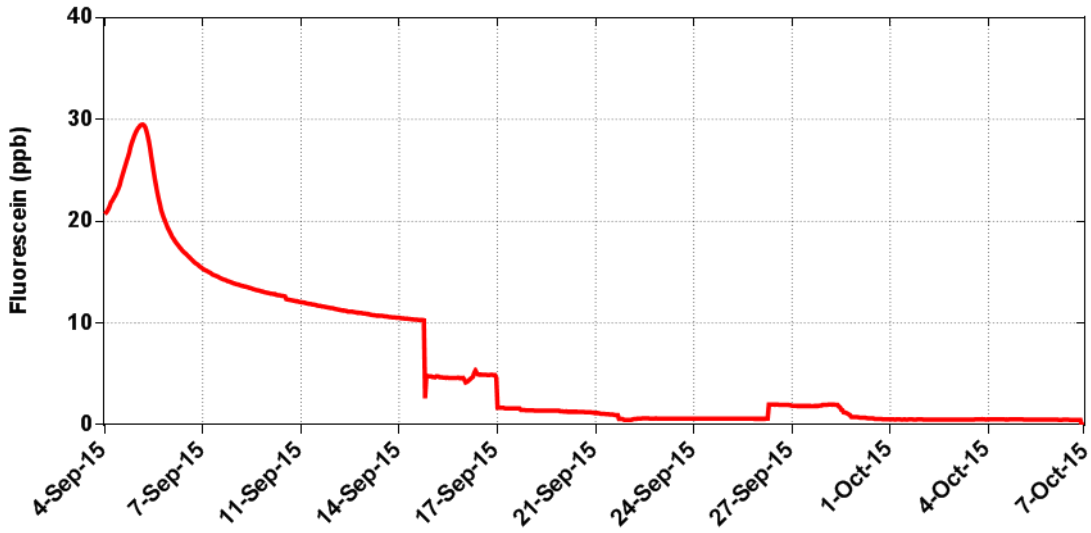

Figure 4.21. Sodium fluorescein concentrations (ppb) measured in OBS.Well

For fine gravel or coarse sand aquifers, the hydraulic conductivity can reach to 5.2×10^{-3} m/s (Morris & Johnson, 1967). So, the value of hydraulic conductivity which calculated by tracer test can be accepted.

For the pumping and laboratory tests the calculated hydraulic conductivity and transmissivity values for various observation wells are listed in Table 4.8.

Table 4.8. Representative values of hydraulic conductivity and transmissivity

Observation well	K (m/d)[1]	K (m/d)[2]	T (m^2/d)[3]
SK-1	2.16	17.46	86.4
SK-2	0.37	12.61	14.3
SK-3	0.13	1.30	4.38
SK-4	2.24	8.81	80.6
SK-5	-	6.62	-
SK-6	0.10	12.22	4.33
SK-7	0.08	9.08	3.27
SK-8	-	4.38	-
SK-9	-	35.70	-

(1, 3) Using pumping test, (2) Laboratory test

- Pumping test was not conducted

The hydraulic conductivity map was created using hydraulic conductivity values which determined from laboratory tests. Figure 4.22 shows the initial distribution of the hydraulic conductivity values interpolated by Kriging interpolation.

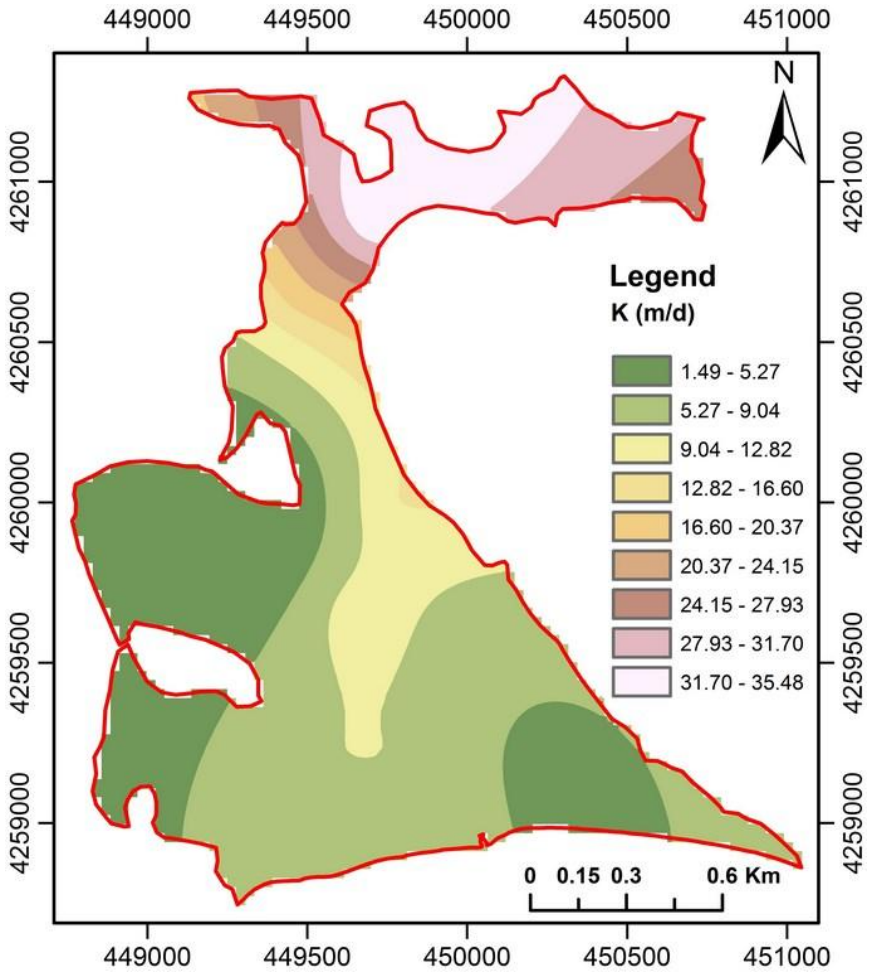

Figure 4.22. Distribution of hydraulic conductivity in longitudinal direction K_x (m/d)

The hydraulic conductivity in longitudinal direction K_x and lateral direction K_y were assumed to be equal in the model and the vertical hydraulic conductivity K_z was set as $0.1\times K_x$. Initial parameters of K_x used in nonlinear parameter estimation software (PEST) calibration was set up as given in Figure 3.29. The aquifer parameters used in simulations are listed in Table 4.9. The values of the longitudinal and vertical transverse dispersivities, is obtained from published data from (Qahman & Larabi, 2006).

Table 4.9. Aquifer parameters assigned for alluvial aquifer of Karareis region

Parameter	Value	Unit
Total porosity	0.30	
Effective porosity	0.25	
Specific yield	0.20	
Longitudinal dispersivity	25	m
Transversal dispersivity	0.25	m
Diffusion coefficient	0.1	m^2/day
Freshwater density	1000	Kg/m^3
Seawater density	1025	Kg/m^3
Seawater concentration	35000	mg/L
Density/Concentration slope	0.7143	
TDS concentration of recharge	0	mg/L

4.2. MODFLOW Results and Calibration

The numerical model output provides contours of head, drawdown, net recharge and water table. It also provides graphs of calculated vs. observed heads, calibration of residual histogram, head vs. time and drawdown vs. time. The model output also provides velocity vectors with direction of flow.

The steady state simulation was employed in order to establish the hydraulic conductivity distributions. The average of the field measurements of groundwater level in the period (2014-2015) were taken as target of steady state calibration (Table 4.2). The calibration is achieved through PEST approach by adjusting the values of hydraulic conductivity, until the hydraulic head values calculated by MODFLOW match the observed values to a satisfactory degree. The model was run a number of times for various values of hydraulic conductivity distributed over the domain. Model calibration was stopped when a reasonable match between the calculated and observed heads was achieved. As illustrated in Figure 4.23, an overall correlation coefficient of 0.972 and a root mean square error (RMSE) of 0.427 m are obtained when the calibration is finished, indicating a good match between the calculated and the observed heads. Table 4.10 shows the residual between the observed and calculated heads. Also, it summarizes the statistics of steady state calibration between observed and calculated head. After

model calibration, the resulting horizontal (longitudinal) hydraulic conductivity for the aquifer layer was ranged from 2.13 to 37.15 m/day. Figure 4.24 shows the distribution of calibrated values of hydraulic conductivity within the model domain.

The simulation results of MODFLOW were exported to ESRI line shape. Figure 4.25. (A) shows the contour lines of the water head calculated by using MODFLOW for the period (2014-2015). While, (B) shows the contour lines for the observed head interpolated by Kriging interpolation for same previously mentioned period.

Table 4.10. Observed and calculated heads with residual of nine observation wells

Target well	Screen depth (m)	Observed head (m)	Calculated head (m)	Residual head (m)
SK-1	40	7.15	7.37	0.22
SK-2	39	4.53	3.95	-0.58
SK-3	34	4.22	4.30	0.07
SK-4	36	1.15	1.42	0.27
SK-5	44	2.62	2.23	-0.39
SK-6	42	2.35	2.80	0.45
SK-7	52	2.25	1.36	-0.89
SK-8	46	0.25	0.45	0.20
SK-9	46	8.23	8.19	-0.04
Max. Residual				-0.89
Min. Residual				-0.04
Residual mean				-0.08
Abs. Residual mean				0.35
Standard error of the estimate				0.14
Normalized RMS				5.35 (%)

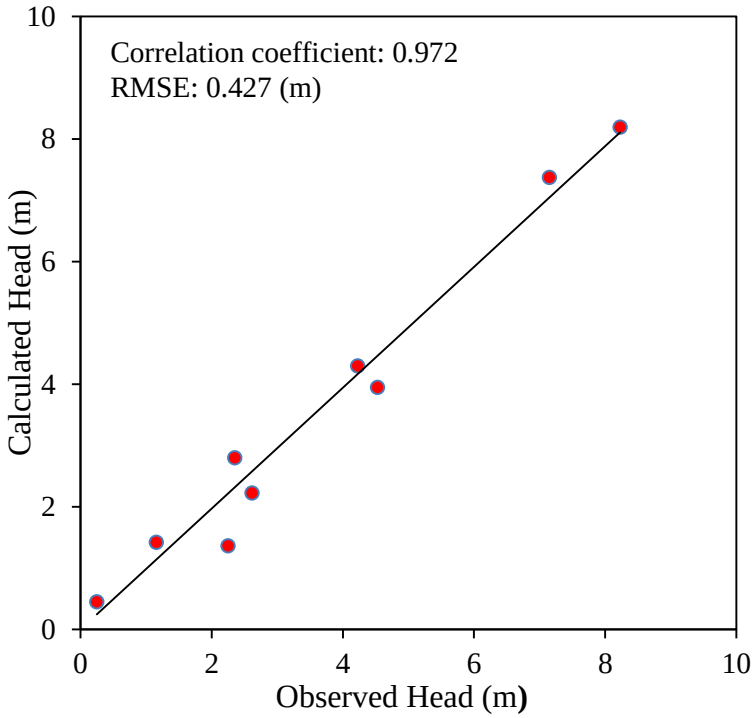

Figure 4.23. Calculated versus observed hydraulic heads

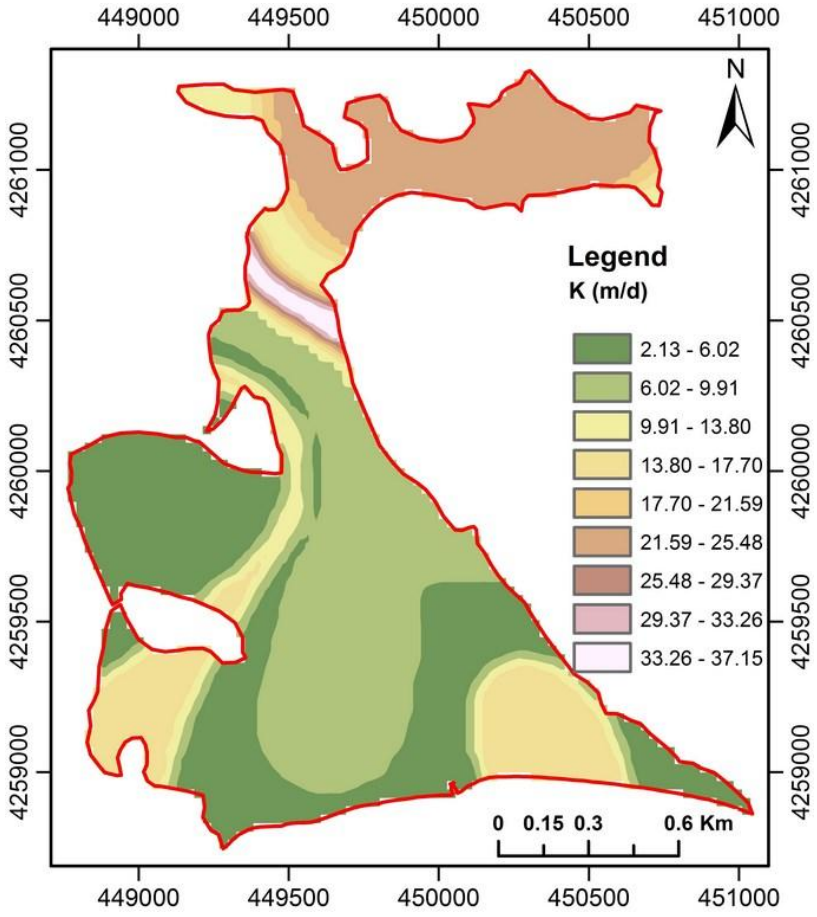

Figure 4.24. Distribution of hydraulic conductivity after calibration (m/d)

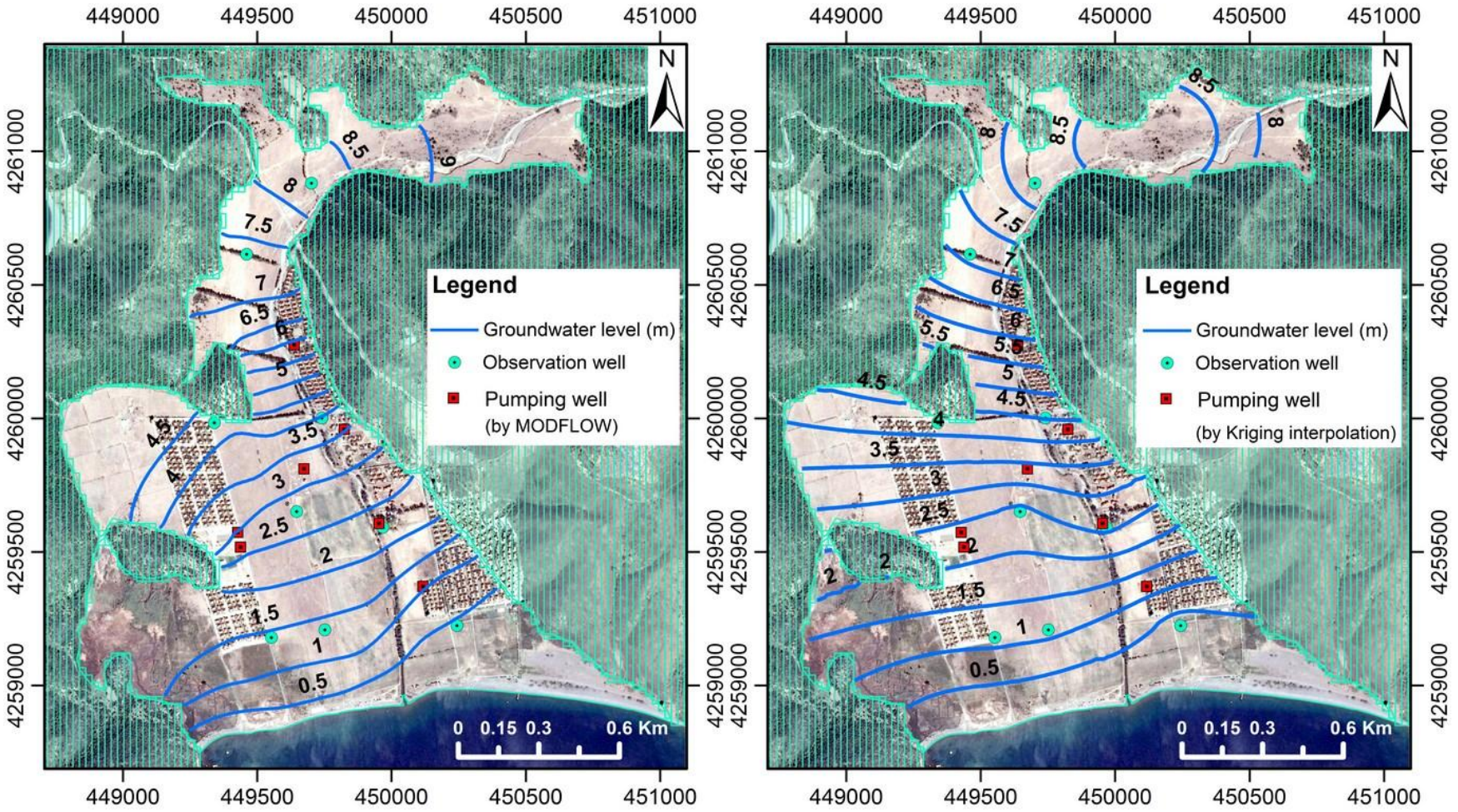

Figure 4.25. (A) Simulated water head for the period (2014-2015) calculated by MODFLOW. (B) Observed water head by using Kriging interpolation for the period (2014-2015)

4.2.1. Water Balance

The steady state water balance was computed based on the available field data for the period (2014-2015). As it is calculated by the program, the total input (721,382 m^3/ year) and output (720,680 m^3/ year) from the model are approximately equal with 1% error without any storage. Water budget inflows include recharge from stream and precipitation (721,382 m^3/ year). While, outflows include pumping for irrigation and domestic use (109,683 m^3/ year) and discharge to the sea (610,996 m^3/ year). The water budget of Karareis region shows that the most of the freshwater comes from the precipitation and discharges to the sea. Also, it shows that there is no deficit in the water balance with (+702 m^3/ year) difference between input and output.

4.2.3. SEAWAT Calibration and Validation

To study the seawater intrusion in Karareis aquifer, SEAWAT was employed to simulate the head and concentration distribution. SEAWAT calibration was conducted for the (2014-2015) target period, using the calibrated (2014-2015) steady state results as an initial condition. Table 4.11 presents the residual between the observed and calculated heads. Also, it summarizes statistics of SEAWAT calibration between observed and calculated heads. Figure 4.26 shows the calibrated and observed water heads. An overall of correlation coefficient of 0.95 and RMSE of 0.474 m are obtained when the calibration was finished. As mentioned previously, in SEAWAT code the density is assumed to be a function of the concentration of dissolved solid, while in MODFLOW the density is assumed to be constant, due to this fact there is a difference in the calculated groundwater levels computed by both codes (Figure 4.29).

For the solute transport model, TDS is the simulated component. During calibration, a total of nine observed TDS values were used in the period of (2014-2015) (Table 4.6). Model calibration was terminated when a reasonably good match between the observed and calculated concentrations was achieved. In the simulation the correlation coefficient of the calculated and observed TDS concentration is 0.89, and the RMSE was 350.6 mg/L (Figure 4.27). A Summary of statistic values and the residual between the calculated and observed TDS was also listed in Table 4.11.

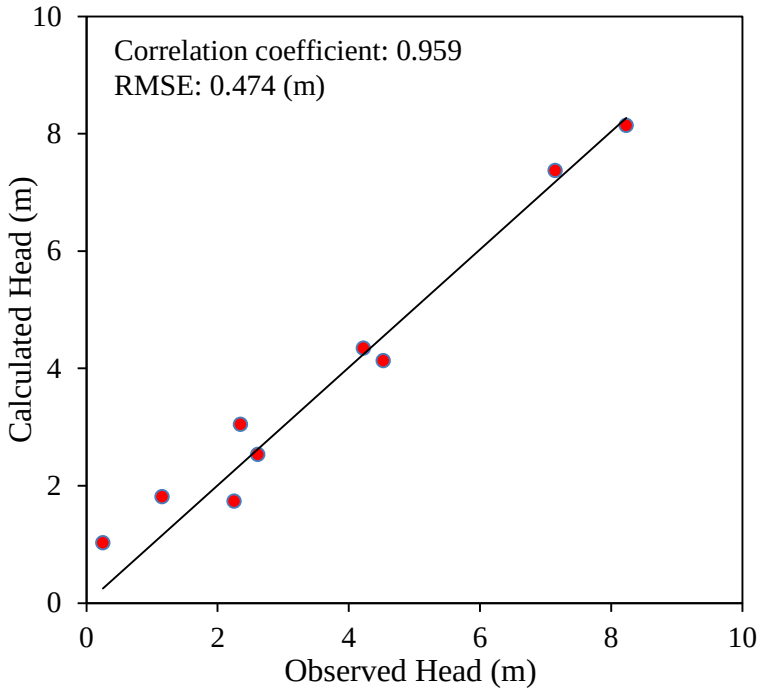

Figure 4.26. Calculated versus observed hydraulic heads

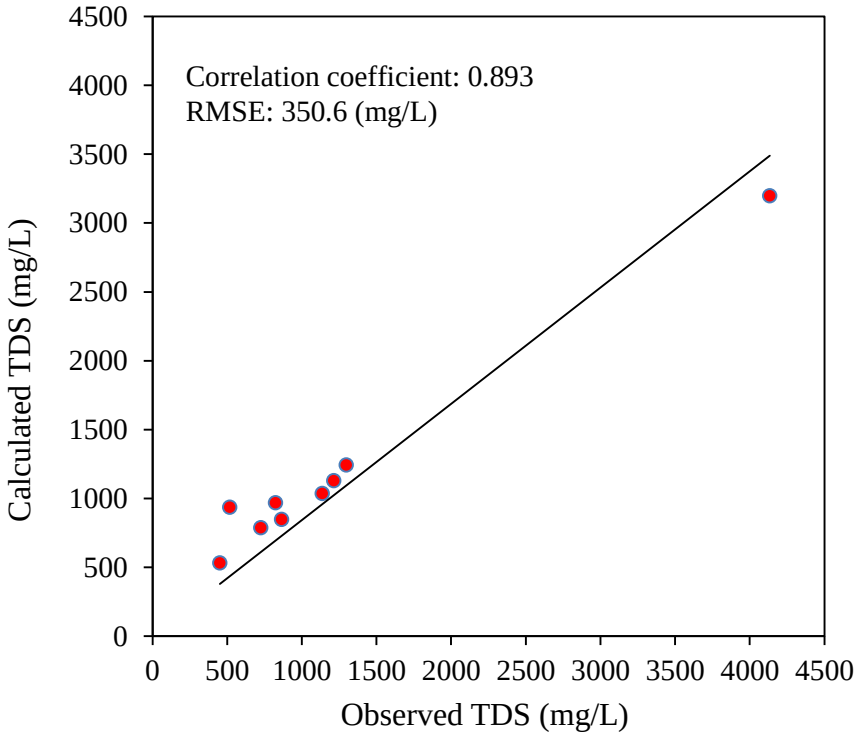

Figure 4.27. Calculated versus observed TDS concentrations

Following calibration, the model was validated by using the field observation data for the next year (2015-2016). The average of the head for the same observation wells was taken for validation of SEAWAT. The statistical analysis reveals that the

correlation coefficient was 0.94 and the RMSE was 1.207 m (Figure 4.28). A summary of statistic values and the residual between the calculated and observed heads are also listed in Table 4.12. The calculated values of the model are matching with the field observed values. Therefore, there is no further calibration or refinement the model is required and it's ready for predictive simulations. Due to scarcity of the observed TDS concentrations and continuously monitored electrical conductivity data, the model was only validated against the observed heads at the end of the simulation.

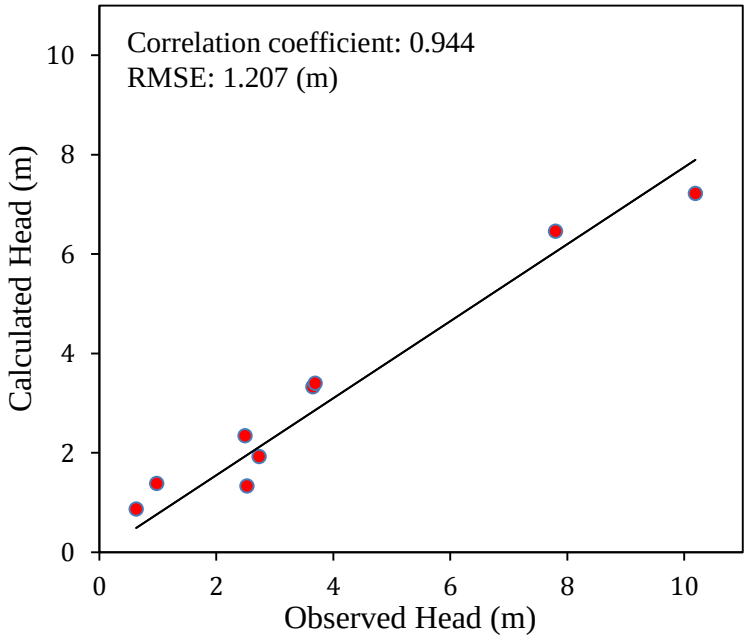

Figure 4.28. Calculated versus observed hydraulic head

Table 4.11. Observed and calculated heads and TDS concentration with residual of nine observation wells

Target well	Screen depth (m)	Observed head (m)	Calculated head (m)	Residual head (m)	Observed TDS (mg/L)	Calculated TDS (mg/L)	Residual head (mg/L)
SK-1	40	7.15	7.37	0.22	725	789	64
SK-2	39	4.53	4.13	-0.39	450	533	83
SK-3	34	4.22	4.35	0.12	1138	1037	-101
SK-4	36	1.15	1.82	0.66	518	938	420
SK-5	44	2.62	2.53	-0.08	1298	1245	-54
SK-6	42	2.35	3.05	0.70	864	850	-14
SK-7	52	2.25	1.74	-0.51	4135	3198	-937
SK-8	46	0.25	1.03	0.78	823	970	147
SK-9	46	8.23	8.14	-0.09	1214	1131	-83
Max. Residual				0.78			937
Min. Residual				-0.08			-14
Residual mean				0.16			-52.7
Abs. Residual mean				0.39			211.3
Standard error of the estimate				0.16			122.54
Normalized RMS				5.94 (%)			9.514 (%)

Table 4.12. Observed and calculated heads with residual of nine observation wells

Target well	Screen depth (m)	Observed head (m)	Calculated head (m)	Residual head (m)
SK-1	40	7.80	6.46	-1.34
SK-2	39	3.65	3.33	-0.32
SK-3	34	3.69	3.40	-0.29
SK-4	36	0.98	1.38	0.40
SK-5	44	2.73	1.92	-0.81
SK-6	42	2.49	2.34	-0.15
SK-7	52	2.52	1.33	-1.19
SK-8	46	0.63	0.87	0.24
SK-9	46	10.19	7.22	-2.97
Max. Residual				-2.97
Min. Residual				-0.15
Residual mean				-0.71
Abs. Residual mean				0.86
Standard error of the estimate				0.344
Normalized RMS				12.62%

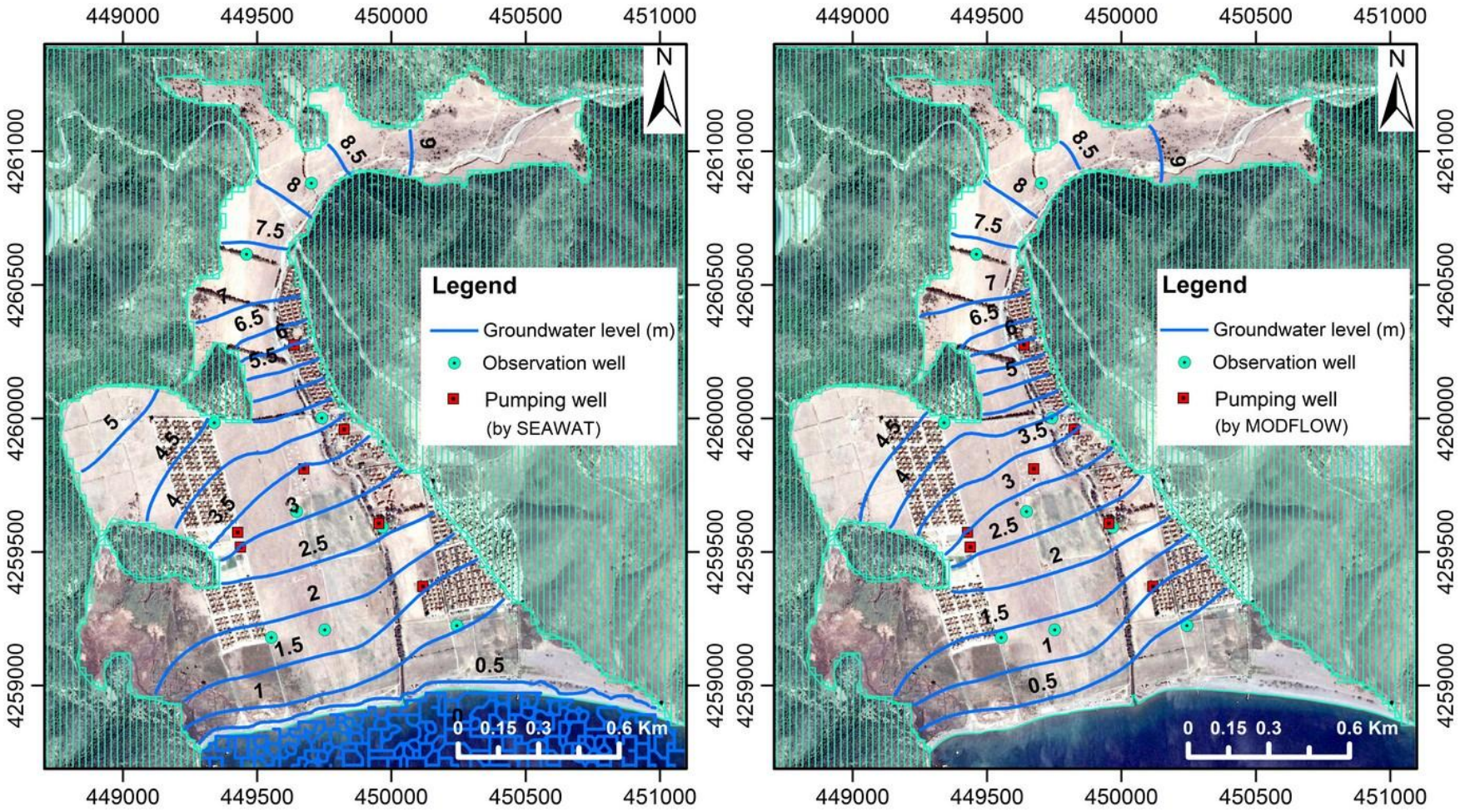

Figure 4.29. (A) Simulated water head for the period (2014-2015) calculated by SEAWAT. (B) Simulated water head for the period (2014-2015) calculated by MODFLOW

4.2.4. Simulation of Seawater Intrusion

At the end of simulation, the salinity distribution (mg/L) is presented in Figure 4.30. Figure 4.31 shows that seawater intrusion near SK-7 extends about 500 m inland and it's clear that the most affected area by seawater intrusion is located around the seventh observation well. One of the main reasons of this intrusion is due to the increase in water withdrawal of both Agricultural and Karareis wells with average rate of pumping equal to 120 m^3/day and 80 m^3/day, respectively (Figure 4.30). In the simulated model, TDS concentration near SK-7 reached to approximately 3000 mg/ L, and then it started to fall progressively to 1000 mg/L near to SK-6.

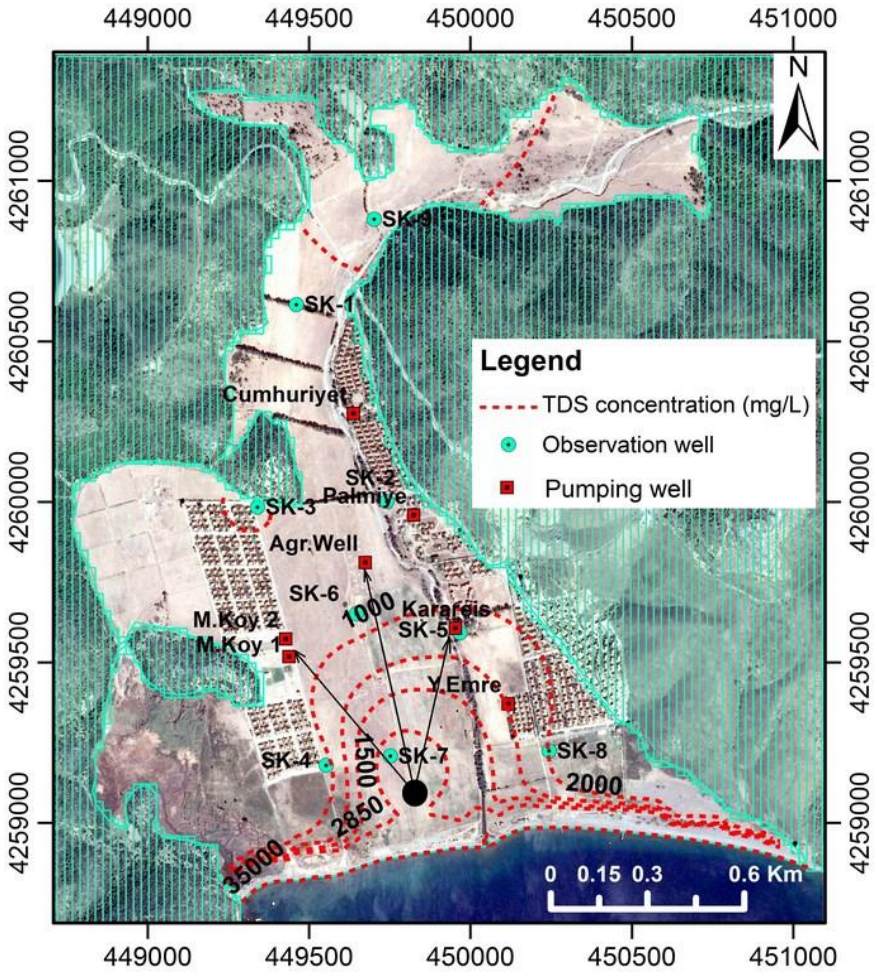

Figure 4.30. Simulated TDS (mg/L) for the period (2014-2015) calculated by SEAWAT

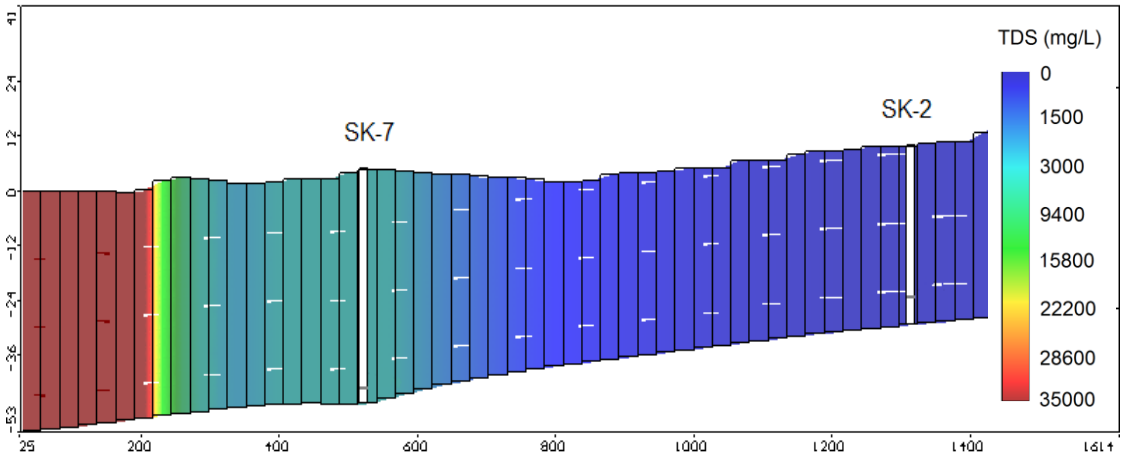

Figure 4.31. Calculated TDS (mg/L) for the period (2014-2015) calculated by SEAWAT along SK-7 cross section

4.2.5. Management Scenarios

Excessive withdrawal of groundwater from wells near the coast is considered to be the main reason of seawater intrusion into the aquifer. In order to prevent further intrusion of seawater into the aquifer, groundwater withdrawal should be decreased near the coast. As mentioned in Section 4.1.2 the groundwater levels depend on the amount of infiltrated water due to precipitation which means any change in the climate will affect the groundwater system.

To demonstrate the effect of future scenarios of groundwater pumpage and the annual precipitation on seawater intrusion, five scenarios were designed to use the calibrated model for calculations of future changes in water levels and TDS concentrations for the next ten years, within (2014-2024). In all scenarios the recharge rate was taken as it was in (2014-2015) which equals to 320 mm/year. The expected scenarios are presented as follow:

- The first scenario: no-change occur on the model
- The second scenario: the annual pumping rate from the aquifer will be equal to the pumping rate in the summer season (none of the people leave summerhouses)
- The third scenario: the pumping from the aquifer increase by doubling in the same pumping wells

- The fourth (worst) scenario: three new agricultural wells will be opened within the third scenario
- The fifth scenario: a change in the annual precipitation rate occurs (20% reduction of annual precipitation)

Table 4.13 presents the amount of abstracted water from the aquifer for the four scenarios. In all scenarios the recharge rater was taken as (2014-2015) which equal to 320 mm/year.

Table 4.13. Abstraction amounts (m^3/d) for management scenarios

Well ID	First scenario	Second scenario	Third scenario	Fourth scenario
Palmiye	12	40	80	80
Cumhuriyet	35	130	260	260
Karareis	74	270	540	540
M.Koy 1	27	100	200	200
M.Koy 2	27	100	200	200
Y.Emre	5	20	40	40
Agr.Well	120	120	240	240
A1	0	0	0	240
A2	0	0	0	240
A3	0	0	0	240

The resulted groundwater levels under normal pumping conditions are compared against those obtained by the previously mentioned scenarios. Figure 4.32 shows the predicted groundwater levels of the first scenario at the end of years 2019 and 2024. It is clear from this Figure that if non extra pumping is allowed, the groundwater levels will not change at the end of simulation periods. Figure 4.33 shows the future changes in the predicted water levels of the second scenario. Obviously, the water levels dropped from 0.75 m to 0.25 m starting from the north towards the sea at the end of the first simulation period and 1 m to 0.5 m at the end of the second simulation period. In the third scenario, the pumping rate at the same wells was doubled (Figure 4.34). The comparison between the normal-simulated groundwater levels shows that the water level dropped by 2.5 m at the end of the first simulation period and 3 m for the second

simulation period. Figure 4.35 represents future change in the fourth scenario (worst scenario). Clearly, the water level in this Figure dropped to be below MSL in the middle part of the studying region near to the new opened agricultural wells. This case may lead to reduction or reversal of groundwater gradient, which permits saline water to displace fresh water. 20% of the annual recharging rate was reduced in the last scenario (Figure 4.36). The ground water level dropped from 1 to 0.5 m and 1.5 to 0.5 m in 2019 and 2024, respectively.

Figures 4.37 to 4.41 show the comparison between the extents of seawater intrusion in the aquifer in year 2019 and 2024 for all scenarios. In the first and fifth scenarios, the results indicate that the extents of the isolines (TDS concentration) in 2024 will be less than 2019 due to the high infiltration and recharge from rainfall (Figures 4.37, 4.41). For the second scenario model results indicate that the seawater intrusion isoline (TDS concentration= 2000 mg/L) will move about an additional 60 m and 70 m in the northern part in 2019 and 2024, respectively (Figure 4.38). While, in the third scenario it will move about an additional 155 m and 270 m in the northern part in 2019 and 2024, respectively (Figure 4.39). Finally, in the worst scenario it will move 250 m and 420 m in the northern part in 2019 and 2024, respectively (Figure 4.40).

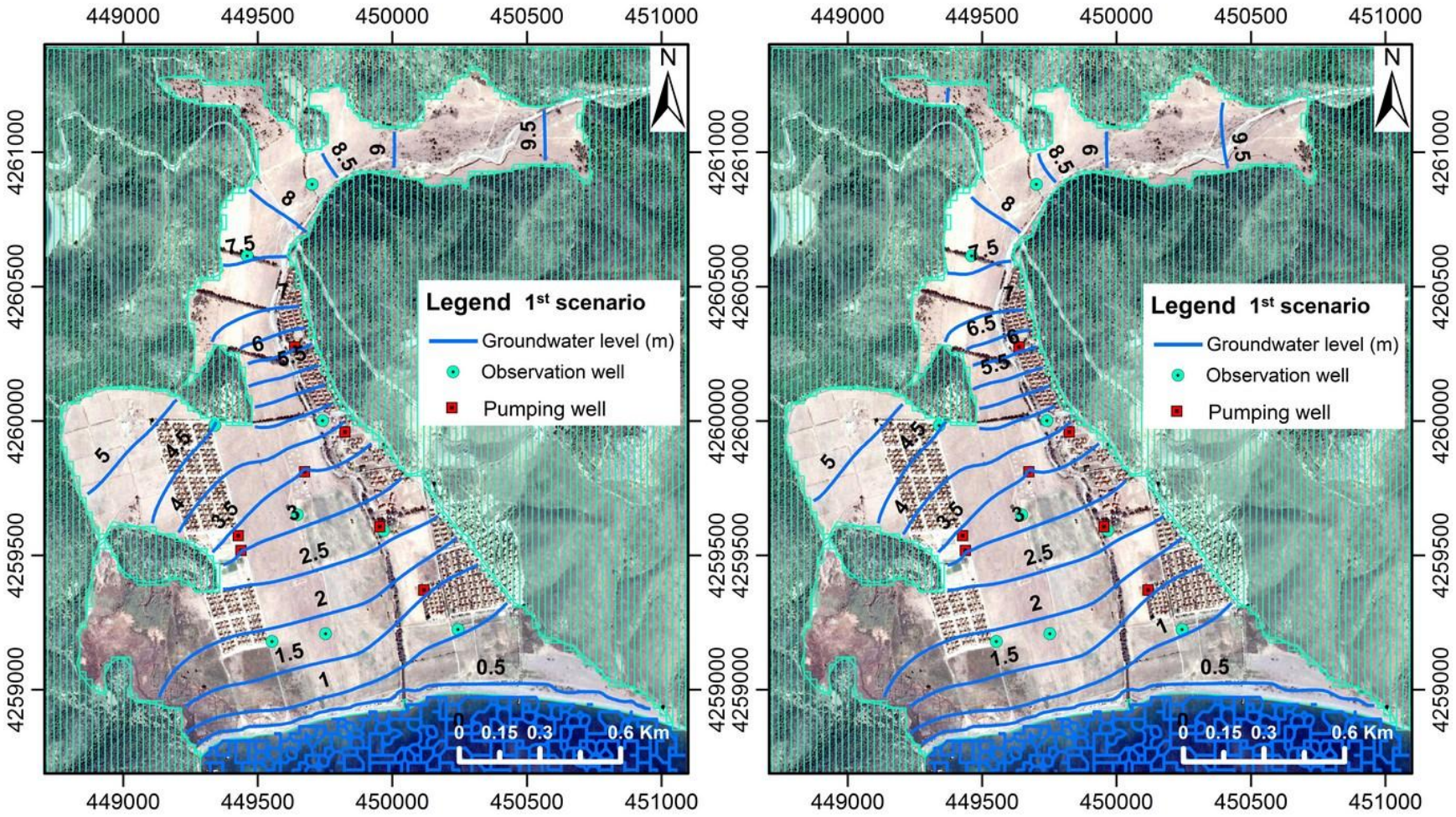

Figure 4.32. (A) Predicted contour lines of groundwater levels for the first scenario in 2019. (B) Predicted contour lines of groundwater levels for the first scenario in 2024

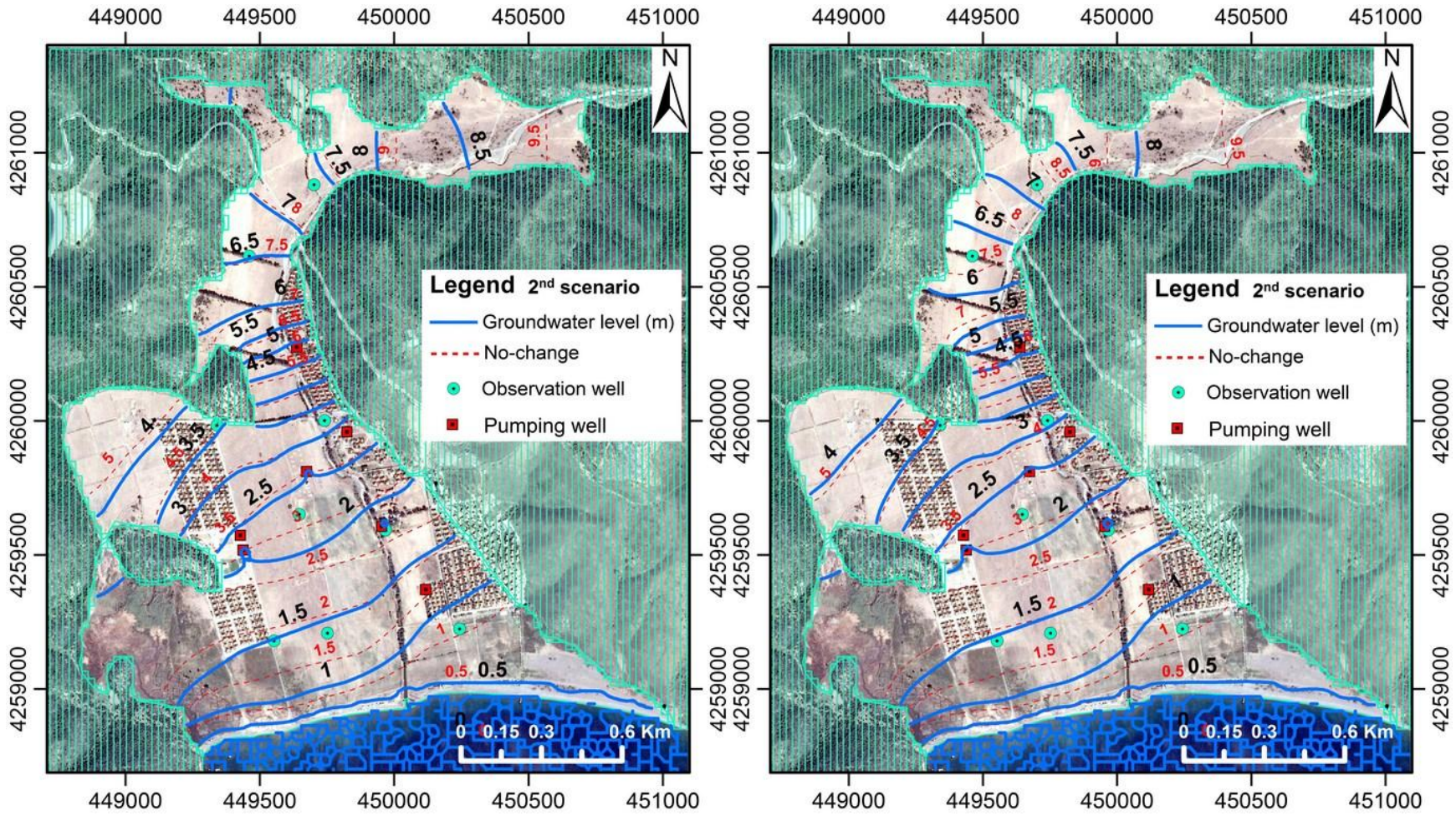

Figure 4.33. (A) Predicted contour lines of groundwater levels for the second scenario in 2019. (B) Predicted contour lines of groundwater levels for the second scenario in 2024

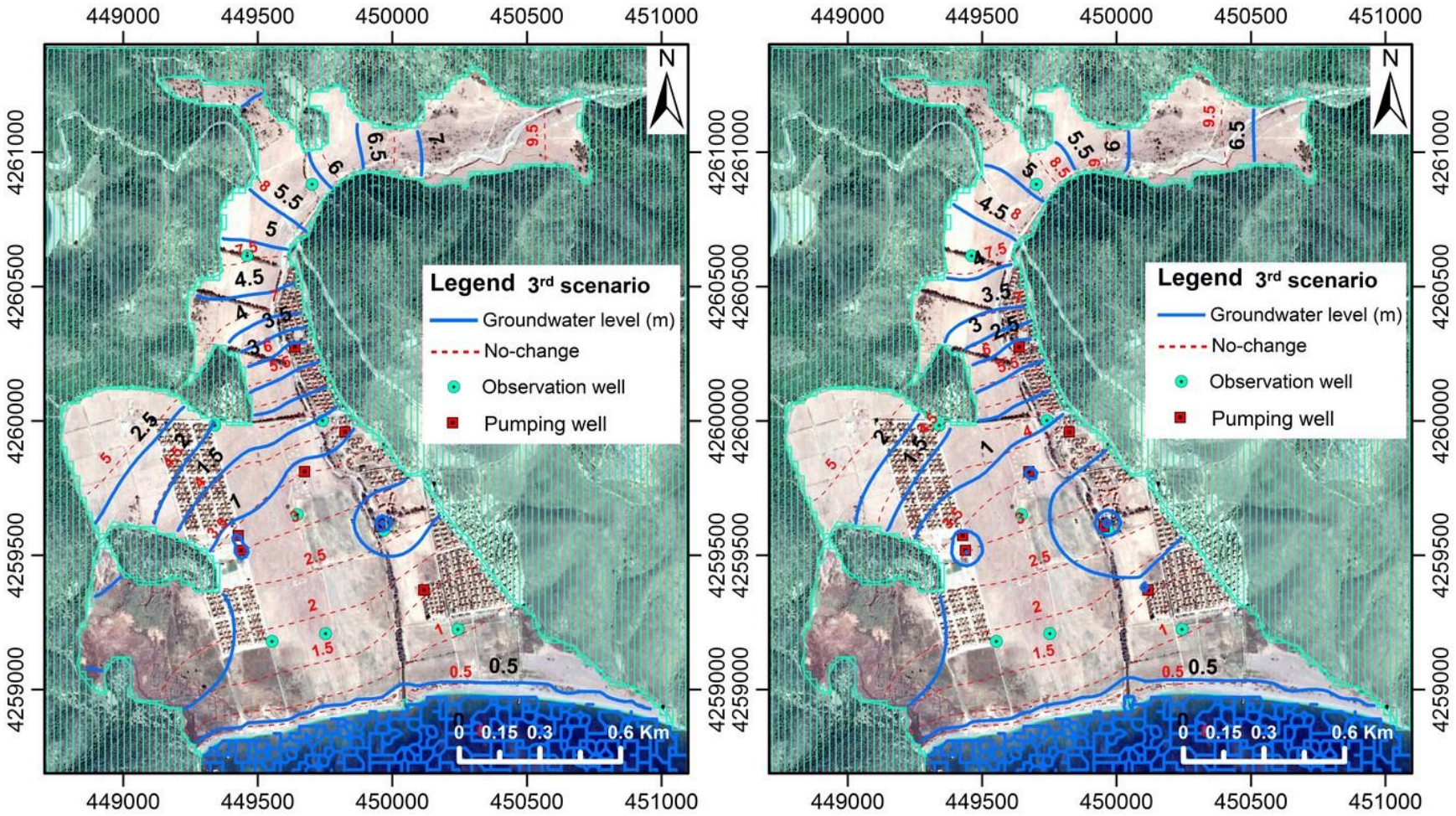

Figure 4.34. (A) Predicted contour lines of groundwater levels for the third scenario in 2019, (B) predicted contour lines of groundwater levels for the third scenario in 2024

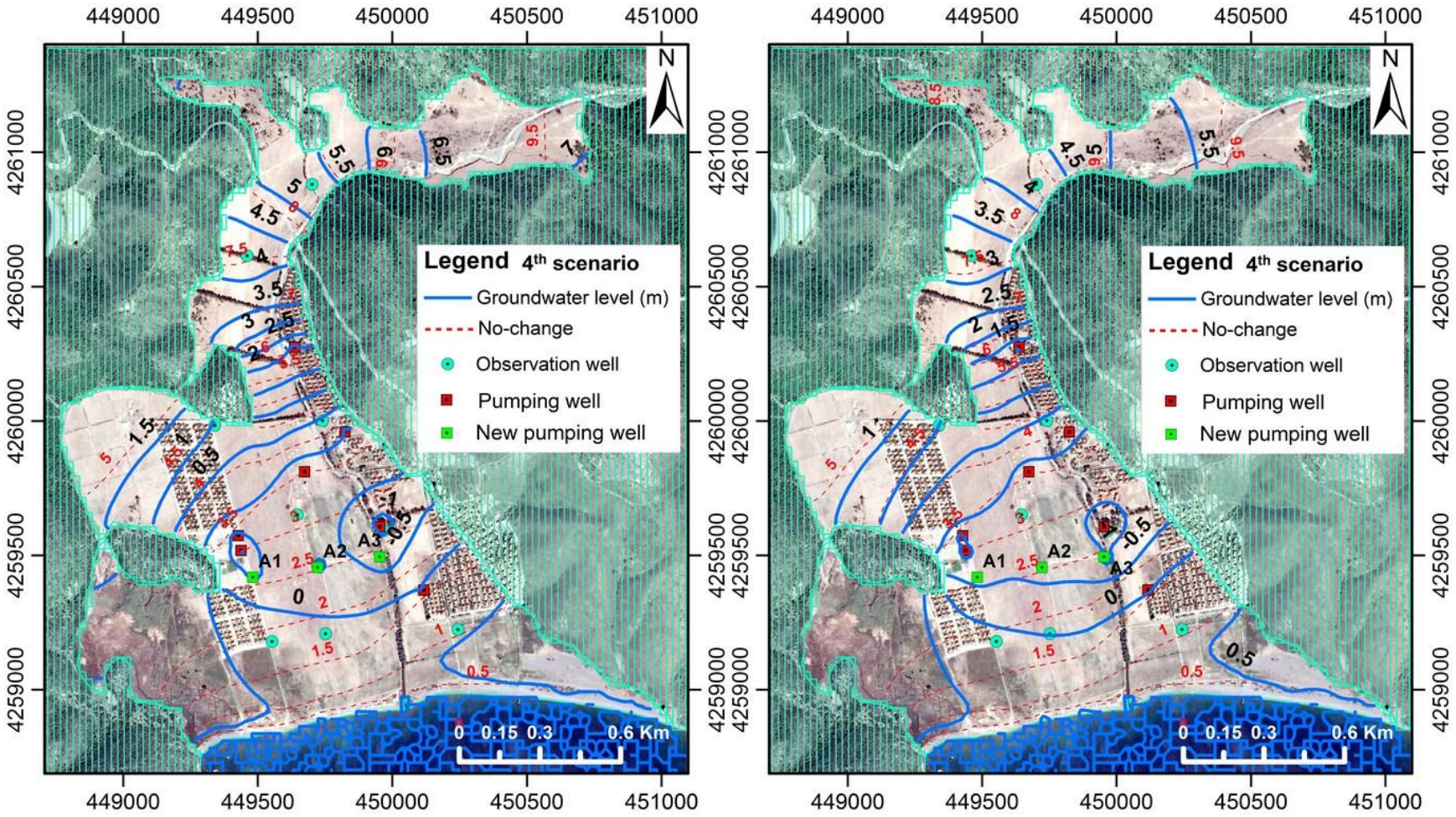

(A) (B)

Figure 4.35. (A) Predicted contour lines of groundwater levels for the fourth scenario in 2019. (B) Predicted contour lines of groundwater levels for the fourth scenario in 2024

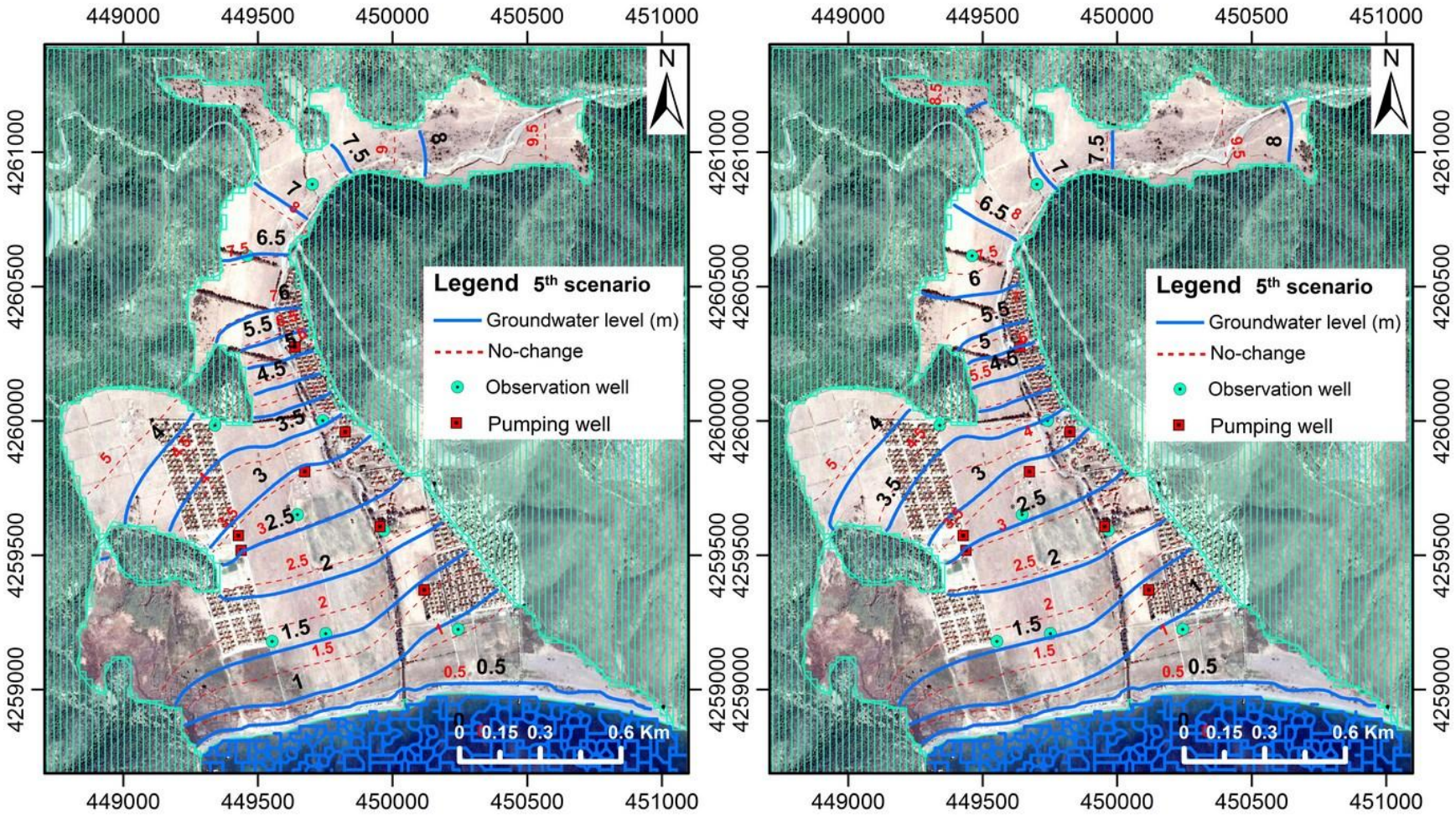

(A) (B)

Figure 4.36. (A) Predicted contour lines of groundwater levels for the fifth scenario in 2019. (B) Predicted contour lines of groundwater levels for the fifth scenario in 2024

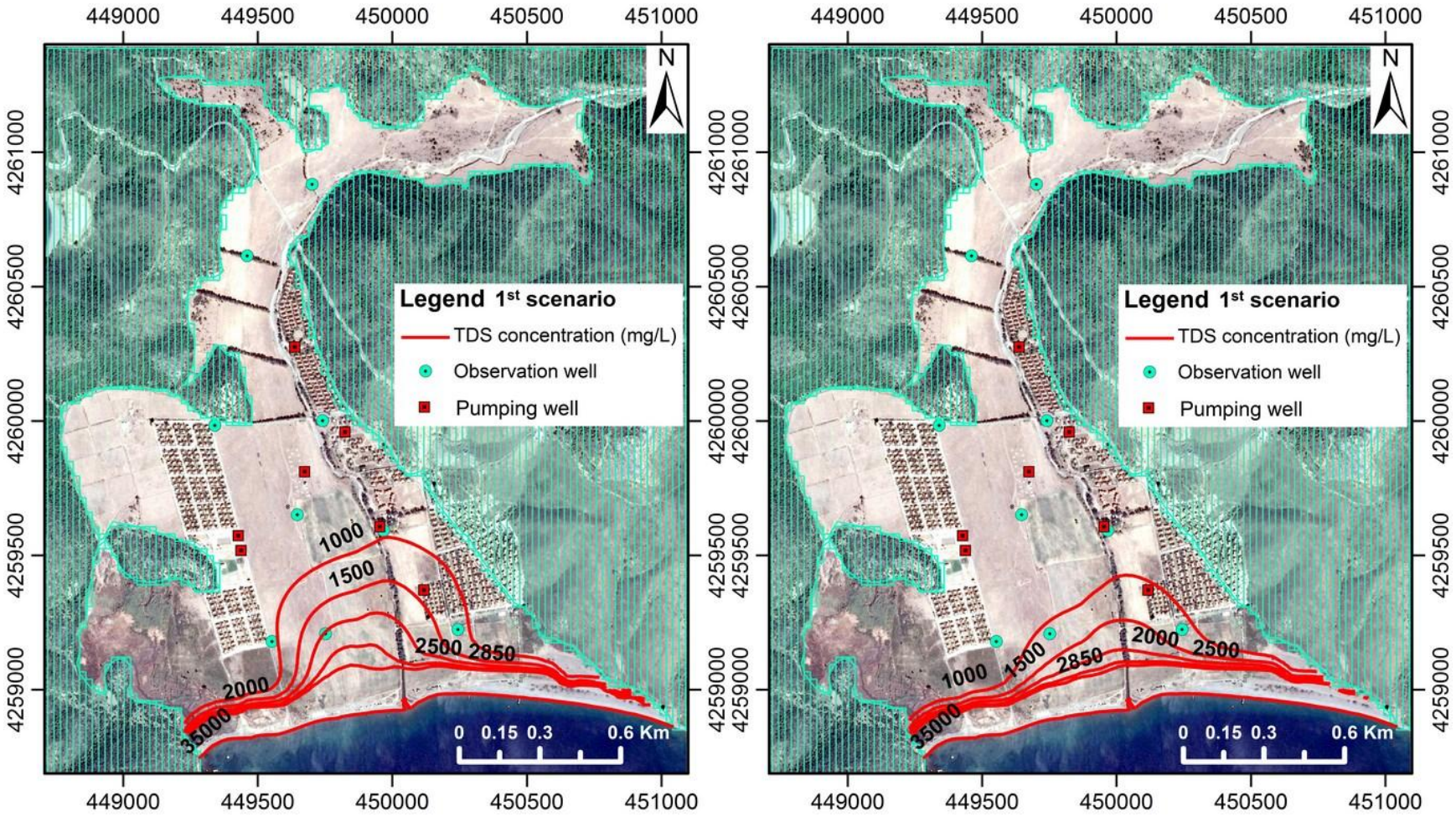

Figure 4.37. (A) Predicted contour lines of TDS concentration mg/L for the first scenario in 2019. (B) Predicted contour lines of TDS concentration mg/L for the first scenario in 2024

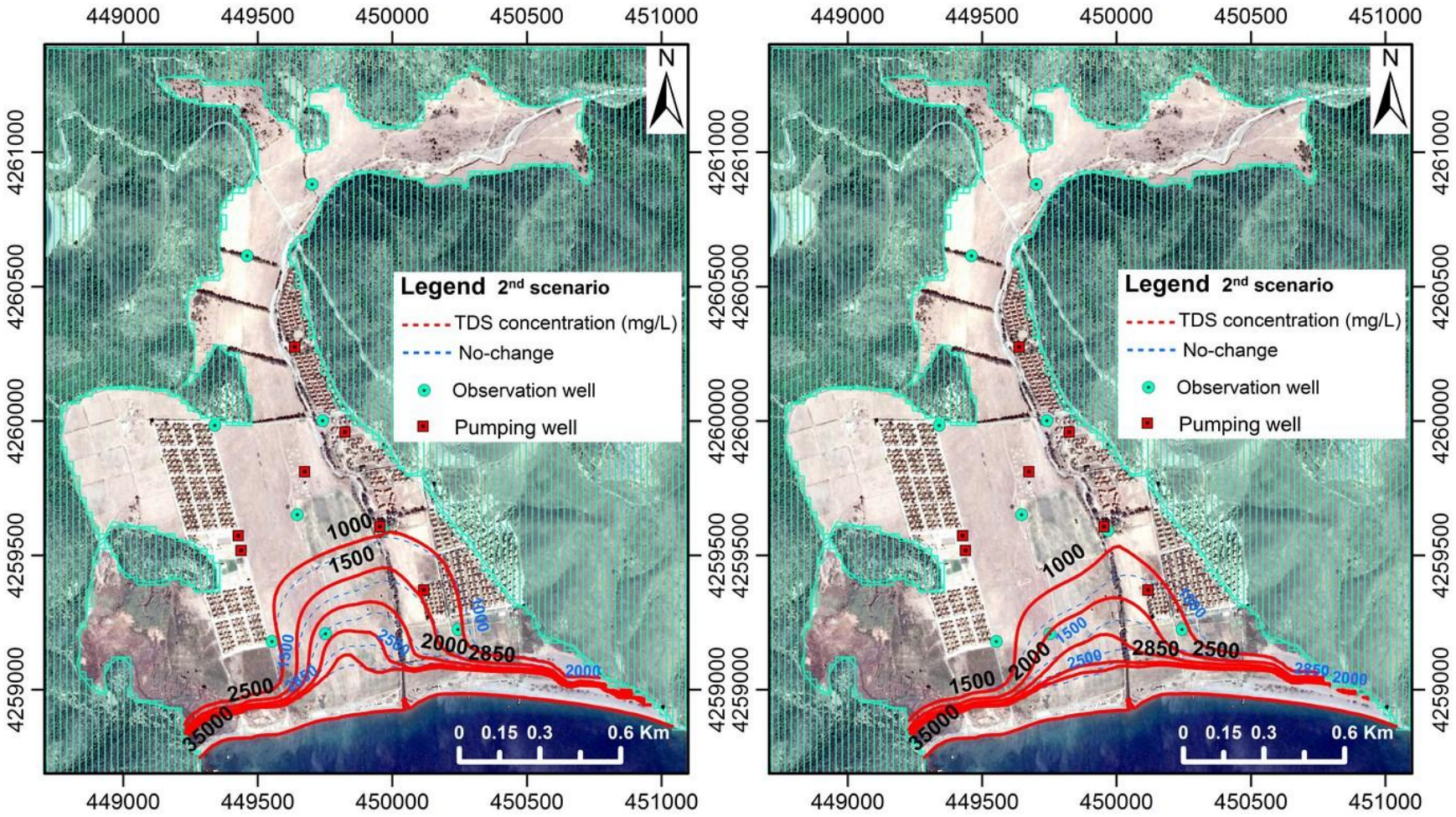

Figure 4.38. (A) Predicted contour lines of TDS concentration mg/L for the second scenario in 2019. (B) Predicted contour lines of TDS concentration mg/L for the second scenario in 2024

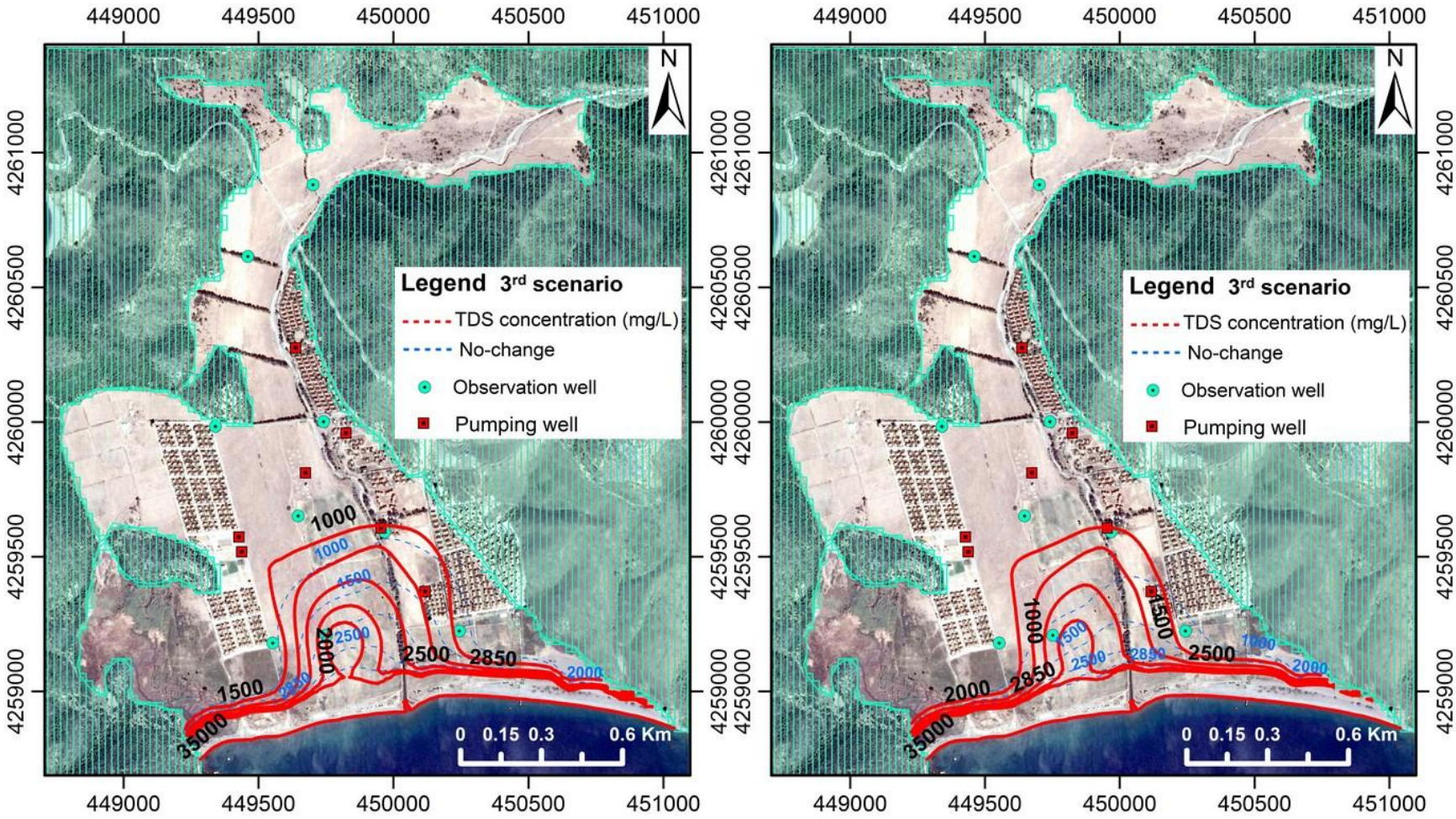

Figure 4.39. (A) Predicted contour lines of TDS concentration mg/L for the third scenario in 2019. (B) Predicted contour lines of TDS concentration mg/L for the third scenario in 2024

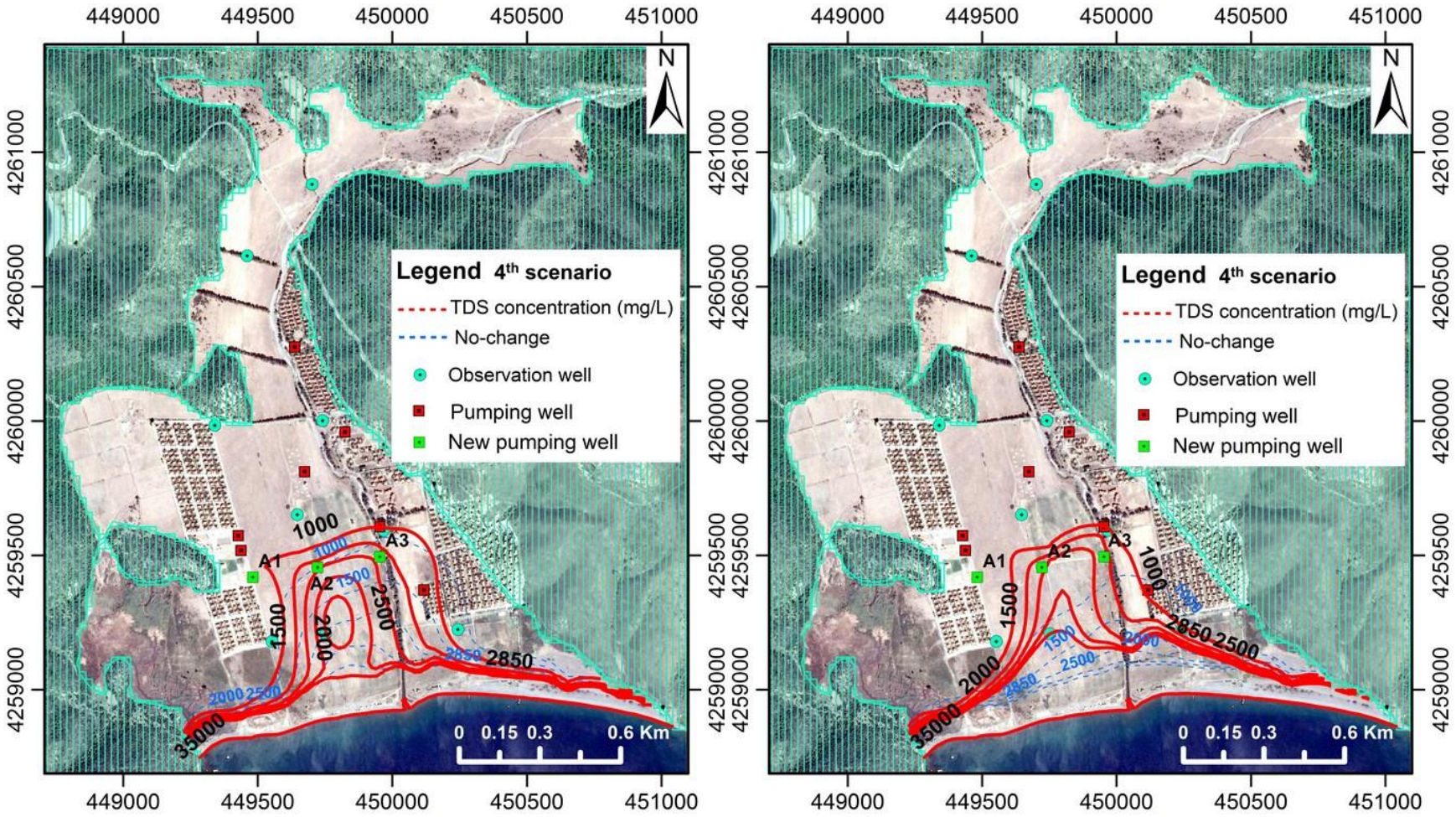

Figure 4.40. (A) Predicted contour lines of TDS concentration mg/L for the fourth scenario in 2019. (B) Predicted contour lines of TDS concentration mg/L for the fourth scenario in 2024

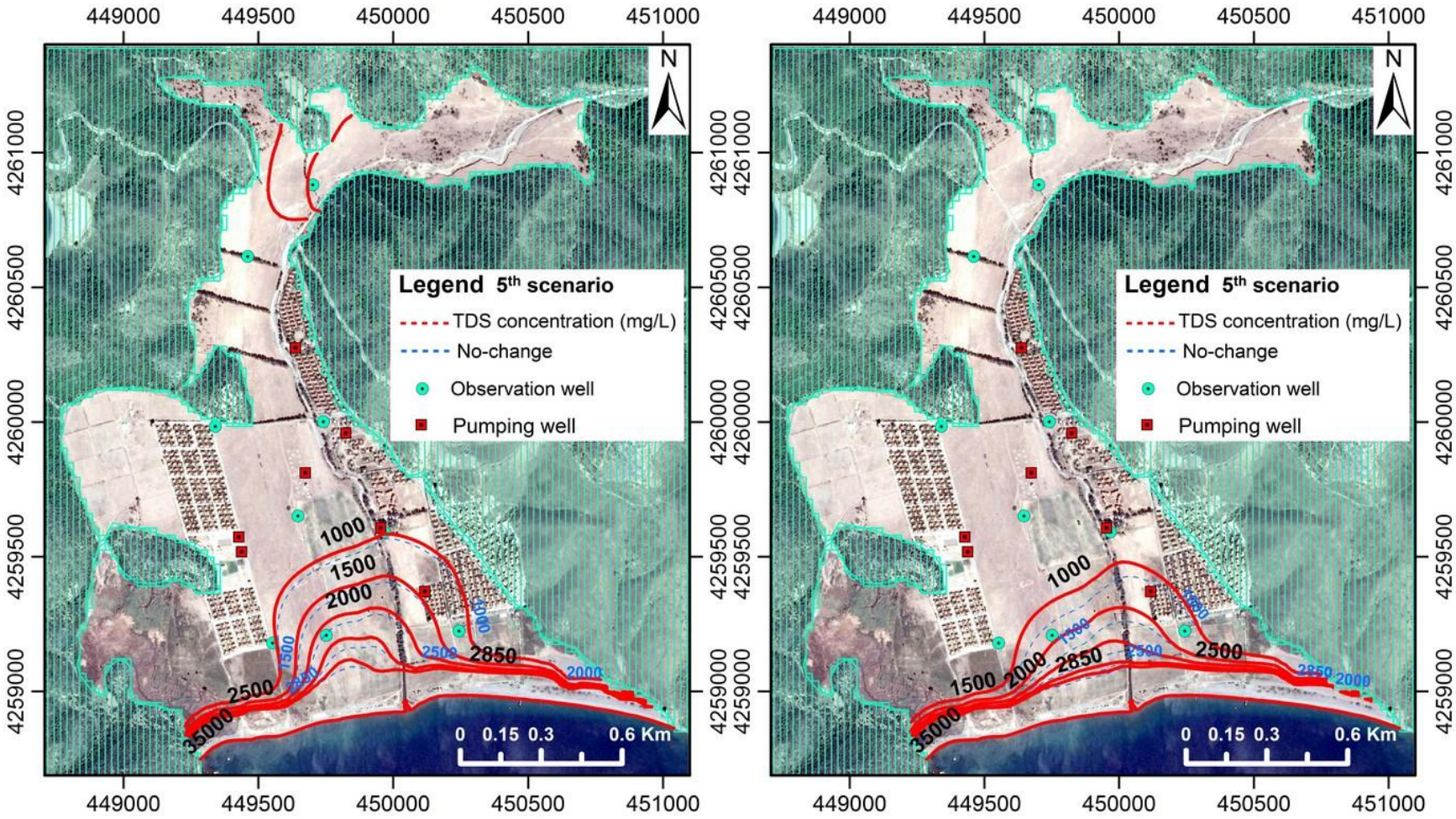

Figure 4.41. (A) Predicted contour lines of TDS concentration mg/L for the fifth scenario in 2019. (B) Predicted contour lines of TDS concentration mg/L for the fifth scenario in 2024

4.3. Control of Seawater Intrusion

Techniques for controlling seawater intrusion vary widely depending on many factors such as the sources of saline water, local geology, and the extent of seawater intrusion (Todd & Mays, 1980). In Karareis region the main reason for seawater intrusion is the excessive pumping from groundwater, due to this fact a modification of pumping pattern should be implemented especially in the summer period. Changing the locations of M.Koy 1, M.Koy 2, Karareis and Agr.Well by dispersing them in land areas, may have positive effects on the groundwater quality by increase the hydraulic gradients towards the sea. Also, reduction in water withdrawal of existing wells can produce the same beneficial effects.

Abd-Elhamid and Javadi (2011) presented a cost-effective method to control the seawater intrusion in the coastal aquifer by desalination the abstracted water and then recharge of desalinated water to the aquifer. Also, artificial recharge of freshwater can raise and maintain the groundwater levels in the aquifer.

There are many methods for controlling seawater intrusion in coastal aquifer; the main factor that is considered in these methods is the economic factor, because some of them tend to be more on the expansive side, such as subsurface barriers.

CHAPTER 5

SUMMARY, CONCLUSIONS AND RECOMMENDATIONS

The purpose of this study is to provide useful information to protect the freshwater resource in the coastal aquifer of Karareis region from contamination by seawater intrusion. In this study 3D variable density groundwater flow model was applied in order to determine how far inland the seawater has moved for the current and future situation. The model input parameters are determined from analysis of geological logs and permeability tests. The SEAWAT code is used to solve the numerical model for the couple density dependent flow system. The model was calibrated using PEST approach by adjusting the horizontal hydraulic conductivities by minimizing the difference between the calculated and observed heads and TDS. Following calibration, the model was validated by using the field observation data of the nine observation wells. A good reasonable match was obtained between the observed and simulated groundwater levels for both calibration and validation periods. The calculated model was then simulated for the next 10 years (2014-2024) using the same hydrological parameters to evaluate the extent of seawater intrusion for five expected scenarios.

Based on model predictions, it is evident that increasing the pumping from Karareis wells will lead to an additional movement of seawater towards populated area. As a result, in 10 years of increased pumping simulation, seawater intrusion will extent about 420 m. It can be expected from model results that the actual extent of seawater intrusion may be more severe than the model prediction, where the used recharge rate was relatively high. Based on the findings of the study, the following conclusions and recommendations have been made:

1. SEAWAT code is considered to be an effective tool for simulating variable density flow and transport under complex geometries and geological settings.
2. During the dry season (summer period) the effect of seawater intrusion is mostly observed in SK-7 near the coast, however model was calibrated for the average head of one year; therefore the actual extent of seawater intrusion doesn’t appear clearly.
3. The effect of the fault lines which pass near to SK-7 may be one of the main reasons causes the increasing of EC and chloride concentration near to SK-7.

4. The lack of rainfall and the effect of pumping in the summer period lead to further intrusion of seawater intrusion in to the aquifer.
5. The water samples were taken randomly at the monitoring wells; these increased the uncertainty of TDS concentration. In order to avoid this problem, the water samples should be taken at different depths on monitoring wells.
6. The model should be discretized vertically into more than one layer; this step is necessary because of transport considerations and because vertical density gradients must be resolved in order to calculate accurate velocity. Also, it is necessary for predicting the concentration of TDS due to upconing phenomena.
7. Model shows a reasonably good match between the observed and calculated data of groundwater levels and TDS concentrations. More data is needed in order to test this model, properly tested with sufficient data, can provide a powerful management tool to make decisions regarding pumping schedules in the study area.
8. The results of this model show that, the aquifer of Karareis region is very sensitive to increase the groundwater pumpage; therefore management techniques should be developed in order to protect the aquifer from deterioration. Also, the aquifer should be continuously monitored in order to determine the progress of seawater intrusion and to suggest the best solutions to prevent the intrusion.
9. In future as new data become available, the model should be updated to reduce the uncertainty in the simulations.
10. This study provides a valuable example that can be used to study the seawater intrusion in other coastal aquifer under similar condition.

REFERENCES

[1] Abd-Elhamid, H. F., & Javadi, A. A. (2011). A cost-effective method to control seawater intrusion in coastal aquifers. *Water Resources Management*, *25*(11), 2755-2780.

[2] Allow, K. A. (2011). Seawater intrusion in Syrian coastal aquifers, past, present and future, case study. *Arabian Journal of Geosciences*, *4*(3-4), 645-653.

[3] Appelo, C. A. J., & Postma, D. (2005). *Geochemistry, groundwater and pollution*: CRC press.

[4] Bakker, M. (2003). A Dupuit formulation for modeling seawater intrusion in regional aquifer systems. *Water Resources Research*, *39*(5).

[5] Bakker, M., Essink, G. H. O., & Langevin, C. D. (2004). The rotating movement of three immiscible fluids—a benchmark problem. *Journal of Hydrology*, *287*(1), 270-278.

[6] Barlow, P. M. (2003). *Ground Water in Fresh Water-salt Water Environments of the Atlantic* (Vol. 1262): Geological Survey (USGS).

[7] Bear, J., & Cheng, A. H.-D. (2010). *Modeling groundwater flow and contaminant transport* (Vol. 23): Springer Science & Business Media.

[8] Bear, J., Cheng, A. H.-D., Sorek, S., Ouazar, D., & Herrera, I. (1999). *Seawater intrusion in coastal aquifers: concepts, methods and practices* (Vol. 14): Springer Science & Business Media.

[9] Boulding, J. R. (1996). *Subsurface Characterization And Monitoring Techniques A Desk Reference Guide: Solids And Ground Water Appendices A And B*: DIANE Publishing.

[10] Causon, D., & Mingham, C. (2010). *Introductory finite difference methods for PDEs*: Bookboon.

[11] Chang, C., Sommerfeldt, T., Carefoot, J., & Schaalje, G. (1983). Relationships of electrical conductivity with total dissolved salts and cation concentration of sulfate-dominant soil extracts. *Canadian Journal of Soil Science*, *63*(1), 79-86.

[12] Cobaner, M., Yurtal, R., Dogan, A., & Motz, L. H. (2012). Three dimensional simulation of seawater intrusion in coastal aquifers: A case study in the Goksu Deltaic Plain. *Journal of Hydrology*, *464*, 262-280.

[13] Cooper, H. H., & Jacob, C. (1946). A generalized graphical method for evaluating formation constants and summarizing well‐field history. *Eos, Transactions American Geophysical Union*, *27*(4), 526-534.

[14] Das, B. M. (2013). *Advanced soil mechanics*: CRC Press.

[15] Dausman, A., & Langevin, C. D. (2005). *Movement of the saltwater interface in the surficial aquifer system in response to hydrologic stresses and water-management practices, Broward County, Florida*: US Department of the Interior, US Geological Survey.

[16] Director, S. D. (2007). M. Thangarajan.

[17] Erdogan, B. (1990). Tectonic relations between Izmir-Ankara zone and Karaburun belt. *Bull. Min. Res. Expl. Inst. Turkey (MTA), 110*, 11-15.

[18] Gaaloul, N., Pliakas, F., Kallioras, A., Schuth, C., & Marinos, P. (2012). Simulation of seawater intrusion in coastal aquifers: Forty five-years exploitation in an eastern coast aquifer in NE Tunisia. *Open Hydrol J, 6*, 31-44.

[19] Geta, J. A. L. (2003). *Coastal aquifers intrusion technology, Mediterranean countries* (Vol. 8): IGME.

[20] Gopinath, S., Srinivasamoorthy, K., Saravanan, K., Suma, C., Prakash, R., Senthilnathan, D., . . . Sarma, V. (2016). Modeling saline water intrusion in Nagapattinam coastal aquifers, Tamilnadu, India. *Modeling Earth Systems and Environment, 2*(1), 1-10.

[21] Guo, W., & Bennett, G. (1998). SEAWAT version 1.1—A computer program for simulations of ground water flow of variable density. *A report prepared by Missimer International Inc.*

[22] Guo, W., & Langevin, C. D. (2002). User's guide to SEAWAT; a computer program for simulation of three-dimensional variable-density ground-water flow.

[23] Harbaugh, A. W. (2005). *MODFLOW-2005, the US Geological Survey modular ground-water model: the ground-water flow process*: US Department of the Interior, US Geological Survey Reston, VA, USA.

[24] Jarvis, A., Reuter, H. I., Nelson, A., & Guevara, E. (2008). Hole-filled SRTM for the globe Version 4. *available from the CGIAR-CSI SRTM 90m Database (http://srtm. csi. cgiar. org).*

[25] Kallioras, A., Pliakas, F., & Diamantis, I. (2006). Conceptual model of a coastal aquifer system in northern Greece and assessment of saline vulnerability due to seawater intrusion conditions. *Environmental Geology, 51*(3), 349-361.

[26] Kaya, M. A., Özürlan, G., & Balkaya, Ç. (2015). Geoelectrical investigation of seawater intrusion in the coastal urban area of Çanakkale, NW Turkey. *Environmental Earth Sciences, 73*(3), 1151-1160.

[27] Land, A. O. o. t. U. N., Division, W. D., East, A. O. o. t. U. N. R. O. f. t. N., & Groundwater, R. I. f. (1997). *Seawater intrusion in coastal aquifers: guidelines for study, monitoring and control* (Vol. 11): Food & Agriculture Org.

[28] Langevin, C. D. (2003). Simulation of submarine ground water discharge to a marine estuary: Biscayne Bay, Florida. *Ground Water, 41*(6), 758-771.

[29] Langevin, C. D., Shoemaker, W. B., & Guo, W. (2003). MODFLOW-2000, the US Geological Survey Modular Ground-Water Model--Documentation of the SEAWAT-2000 Version with the Variable-Density Flow Process (VDF) and the Integrated MT3DMS Transport Process (IMT).

[30] Lin, J., Snodsmith, J. B., Zheng, C., & Wu, J. (2009). A modeling study of seawater intrusion in Alabama Gulf Coast, USA. *Environmental Geology, 57*(1), 119-130.

[31] Logan, B. E. (2012). *Environmental transport processes*: John Wiley & Sons.

[32] Lollar, B. S. (2005). *Environmental geochemistry* (Vol. 9): Elsevier.

[33] Magnus U, I. (2011). Finite difference method of modelling groundwater flow. *Journal of Water Resource and Protection, 2011*.

[34] Marinos, V., Fortsakis, P., Prountzopoulos, G., & Marinos, P. (2011). Permeability in flysch—distribution decrease with depth and grout curtains under dams. *Journal of Mountain Science, 8*(2), 234-238.

[35] McDonald, J., & Harbaugh, A. (1988). MODFLOW, a modular 3D finite difference ground-water flow model. *US Geological Survey. Open File Report*, 83-875.

[36] Morris, D. A., & Johnson, A. I. (1967). Summary of hydrologic and physical properties of rock and soil materials, as analyzed by the hydrologic laboratory of the US Geological Survey, 1948-60: US Govt. Print. Off.

[37] Nair, I. S., Rajaveni, S., Schneider, M., & Elango, L. (2015). Geochemical and isotopic signatures for the identification of seawater intrusion in an alluvial aquifer. *Journal of Earth System Science, 124*(6), 1281-1291.

[38] Paniconi, C., Khlaifi, I., Lecca, G., Giacomelli, A., & Tarhouni, J. (2001). A modelling study of seawater intrusion in the Korba coastal plain, Tunisia. *Physics and Chemistry of the Earth, Part B: Hydrology, Oceans and Atmosphere, 26*(4), 345-351.

[39] Qahman, K., & Larabi, A. (2006). Evaluation and numerical modeling of seawater intrusion in the Gaza aquifer (Palestine). *Hydrogeology Journal, 14*(5), 713-728.

[40] Reilly, T., & Goodman, A. (1987). Analysis of saltwater upconing beneath a pumping well. *Journal of Hydrology, 89*(3), 169-204.

[41] Sarsak, R., & Almasri, M. N. (2013). Seawater intrusion into the coastal aquifer in the Gaza Strip: a computer-modelling study. *The Lancet, 382*, S32.

[42] Schneider, J. C., & Kruse, S. E. (2006). Assessing selected natural and anthropogenic impacts on freshwater lens morphology on small barrier Islands: Dog Island and St. George Island, Florida, USA. *Hydrogeology Journal, 14*(1-2), 131-145.

[43] Sherif, M., Kacimov, A., Javadi, A., & Ebraheem, A. A. (2012). Modeling groundwater flow and seawater intrusion in the coastal aquifer of Wadi Ham, UAE. *Water Resources Management, 26*(3), 751-774.

[44] Strack, O. (1976). A single‐potential solution for regional interface problems in coastal aquifers. *Water Resources Research, 12*(6), 1165-1174.

[45] Todd, D. K., & Mays, L. W. (1980). Groundwater hydrology.

[46] Walton, N. (1989). Electrical conductivity and total dissolved solids—What is their precise relationship? *Desalination, 72*(3), 275-292.

[47] Zheng, C. (1990). {MT3D}, A modular three-dimensional transport model.

[48] Zheng, C. (2006). MT3DMS v5. 2 supplemental user's guide. *Department of Geological Sciences, University of Alabama, Tuscaloosa, AL*

[49] Zheng, C., & Bennett, G. D. (2002). *Applied contaminant transport modeling* (Vol. 2): Wiley-Interscience New York.

[50] Zheng, C., & Wang, P. P. (1999). MT3DMS: a modular three-dimensional multispecies transport model for simulation of advection, dispersion, and chemical reactions of contaminants in groundwater systems; documentation and user's guide: DTIC Document.

[51] Zhou, Q., Bear, J., & Bensabat, J. (2005). Saltwater upconing and decay beneath a well pumping above an interface zone. *Transport in Porous Media, 61*(3), 337-363.

[52] Zimmermann, S., Bauer, P., Held, R., Kinzelbach, W., & Walther, J. H. (2006). Salt transport on islands in the Okavango Delta: numerical investigations. *Advances in Water Resources, 29*(1), 11-29.